December 1968

Final Report

# EXISTING STRUCTURES EVALUATION
## Part II: Window Glass and Applications



Prepared for:
OFFICE OF CIVIL DEFENSE
OFFICE OF THE SECRETARY OF THE ARMY
WASHINGTON, D.C. 20310

STANFORD
RESEARCH
INSTITUTE

SRI

MENLO PARK
CALIFORNIA

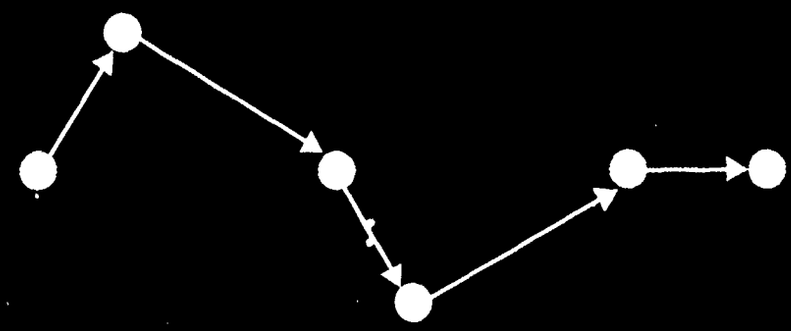

Final Report

# SUMMARY OF EXISTING STRUCTURES EVALUATION Part II: Window Glass and Applications

December 1968

Contract No.
OCD-DAHC20-67-C-0136

OCD Work Unit
No. 1126C

Prepared for:
OFFICE OF CIVIL DEFENSE
OFFICE OF THE SECRETARY OF THE ARMY
WASHINGTON, D.C. 20310

STANFORD
RESEARCH
INSTITUTE

MENLO PARK
CALIFORNIA

By:

J.H. Iverson
Public Works Systems

## SUMMARY

### Introduction

This report covers one portion of a research project to evaluate existing NFSS structures for resistance to combined nuclear weapons effects. The objective of this investigation was to determine the response of windows to air blast overpressures generated by nuclear explosions, including glass fragment data (weights, velocities, numbers produced, and spatial densities) that could be used to predict statistically the effects of window glass failure on humans.

Glass, a brittle material, conforms to elastic theory to the point of failure. Unfortunately, the usual methods of structural analysis based on material ultimate strength or breaking stress were found to be inapplicable to glass panes. Glass strength depends almost completely on flaws or defects. Therefore, failure strongly depends on the probabilities of the number, size, and location of flaws.

### Incipient Failure Load Prediction

Windows exposed to explosions were found to behave similarly to a simple oscillator. Thus, the differential equation of motion for a single-degree-of-freedom system with no damping was usable. Window glass response predictions were based on a load-deflection relationship. The loading with about 50 percent probability of causing failure was reported.

The analytical work was begun with a theoretical load-deflection equation for large deflections of plates since deflections from one to

seven times the glass thicknesses were found in test data. The equation, which includes both bending and membrane action, was then modified slightly (in the membrane term) to fit available static test data. Failure loads, which serve as end points to the equation for various pane sizes and thicknesses, were selected from design data. Thus, a static resistance function describing window response including failure was established.

Data relating breaking stress to various loading rates were used to select 1.8 as the ratio of dynamic to static failure loads.

The air blast loading function selected was the pressure-time relationship that describes the interaction of a nuclear blast wave with the front face of a closed rectangular structure. The clearing distance was set equal to zero for side-face loading.

A computer program was developed that numerically solved the differential equation of motion using the Newmark $\beta$ Method. The resistance function and the loading function were included in the program as subroutines. Inputs to the program include window size and load parameters. The print-out includes the load causing incipient failure and a complete time-history of the response, if desired. The results of several runs were plotted. Figure S-1 provides predictions of the free-field overpressure with a 50 percent probability of causing incipient failure in windows containing sheet glass subjected to front-face loading. Similar figures for side-on loading and for plate glass are included in the report.

## Glass Fragment Characteristics

Data on weight, velocity, and spatial density of glass missiles resulting from window failure caused by a nuclear explosion were reported for Operation Teapot tests. Glass missiles emanating from multipane windows having either steel or wood frames were trapped in Styrofoam absorbers.

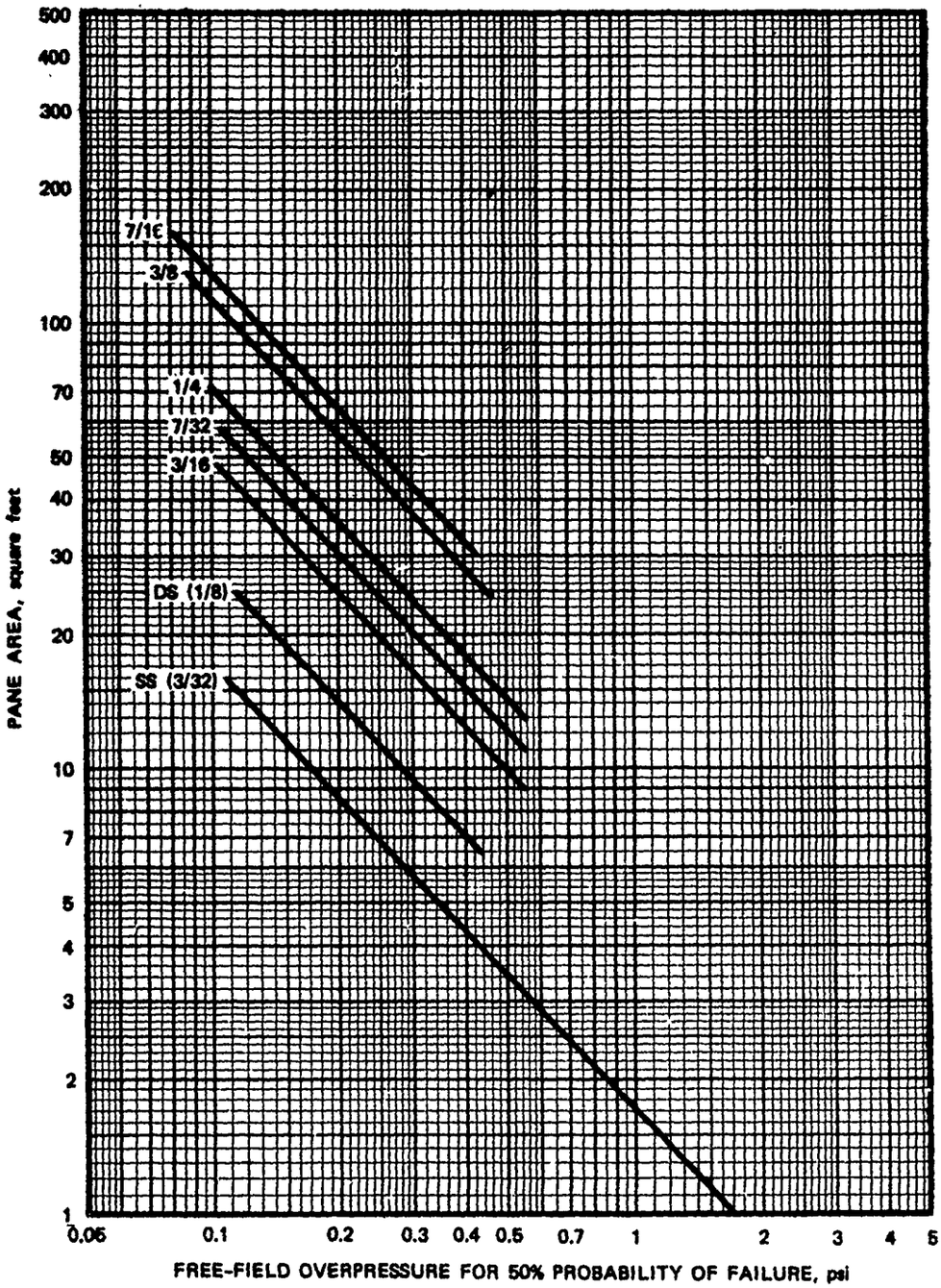


FIG. S-1 SHEET GLASS INCIPIENT FAILURE PRESSURES FOR FRONT-FACE LOADING AS A FUNCTION OF PANE AREA AND THICKNESS

These test data were used to develop the curves presented in Figure S-2, which can be used to predict average and geometric mean fragment weights. The geometric mean fragment weight was found to be indicative of the most likely fragment weight. The average fragment weight is needed in calculations of the number and spatial density of fragments.

The spatial density of fragments very near a window can be estimated by

$$N_0 = \frac{\gamma h}{\bar{M}} \qquad \text{(S-1)}$$

where $N_0$ is the spatial density of fragments zero feet from a window (units are fragments per area), $\gamma$ is the unit weight of glass (0.090 $lb/in^3$), h is the pane thickness, and $\bar{M}$ is the average fragment weight. The total number of fragments produced by a given window may be found by multiplying $N_0$ by the total glass area of the window.

The spatial density of fragments 10 feet from a window ($N_{10}$), based on the Operation Teapot data, can be found by using Figure S-3.

Fragment velocities calculated in this report were based on Bowen's (1961) translation model. Examples of some calculated velocities appear in Table S-1.

The procedures described above for estimating incipient failure and weights, spatial densities, numbers, and velocities of fragments were applied to windows in 14 buildings located in San Jose and Palo Alto, California, which were part of the National Fallout Shelter Survey (NFSS). The results can be found in Chapter VII of the report.

## Biological Considerations

Figure S-4, adapted from work by Bowen, et al. (1956), is presented to relate fragment characteristics to injuries. This figure is presented for illustrative purposes only, since original work on the biological

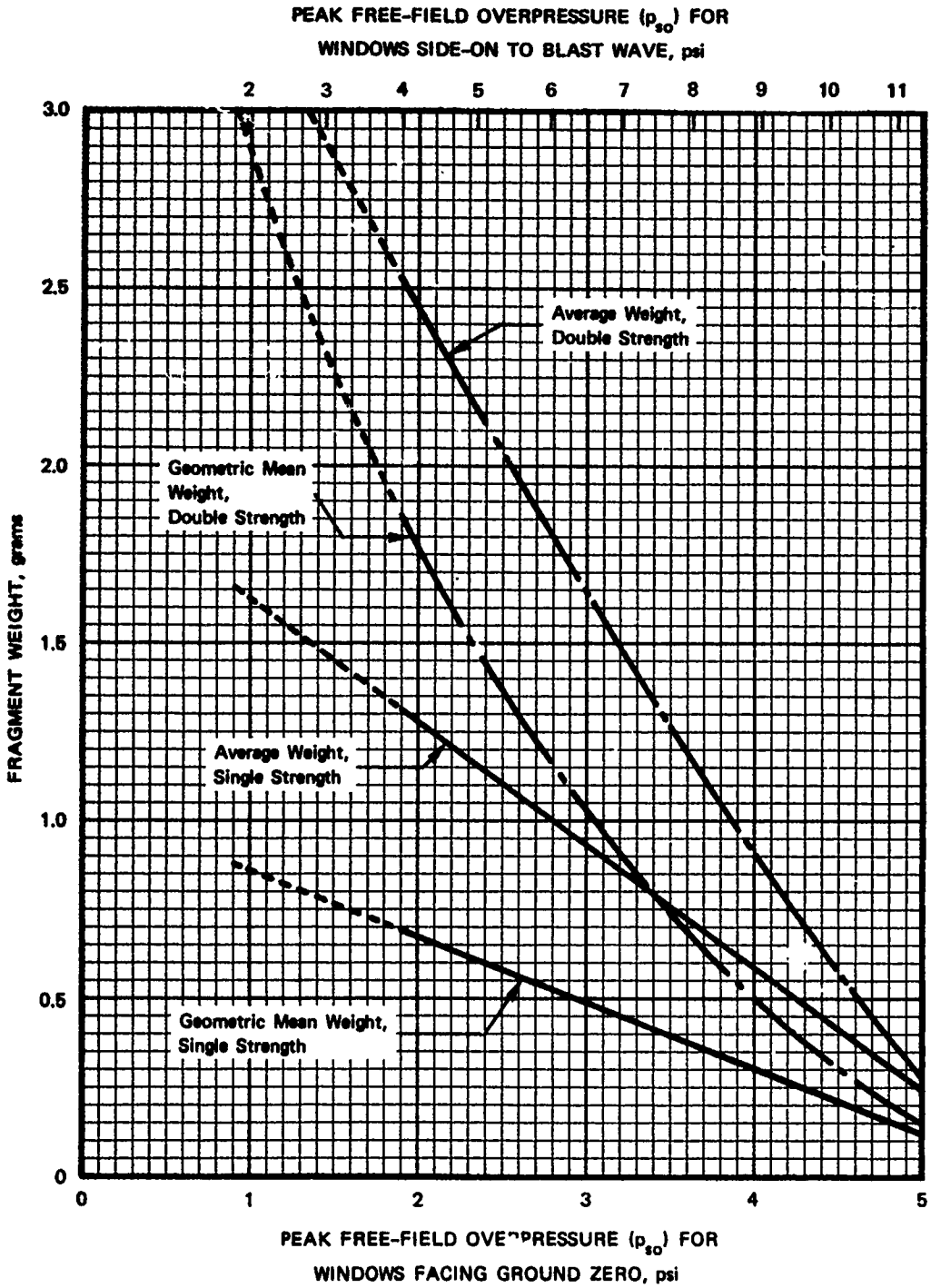


FIG. S-2 FRAGMENT WEIGHT PREDICTIONS

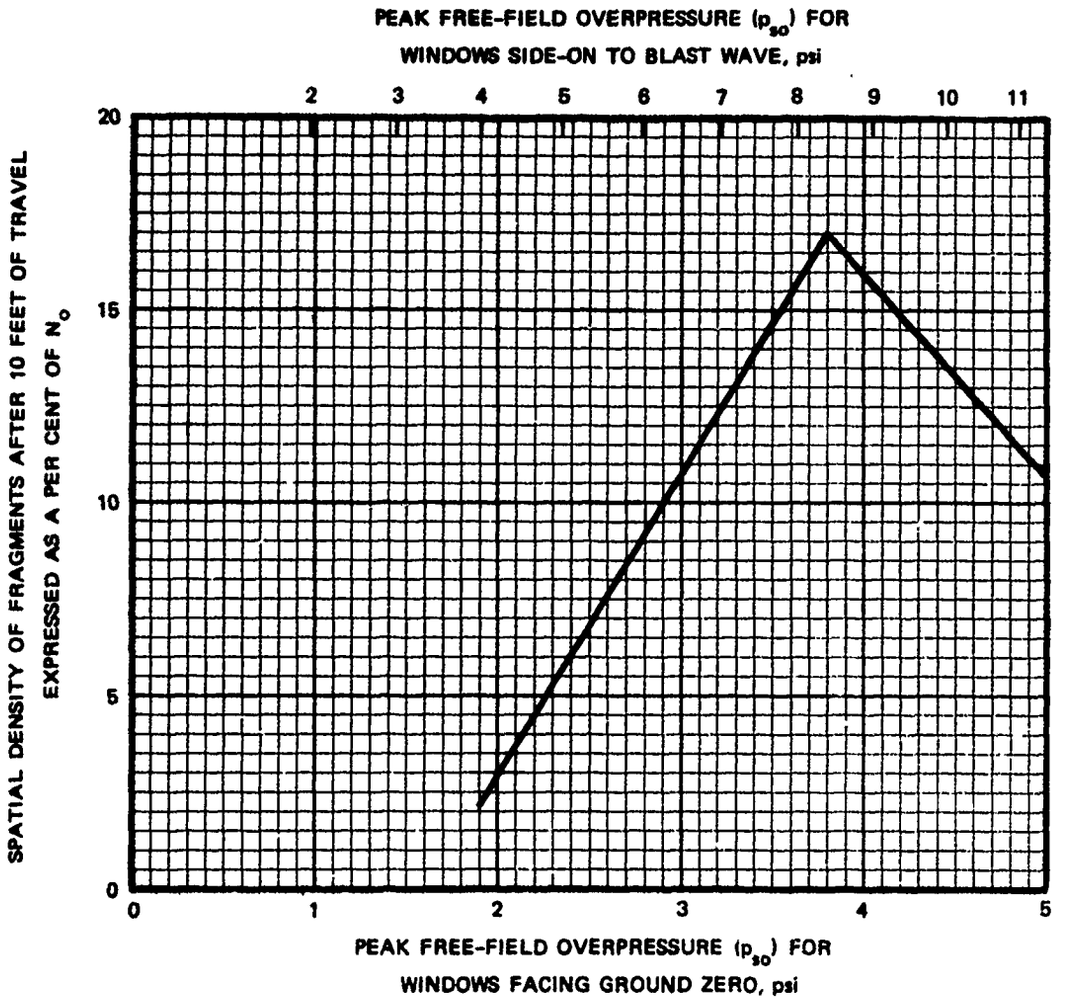


FIG. S-3 SPATIAL DENSITY PREDICTIONS AFTER 10 FEET OF TRAVEL AS A FUNCTION OF OVERPRESSURE

Table S-1

FRAGMENT WEIGHT AND VELOCITY PREDICTIONS
FOR OVERPRESSURES ABOVE INCIPIENT FAILURE

| | Free Field Overpressure (psi) | | Geometric Mean Fragment Weight $M_{50}$, (gm) | Average Fragment Weight $\bar{M}$, (gm) | Velocity of Geometric Mean Weight Fragment After 10 Feet of Travel (fps)* |
|---|---|---|---|---|---|
| | Front Facing | Side Facing | | | |
| Single strength | 2.0 | 4.2 | 0.67 | 1.27 | 87 |
| | 3.0 | 6.5 | 0.48 | 0.93 | 132 |
| | 5.0 | 11.4 | 0.12 | 0.24 | 238 |
| Double strength | 2.0 | 4.2 | 1.85 | 2.43 | 92 |
| | 3.0 | 6.5 | 1.07 | 1.63 | 130 |
| | 5.0 | 11.4 | 0.14 | 0.28 | 234 |
| 3/16-in. sheet | 2.0 | 4.2 | 4.3 | 5.6 | 93 |
| | 3.0 | 6.5 | 2.1 | 3.3 | 138 |
| | 5.0 | 11.4 | 0.14 | 0.28 | 234 |
| 1/4-in. sheet | 2.0 | 4.2 | 9.8 | 13.0 | 94 |
| | 3.0 | 6.5 | 4.2 | 6.6 | 139 |
| | 5.0 | 11.4 | 0.14 | 0.28 | 234 |

* Velocities are given for a weapon yield of 1 Mt, ambient atmospheric pressure of 14.7 psi, and speed of sound in undisturbed air of 1126 fps.

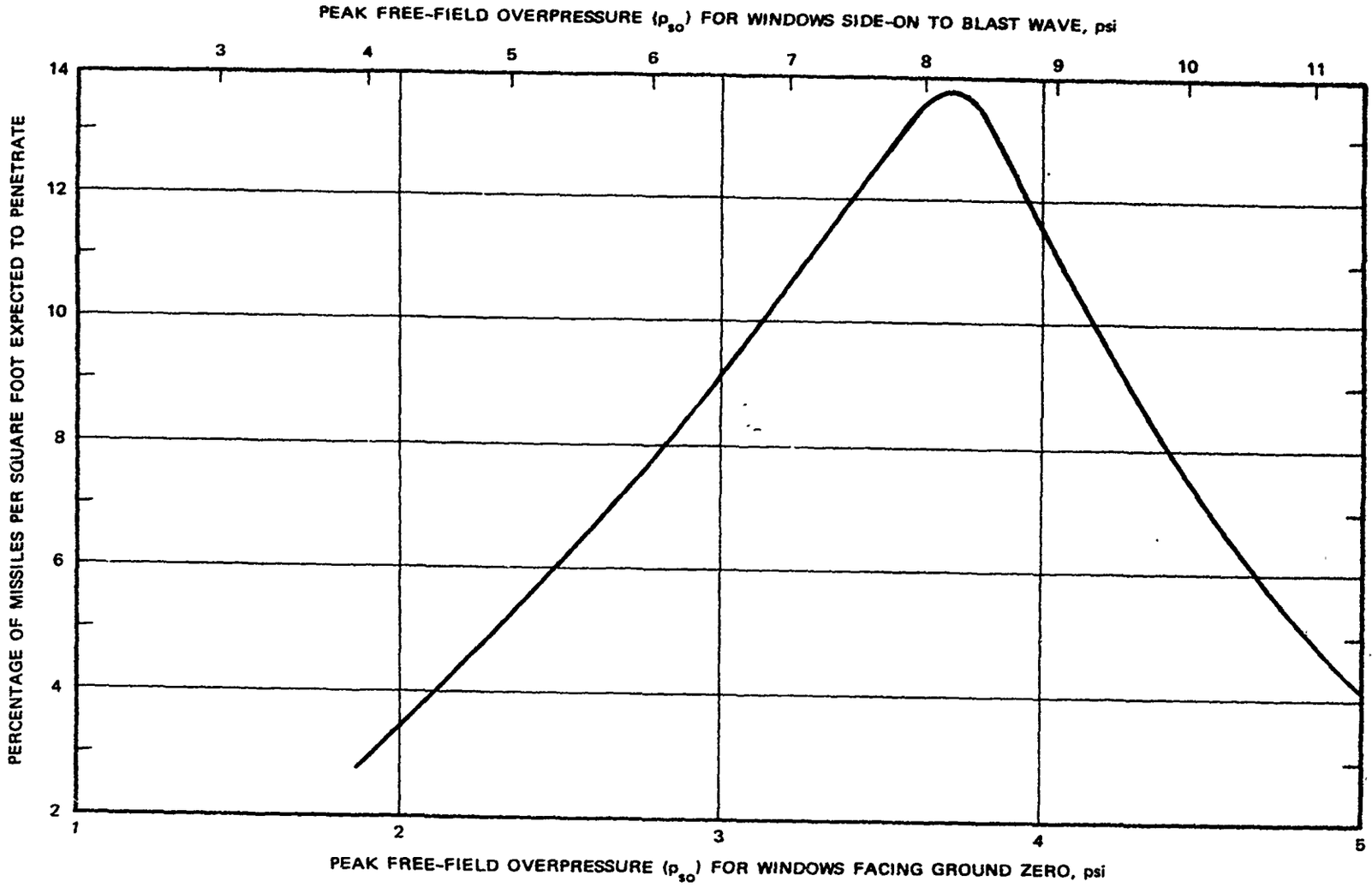


FIG. S-4 EXPECTED FREQUENCY OF PENETRATION AS A FUNCTION OF PEAK OVERPRESSURE*

* Computed for glass missiles occurring about 10 feet behind windows in house walls facing blast. Penetration criterion derived from dog abdomen studies.

aspects of flying glass missiles was outside the scope of this investigation.

Other Work

Five appendixes are included in the report. Appendix A provides the Uniform Building Code approach to selecting the minimum glass thickness for a window; common window types and sizes are recorded in Appendix B; test data on the modulus of rupture of glass may be found in Appendix C; Appendix D contains general information on various dynamic loadings to windows in relation to nuclear explosion, conventional explosion, shock tube, and sonic boom tests; and figures describing the elapsed time between loading and failure for windows are in Appendix E.

Final Report

# EXISTING STRUCTURES EVALUATION
## Part II: Window Glass and Applications

December 1968

SRI Project No. MU-6300-020

Contract No.
OCD-DAHC20-67-C-0136

OCD Work Unit
No. 1126C

Prepared for:
OFFICE OF CIVIL DEFENSE
OFFICE OF THE SECRETARY OF THE ARMY
WASHINGTON, D.C. 20310

STANFORD
RESEARCH
INSTITUTE

MENLO PARK
CALIFORNIA

By:

J.H. Iverson
Public Works Systems

## FOREWORD

This report is one of a series covering research of a continuing nature under a project for blast resistance evaluation of existing structures in the National Fallout Shelter Survey (NFSS) inventory of the U.S. Office of Civil Defense (OCD).

The objective is to develop an evaluation method for estimating blast resistance and the cost-effectiveness of structure modifications to improve blast protection.

The evaluation method differs from vulnerability analysis techniques by carrying along significant statistical yardsticks (e.g., on strengths of materials) in the calculations sufficient to meet the needs of shelter operations research or war-gaming. It differs from protective design/analysis by aiming at a 50% probability basis, rather than the 90%-99% probability basis intended in design/analysis methods.

The results expected of the evaluation method will provide inputs for systems analyses related to performance of structures and effects on shelterees. For the latter purpose, the evaluation method results will include data on fragments and their sizes, masses, accelerations, velocities, and displacements.

The approach used for the continuing research was to develop an evaluation method for each of several structural elements (e.g., window glass, walls, and slabs), including reaction load-time history, and then for structural frames.

The research includes applications to specific buildings, such as those selected in a statistically adequate sample of NFSS structures under another OCD project, thereby making possible various extrapolations to the overall NFSS structures picture.

## ABSTRACT

This report covers one portion of a research project to evaluate existing National Fallout Shelter Survey (NFSS) structures for resistance to combined nuclear weapons effects. The objective of this investigation was to determine the response of windows to air blast overpressures generated by nuclear explosions, including glass fragment characteristics (weights, velocities, numbers produced, and spatial densities) that could be used to predict statistically the effects of window glass failure on humans.

The analysis leading to the presentation of graphs, which can be used to predict the free-field overpressure at incipient failure for sheet and plate glass, was based on the theoretical load-deflection equation for large deflections of plates, modified by test results found in the literature. Glass panes were changed to equivalent single-degree-of-freedom systems in the analysis. The analysis was also used to estimate the time to failure for windows at various overpressures. Methods for predicting glass fragment characteristics were obtained empirically from Operation Teapot nuclear test data. The procedures for estimating incipient failure overpressures and fragment weights, spatial densities, numbers, and velocities were applied to windows in 14 buildings (located in San Jose and Palo Alto, California) that were part of the NFSS.

CONTENTS


SUMMARY . . . . . S-1

FOREWORD . . . . . iii

ABSTRACT . . . . . v

I INTRODUCTION . . . . . 1

Relationship to Parent Investigation . . . . . 1
Objective . . . . . 1
Types of Glass . . . . . 2
Properties of Glass . . . . . 3
Acknowledgments . . . . . 6

II INCIPIENT FAILURE LOAD PREDICTION . . . . . 7

Discussion of Approach . . . . . 7
Development of a Static Resistance Function . . . . . 9
Static Failure Load Determination . . . . . 14
Transition from Static to Dynamic Response . . . . . 18
Air Blast Loading . . . . . 21
Window Pane Response to Nuclear Blast Wave Loading . . . . . 23
Incipient Failure Prediction Results . . . . . 24

III WEIGHT, NUMBER, AND SPATIAL DENSITY OF GLASS FRAGMENTS . . . 37

Introduction . . . . . 37
Fragment Weight . . . . . 38
Number of Fragments . . . . . 41
Spatial Density of Fragments . . . . . 41

IV FRAGMENT TRANSLATION MODEL . . . . . 47

V BIOLOGICAL CONSIDERATIONS . . . . . 69

VI RECOMMENDED ADDITIONAL STUDY . . . . . 75

VII APPLICATIONS . . . . . 77

CONTENTS

APPENDIXES

A GLASS SELECTION PROCEDURE . . . . . A-1

B COMMON WINDOW TYPES AND SIZES . . . . . B-1

C MODULUS OF RUPTURE DATA . . . . . C-1

D WINDOWS SUBJECTED TO VARIOUS DYNAMIC LOADINGS . . . . . D-1

E TIME TO FAILURE . . . . . E-1

ADDENDUM A MULTIPLE REGRESSION ANALYSIS APPROACH . . . . . An-1

REFERENCES . . . . . R-1

BIBLIOGRAPHY . . . . . Bi-1

NOTATION . . . . . N-1

## FIGURES


| | | |
|---|---|---|
| 1 | Static Load Versus Central Deflection for Square Panes of Sheet and Plate Glass | 15 |
| 2 | Plate Glass Failure Loads for Time to Failure of 60 Seconds | 16 |
| 3 | Sheet Glass Failure Loads for Time to Failure of 60 Seconds | 17 |
| 4 | Effect of Loading Rate on Normalized Breaking Stress | 20 |
| 5 | Front-Face Air Blast Loading | 22 |
| 6 | Computer Program Flow Chart | 25 |
| 7 | Plate Glass Incipient Failure Pressures for Side-Wall Loading as a Function of Pane Area and Thickness | 32 |
| 8 | Plate Glass Incipient Failure Pressures for Front-Face Loading as a Function of Pane Area and Thickness | 33 |
| 9 | Sheet Glass Incipient Failure Pressures for Side-Wall Loading as a Function of Pane Area and Thickness | 34 |
| 10 | Sheet Glass Incipient Failure Pressures for Front-Face Loading as a Function of Pane Area and Thickness | 35 |
| 11 | Fragment Weight Predictions | 40 |
| 12 | Spatial Density Predictions After 10 Feet of Travel as a Function of Overpressure | 44 |
| 13 | Ratio of Duration of Wind to Positive Phase Duration as a Function of Overpressure | 55 |
| 14 | Summary of Acceleration Coefficient Data for Glass Fragments | 56 |
| 15 | Predicted Maximum Velocity as a Function of Acceleration Coefficient and Nondimensional Peak Overpressure (W = 1 kt) | 58 |
| 16 | Predicted Displacement at Maximum Velocity as a Function of Acceleration Coefficient and Nondimensional Peak Overpressure (W = 1 kt) | 59 |
| 17 | Predicted Maximum Velocity as a Function of Acceleration Coefficient and Nondimensional Peak Overpressure (W = 20 kt) | 60 |
| 18 | Predicted Displacement at Maximum Velocity as a Function of Accelerated Coefficient and Nondimensional Peak Overpressure (W = 20 kt) | 61 |

## FIGURES


| | | |
|---|---|---|
| 19 | Predicted Maximum Velocity as a Function of Acceleration Coefficient and Nondimensional Peak Overpressure (W= 1 Mt) . | 62 |
| 20 | Predicted Displacement at Maximum Velocity as a Function of Acceleration Coefficient and Nondimensional Peak Overpressure (W = 1 Mt) . . . . . | 63 |
| 21 | Operation Plumbbob: Analysis of Window Glass Fragments from 14 Traps . . . . . | 66 |
| 22 | Probability of Penetration of Glass Fragments into the Abdomen of a Dog as a Function of Missile Weight and Impact Velocity . . . . . | 70 |
| 23 | Expected Frequency of Penetration as a Function of Peak Overpressure . . . . . | 72 |
| A-1 | Allowable Resultant Wind Pressures . . . . . | A-4 |
| B-1 | Common Window Types . . . . . | B-4 |
| C-1 | Diagram of Test Method . . . . . | C-3 |
| E-1 | Free-Field Overpressure Versus Time to Failure for Panes of Glass Mounted in House Walls Single Strength Glass, Front-Face Loading . . . . . | E-4 |
| -2 | Free-Field Overpressure Versus Time to Failure for Panes of Glass Mounted in House Walls Single Strength Glass, Side-Face Loading . . . . . | -5 |
| -3 | Free-Field Overpressure Versus Time to Failure for Panes of Glass Mounted in House Walls Double Strength Glass, Front-Face Loading . . . . . | -6 |
| -4 | Free-Field Overpressure Versus Time to Failure for Panes of Glass Mounted in House Walls Double Strength Glass, Side-Face Loading . . . . . | -7 |

## TABLES


| | | |
|---|---|---|
| 1 | Sheet Glass Specifications | 4 |
| 2 | Plate Glass Specifications | 4 |
| 3 | Load - Central Deflection Failure Data for Square Panes | 11 |
| 4 | Stress Data | 12 |
| 5 | Failure Load - Central Deflection Data for Large Plate Glass Panes | 13 |
| 6 | Computer Program | 26 |
| 7 | Window Glass Fragment Weight Data | 39 |
| 8 | Window Glass Spatial Density Data | 42 |
| 9 | Computed Motion Parameters for Objects Displaced by Classical Blast Waves | 49 |
| 10 | Tentative Criteria for Secondary Blast Effects | 71 |
| 11 | Window Field Data | 78 |
| 12 | Incipient Failure Overpressure Predictions | 80 |
| 13 | Fragment Weight and Velocity Predictions for Overpressures Above Incipient Failure | 82 |
| 14 | Predictions of Spatial Density and Number of Fragments for Overpressures Above Incipient Failure | 86 |
| A-1 | Wind Pressures at Various Elevations Above Grade | A-5 |
| -2 | Maximum Allowable Area of Glass | -6 |
| C-1 | Modulus of Rupture Tests on Plate Glass | C-4 |
| -2 | Summary of Table C-1 Data | -5 |
| -3 | Modulus of Rupture Tests | -5 |
| -4 | Modulus of Rupture Tests | -7 |
| D-1 | The Relationship of Loading to Breaking Stress | D-3 |
| -2 | Blast Effects on Window Construction and Grazing | -7 |
| -3 | Sonic Boom Exposure | -11 |

## TABLES


An-1 Window Glass Fragment Weight Data . . . . . An-6

-2 B = f(A,C,D,E) . . . . . -7

-3 B = f(A,C,E) . . . . . -8

-4 B = f(A,D,E) . . . . . -9

-5 B = f(A,E) . . . . . -10

-6 B = f(A) . . . . . -11

-7 H = f(A) . . . . . -12

-8 J = f(A,K) . . . . . -13

# I INTRODUCTION

## Relationship to Parent Investigation

This report covers one portion of a research project to evaluate existing NPSS structures for resistance to combined nuclear weapons effects. In the overall program, an analytical approach is taken to the evaluation of the blast protection available in existing buildings and is related to confidence levels and people-damage.

If a structure were examined to determine its response to a range of air blast overpressures, the lowest overpressure causing building damage would be that associated with window glass failure.* Glass failure is not structurally detrimental; however, if the glass fragments accelerated by air blast attain sufficient velocity, the injury to humans is of major concern. Thus, the need existed for a study of window† behavior, ranging from the overpressure causing incipient failure to the overpressure causing failure of the wall containing the window.

## Objective

The objective of this investigation was to determine the response of windows to air blast overpressures generated by nuclear explosions, including development of output useful in estimating the probability and degree of injury to humans caused by glass fragments. It was expected

---

* Failure is defined as the dislodging of pieces of glass or frame from their original position in a window.

† Even though the precise definition of a window is an opening in a wall of a building to admit light, or light and air, the term window as used herein is the opening, including one or more glass panes mounted in a sash (casement or frame).

that such an investigation could be profitably used by others to make statistical predictions of the effects of window glass failure on humans in specific situations. The following sequence of effort was used to achieve the objective:

- Development of a method to predict incipient window failure (Chapter II)
- Development of a method to predict number, weight, and spatial density of fragments (Chapter III)
- Reporting of a method to predict the velocity of glass fragments (Chapter IV)
- Use of the above methods to predict human injuries (Chapter V)
- Application of the incipient failure and fragment number, weight, spatial density, and velocity prediction procedures to 14 NFSS structures (Chapter VII)

## Types of Glass[1-3]*

Glass is basically a product of the fusion of silica. The principal compounds added during the manufacturing of window glass are soda to improve quality and lime to improve chemical durability, thus soda-lime-silica or more commonly soda-lime glass. Further classification of soda-lime glass is done on the basis of differences in the manufacturing processes. Sheet glass, one type of soda-lime glass sometimes referred to as window-sheet, is drawn from large melting tanks and annealed. Annealing is a process of controlled cooling from a suitable temperature to prevent or remove objectionable stresses. Polished plate glass, another type of soda-lime glass, is manufactured from rolled sheets that are

---

* Superscripts refer to the references listed at the end of this report.

annealed, cooled, and then mechanically ground and polished to produce flat, parallel, and bright surfaces. Float glass, a type of plate glass, is manufactured by floating molten glass on a dead flat surface of molten metal where it flows to a uniform thickness.

Sheet glass and polished plate are the most commonly used, accounting for the major portion of glass in existing buildings. Therefore, they are the two types that are conside ed in this report. Tables 1 and 2 indicate the weights, thicknesses, and maximum sizes of sheet and plate that are available commercially. Other types of glass such as tempered, safety, laminated, and wire glass are available, but they are not discussed in this report since their use is generally limited to special applications.

A design procedure for the selection of glass for windows is given in Appendix A. Common window types and sizes and associated glass sizes are given in Appendix B.

## Properties of Glass

Glass, which is both homogeneous and isotropic, qualifies as a brittle material. It conforms to elastic theory to the point of fracture; that is, either fracture occurs or the specimen returns to its original shape on release of applied loads.[2] One property agreed on in current literature is that glass always fails in tension.

The ultimate tensile strength of glass[5-7] theoretically approaches 3 million psi. Experimentally, values exceeding 1 million psi have been observed in fine fibers. That such tensile strengths are not achieved in use is evidenced by considering modulus of rupture values as approximate peak tensile strengths, then noting that the $\sigma_r$* values for glass

---

* Symbols are explained in the Notation section; only special usages will be defined in the text.

Table 1

SHEET GLASS SPECIFICATIONS

| Type | Thickness (in.) Nominal | Thickness (in.) Range | Approximate Weight per Square Foot Ounces | Approximate Weight per Square Foot Pounds | Maximum Size (in.) |
|---|---|---|---|---|---|
| Single strength | 3/32 | (.085-.097) | 19 | 1.20 | 40 X 50 |
| Double strength | 1/8 | (.117-.131) | 26 | 1.60 | 60 X 80 |
| 3/16" heavy sheet | 3/16 | (.182-.200) | 40 | 2.51 | 120 X 84 |
| 7/32" heavy sheet | 7/32 | (.212-.230) | 45 | 2.82 | 120 X 84 |
| 1/4" heavy sheet | 1/4 | (.240-.260) | 52 | 3.23 | 120 X 84 |
| 3/8" heavy sheet | 3/8 | (.356-.384) | 77 | 4.78 | 60 X 84 |
| 7/16" heavy sheet | 7/16 | (.400-.430) | 86 | 5.36 | 60 X 84 |

Source: Reference 4.

Table 2

PLATE GLASS SPECIFICATIONS

| Type | Thickness (in.) Nominal | Thickness (in.) Tolerance | Approximate Weight per Square Foot (pounds) | Maximum Size (in.) |
|---|---|---|---|---|
| Float | 1/4 | ±1/32 | 3.24 | 122 X 200 |
| Regular plate | 1/8 | ±1/32 | 1.64 | 76 X 128 |
| Regular plate | 1/4 | ±1/32 | 3.28 | 127 X 226 |
| Regular plate | 5/16 | ±1/32 | 4.10 | 127 X 226 |
| Regular plate | 3/8 | ±1/32 | 4.92 | 125 X 281 |
| Regular plate | 1/2 | ±1/32 | 6.56 | 125 X 281 |
| Regular plate | 3/4 | +1/32 -3/64 | 9.85 | 120 X 280 |
| Regular plate | 1 | +3/64 -1/16 | 13.13 | 74 X 148 |

Source: Reference 4.

laths* (Table C-1) are all under 50,000 psi, or less than 5 percent of the observed tensile strength of fibers.

Glass strength depends almost completely on flaws or defects[2,5-8] most of which are found on the surface. If glass were ductile, yielding near the flaws would tend to equalize somewhat the stress concentrations before failure. Since glass is brittle and does not yield, stress concentrations at flaws are not relieved, and failure is caused by the propagation of one of the flaws. The flaw size that causes failure or the number of flaws in a specimen is a matter of probability. This is the reason for the wide dispersion of strength values reported in tests and for the difficulty in predicting the performance of an individual specimen within reasonably close limits. Therefore, a standard deviation value or a coefficient of variation is usually reported with an average value of the ultimate tensile strength, load carrying capacity, or modulus of rupture of glass.

Flaws or defects in glass can occur in several forms:[2,3,6,9,10] submicroscopic voids, bubbles, foreign matter on the surface of reheated glass, and mechanical damage. The usable strength of plate glass is reduced by the process of grinding and polishing the surfaces.[1] Other factors affecting strength are moisture, temperature, duration of stress, age, and induced stresses. It would have been desirable to place a strength adjusting factor on each variable but such information was not found in the literature; however, a few comments on some of the variables were found. In one series of static tests on panes,[11] it was found that only 85 percent of the established failure pressure was required to cause failure when a surface scratch appeared on the tension side. Temperature variations within the range of interest of this report were found to have

---

* A standard glass lath used in determining the modulus of rupture of glass is 10 in. long, 1-1/2 in. wide, and 1/4 in. thick.

little effect on strength.[2,12] The strength of a lath or pane is sometimes reduced by as much as one-half if its edges are rounded by grinding instead of cut as they usually are.[12]

Strength values are purposely not reported here since a further discussion of strength related to glass panes is found in Chapter II. Necessary values for material properties of glass were found in several references.[2-4,6,13] The values selected for use are:

- Modulus of elasticity, $E = 10^7$ psi
- Poisson's ratio, $\nu = 0.23$
- Unit weight, $\gamma = 0.090$ lb/in$^3$ $\approx$ 155 lb/ft$^3$

Acknowledgments

The author gratefully acknowledges the assistance and guidance of H. L. Murphy, C. K. Wiehle, and L. Seaman of Stanford Research Institute. In addition, a special acknowledgment is due J. L. Bockholt of SRI for preparation of the window response computer program.

# II INCIPIENT FAILURE LOAD PREDICTION

## Discussion of Approach

This chapter was prepared to illustrate the approach taken in the development of a method for predicting the probability of glass failure in a window subjected to air blast loading caused by a nuclear explosion. Window parameters, namely glass size, thickness, and type, were assumed to be known. Loading parameters also assumed to be known were approximate weapon yield, ambient air pressure, speed of sound in undisturbed air, and clearing distance.

In work done by Schardin,[14] windows exposed to explosions were found to behave similarly to a simple oscillator. Therefore, the differential equation of motion for a single-degree-of-freedom system with no damping was selected for use in this investigation, as follows:

$$\frac{d^2x}{dt^2} = \frac{1}{m}\left[F(t) - R(x)\right] \tag{1}$$

where F(t) = a time dependent forcing function and

R(x) = a resistance-displacement function.

The first step in determining a resistance-displacement function for glass panes was to select an analytical approach. Window glass was considered in the literature as a flat plate with length and width corresponding to the exposed length and width of the pane and thickness equal to the pane thickness. Actual edge conditions are probably somewhere between simply supported and fixed; however, the frame offers little resistance to rotation[15] and lateral movement[15,16] during loading. Therefore, the assumption of simply supported edges is generally accepted

in the literature. From static tests on glass panes,[11,15,16] central deflections at failure are reported to be from one to seven times the glass thickness. Deflections of this magnitude preclude the use of small deflection plate theory, which is invalid for deflections exceeding one-half of the thickness. Thus, it seemed appropriate that window glass should be analyzed as a simply supported, rectangular plate with large deflections. The development of the incipient failure prediction method herein was accomplished for square plates for reasons that are discussed in the last section of this chapter.

In small deflection plate analysis, it is assumed that applied loads are resisted by bending stresses alone. When analyzing thin plates with deflections equal to several thicknesses but still small relative to other plate dimensions, maximum stresses may still be within the elastic strength of the material. Under these conditions, the load carrying ability is greatly enhanced by the addition of direct tensile stresses to the bending stresses.[17] The direct tensile stresses are a result of stretching the middle plane of the plate. One step beyond this type of load resistance is membrane action in which the stresses developed by stretching the middle surface carry all of the load with no bending action present.

Timoshenko[18] provides the basic approach to large deflection plate theory, which includes the strain of the middle plane as a result of bending. The result is two nonlinear differential equations for which the solution in the general case is not known. As an alternative, he provides an approximate solution originally recommended by Föppl in which small deflection plate theory and membrane theory are combined to account for bending and direct tension, respectively. The approach is discussed in the next section of this chapter.

The next step in the analysis was to have been a development of the Föppl approach such that maximum stresses occurring in the plate could be

compared with allowable stresses for glass panes. Attempts were made to establish such a procedure during this investigation but they were suspended for two reasons. First, available test data did not provide strain gage results near failure, thus an understanding of how bending and membrane stresses combine could not be obtained. Second, available breaking stress or strength data were found to be modulus of rupture data adequate for predicting probable failure of glass laths but not comparable to the stresses developed in a window pane. It was concluded that ultimate strength or breaking stress of glass panes was too elusive a quantity to be considered as a failure criterion. This conclusion is supported in the literature by Greene[19] who observed that the concept of glass strength as a material property has no real meaning or existence. Further support was derived from Mould[20] who concludes that a meaningful failure criterion for glass would be a complete theory of the kinetics of flaw behavior. (Glass strength as related to flaws was discussed in Chapter I.)

For the reasons stated above, window glass response was based on a load-deflection relationship rather than on an ultimate strength relationship. Because of the spread in glass test data, the loading with about a 50 percent probability of causing failure is reported. Sufficient test data were found to support the establishment of a load-deflection equation, the selection of a static failure load, and the estimation of a static to dynamic response transition. These subjects are discussed in subsequent sections of this chapter.

## Development of a Static Resistance Function

The approximate solution to plate problems containing a combination of bending and membrane stresses has been discussed. That solution was used to derive the following load-central deflection relationship for $\nu = 0.25$:

$$\frac{q}{E}\left(\frac{s}{h}\right)^4 = 21.9\left(\frac{w_o}{h}\right) + 31.0\left(\frac{w_o}{h}\right)^3 \qquad (2)$$

where $21.9\ w_o/h$ is the bending term and $31.0(w_o/h)^3$ is the membrane term.

Seaman[21] continued the same approach by first incorporating $\nu = 0.23$ for glass:

$$\frac{q}{E}\left(\frac{s}{h}\right)^4 = 21.7\left(\frac{w_o}{h}\right) + 28.6\left(\frac{w_o}{h}\right)^3. \qquad (3)$$

Then he corrected the membrane coefficient to allow for movable-edge rather than immovable-edge membrane action:

$$\frac{q}{E}\left(\frac{s}{h}\right)^4 = 21.7\left(\frac{w_o}{h}\right) + 12.8\left(\frac{w_o}{h}\right)^3. \qquad (4)$$

Equation 4 provides one possible form of a static load-central deflection relationship. Before accepting this equation derived from plate and membrane theory, actual test data were required for comparison and validation. Test data are limited; however, the work done by Bowles and Sugarman[16] was considered the best available because of the number of tests performed. Their failure tests, the results of which are presented in Table 3, were all performed on 40-in. square panes. Tests were designed such that failure occurred in approximately 30 seconds. The equation they derived to fit their test data is:

$$\frac{q}{E}\left(\frac{s}{h}\right)^4 = 21.9\left(\frac{w_o}{h}\right) + 2.72\left(\frac{w_o}{h}\right)^3. \qquad (5)$$

In an attempt to compare their equation with Equation 2, they suggest that "the difference in the membrane coefficient is partially due to lateral movement of the panel during loading." Table 4 contains more of their test results for loads far below failure.

The load-central deflection data for very large panes presented in Table 5 were taken from Orr.[15] Two shortcomings of these data are that

Table 3

LOAD - CENTRAL DEFLECTION FAILURE DATA FOR SQUARE PANES

| Sample | Number of Panes Tested | Mean Thickness, h (in.) | $\frac{s}{h}$* | Mean Bursting Pressure (psi) | Mean Central Deflection, $w_o$ (in.) | $\frac{q}{E}\left(\frac{s}{h}\right)^4$† | $\frac{w_o}{h}$ |
|---|---|---|---|---|---|---|---|
| 1/8-in. plate | 40 | 0.122 | 328 | 0.754 | 0.760 | 871 | 6.23 |
| 3/16-in.plate | 30 | 0.197 | 203 | 1.412 | 0.726 | 240 | 3.68 |
| 1/4-in. plate | 30 | ‡ | 160 | 1.811 | 0.651 | 119 | 2.60 |
| 3/8-in. plate | 30 | 0.373 | 107 | 3.625 | 0.610 | 47.9 | 1.64 |
| 24-oz sheet§ | 30 | 0.110 | 364 | 0.692 | 0.807 | 1210 | 7.34 |
| 32-oz sheet§ | 30 | 0.158 | 253 | 1.369 | 0.870 | 562 | 5.51 |
| 3/16-in. sheet | 30 | 0.195 | 205 | 1.910 | 0.860 | 338 | 4.41 |

* s = 40 inches for all samples.

† $E = 10^7$ psi.

‡ Since no value was given, h = 0.250 in. was assumed.

§ This work was done in England where pane thicknesses differ slightly from the U.S. thicknesses shown in Table 1.

Source: Data from Reference 16 appear in columns 1, 2, 3, 5, and 6. Calculations based on the data (Reference 21) were added in columns 4, 7, and 8.

Table 4

STRESS DATA

| Sample | Pressure (psi) | $\frac{w_o}{h}$ | Measured Central Stress (psi) Upper Surface | Measured Central Stress (psi) Lower Surface | Bending Stress (psi) | Membrane Stress (psi) | $\frac{q}{E}\left(\frac{s}{h}\right)^{4}$ ** |
|---|---|---|---|---|---|---|---|
| 1/8-in. plate | 0.05 | 1.61 | 810 | -380 | 595 | 215 | 57.8 |
| | 0.1 | 2.40 | 1210 | -380 | 795 | 415 | 115.6 |
| | 0.15 | 2.98 | 1480 | -320 | 900 | 580 | 173.3 |
| | 0.2 | 3.43 | 1700 | -200 | 950 | 750 | 231.1 |
| | 0.25 | 3.78 | 2880 | | | | 288.9 |
| 3/16-in. sheet | 0.05 | 0.59 | 670 | -485 | 577 | 93 | 8.8 |
| | 0.10 | 0.92 | 1150 | -750 | 950 | 200 | 17.7 |
| | 0.15 | 1.19 | 1520 | -925 | 1222 | 298 | 26.6 |
| | 0.2 | 1.41 | 1830 | -1030 | 1430 | 400 | 35.4 |
| | 0.25 | 1.62 | 2120 | -1070 | 1595 | 525 | 44.3 |
| | 0.3 | 1.81 | 2370 | -1080 | 1725 | 645 | 53.1 |
| | 0.35 | 1.96 | 2580 | -1075 | 1827 | 753 | 62.0 |
| 1/4-in. plate | 0.1 | 0.42 | 710 | -630 | 670 | 40 | 6.6 |
| | 0.2 | 0.70 | 1400 | -1080 | 1240 | 160 | 13.1 |
| | 0.3 | 0.93 | 2000 | -1410 | 1705 | 295 | 19.7 |
| | 0.4 | 1.13 | 2510 | -1640 | 2075 | 435 | 26.2 |
| | 0.5 | 1.32 | 2930 | -1805 | 2367 | 563 | 32.8 |
| | 0.6 | 1.48 | 3300 | -1930 | 2615 | 685 | 39.3 |
| | 0.7 | 1.63 | 3640 | -2010 | 2825 | 815 | 45.9 |
| | 0.8 | 1.76 | 3940 | -2040 | 2990 | 950 | 52.4 |
| 3/8-in. plate | 0.2 | 0.25 | 640 | -550 | 595 | 45 | 2.6 |
| | 0.4 | 0.41 | 1270 | -1070 | 1170 | 100 | 5.3 |
| | 0.6 | 0.57 | 1910 | -1550 | 1730 | 180 | 7.9 |
| | 0.8 | 0.70 | 2540 | -2000 | 2270 | 270 | 10.6 |
| | 1.0 | 0.81 | 3120 | -2360 | 2740 | 380 | 13.2 |
| | 1.2 | 0.92 | 3690 | -2650 | 3170 | 520 | 15.9 |
| | 1.4 | 1.03 | 4010 | | | | 18.5 |
| | 1.6 | 1.12 | 4530 | | | | 21.2 |
| | 1.8 | 1.21 | 5040 | | | | 23.8 |
| | 2.0 | 1.30 | 5570 | | | | 26.4 |
| | 2.20 | 1.38 | 6060 | | | | 29.1 |

* Mean values of h presented in Table 3 were used since thickness values were not given with these data.

Source: Data from Reference 16 appear in columns 1 through 5. Calculations assuming elastic theory (Reference 21) appear in Columns 6, 7, and 8.

Table 5

FAILURE LOAD - CENTRAL DEFLECTION DATA FOR LARGE PLATE GLASS PANES

| Glass Size (in.) | Average Thickness, h (in.) | Pane Area ($in^2$) | $\frac{\sqrt{A}}{h}$ or $\frac{s^*}{h}$ | Failure Pressure (psi) | Maximum Deflection, $w_o$ (psi) | $\frac{q}{E}\left(\frac{s}{h}\right)^4$ | $\frac{w_o}{h}$ |
|---|---|---|---|---|---|---|---|
| 82 X 82 | 0.2373 | 6724 | 345.6 | 0.3628 | 1.200 | 517.3 | 5.06 |
| | 0.240 | 6724 | 341.7 | 0.3602 | 1.189 | 490.8 | 4.95 |
| | 0.303 | 6724 | 270.6 | 0.5601 | 1.200 | 300.4 | 3.96 |
| | 0.301 | 6724 | 272.4 | 0.3901 | 1.000 | 214.9 | 3.32 |
| 82 X 102 | 0.2344 | 8364 | 390.2 | 0.2726 | 1.300 | 631.7 | 5.55 |
| | 0.2453 | 8364 | 372.8 | 0.2501 | 1.200 | 483.2 | 4.89 |
| | 0.3045 | 8364 | 300.3 | 0.3756 | 1.200 | 305.6 | 3.94 |
| | 0.305 | 8364 | 299.8 | 0.3751 | 1.200 | 303.2 | 3.93 |
| 82 X 120 | 0.242 | 9840 | 409.9 | 0.2258 | 1.400 | 637.4 | 5.78 |
| | 0.239 | 9840 | 415.0 | 0.1638 | 1.200 | 486.1 | 5.02 |
| | 0.303 | 9840 | 327.4 | 0.3094 | 1.311 | 355.4 | 4.33 |
| | 0.304 | 9840 | 326.3 | 0.3056 | 1.300 | 346.4 | 4.28 |
| | 0.369 | 9840 | 268.8 | 0.3898 | 1.200 | 203.6 | 3.25 |
| | 0.372 | 9840 | 266.6 | 0.4017 | 1.200 | 203.1 | 3.23 |
| 72 X 120 | 0.114 | 8640 | 815.4 | 0.1161 | 1.400 | 5131.4 | 12.28 |

* All panes were analyzed as squares. In the case of a rectangular pane, s is the side of a square having an area, A, equal to the actual area of the rectangle.

Source: Data from Reference 15 appear in columns 1, 2, and 6. Original data reported in psf are presented in psi in column 5. Calculations using the data (Reference 21) appear in columns 3, 4, 7, and 8.

each value represents only a single test and that the panes were very slowly loaded with several 5- to 25-minute breaks in the loading for measurements to be taken. The tests were performed on rectangular and square plates with aspect ratios between 0.6:1 and 1:1.

Seaman[21] used the nondimensional load values, $(q/E)(s/h)^4$, and the nondimensional deflection values, $w_o/h$, of Tables 3, 4, and 5 to establish the following static load-central deflection relationship for square panes at rupture:

$$\frac{q}{E}\left(\frac{s}{h}\right)^4 = 21.7\left(\frac{w_o}{h}\right) + 2.80\left(\frac{w_o}{h}\right)^3. \qquad (6)$$

Equation 6 and the data of Tables 3, 4, and 5 are shown in Figure 1. Unsuccessful attempts to obtain a better fit of the data were made in this investigation by allowing adjustment of the bending coefficient as well as the membrane coefficient. Also, curve fitting procedures were applied so that other equations fitting the data might be studied for validity. A better fit was hard to find. Also, it was futile to give meaning to the results of the curve fitting equations. Therefore, Equation 6 was adopted for use as the static resistance function since it displayed a direct relationship to accepted theory.

## Static Failure Load Determination

Equation 6 provided a relationship between applied static load and central deflection for square panes of either plate or sheet glass. To use the equation, the static failure load (or deflection) for each specific case of area, thickness, and type of glass was required. Charts 1 and 4 of Reference 22 were selected for this purpose. The charts, with the following modifications, appear as Figures 2 and 3:

- A scale showing the load in psi was added

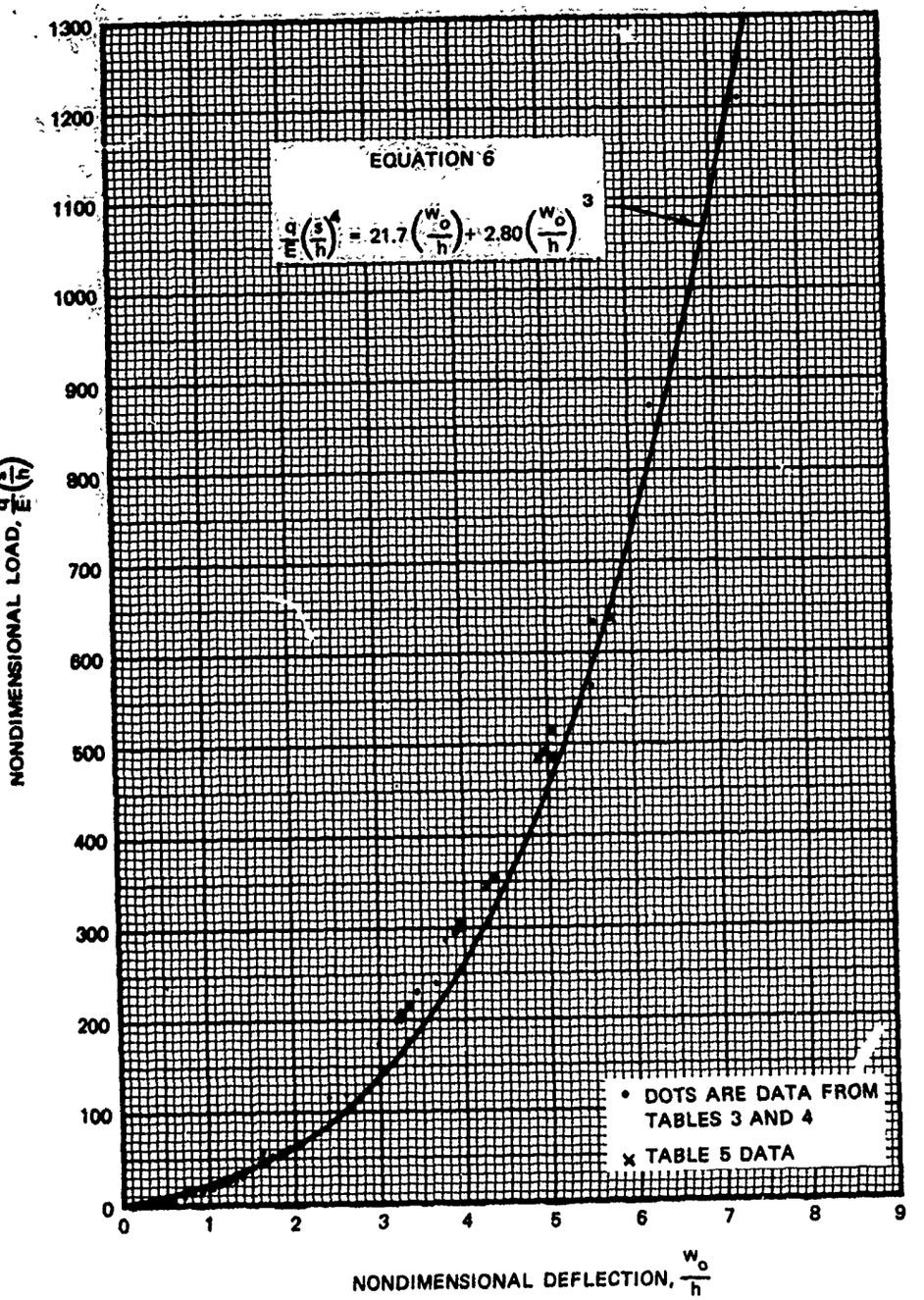


FIG. 1 STATIC LOAD VERSUS CENTRAL DEFLECTION FOR SQUARE PANES OF SHEET AND PLATE GLASS

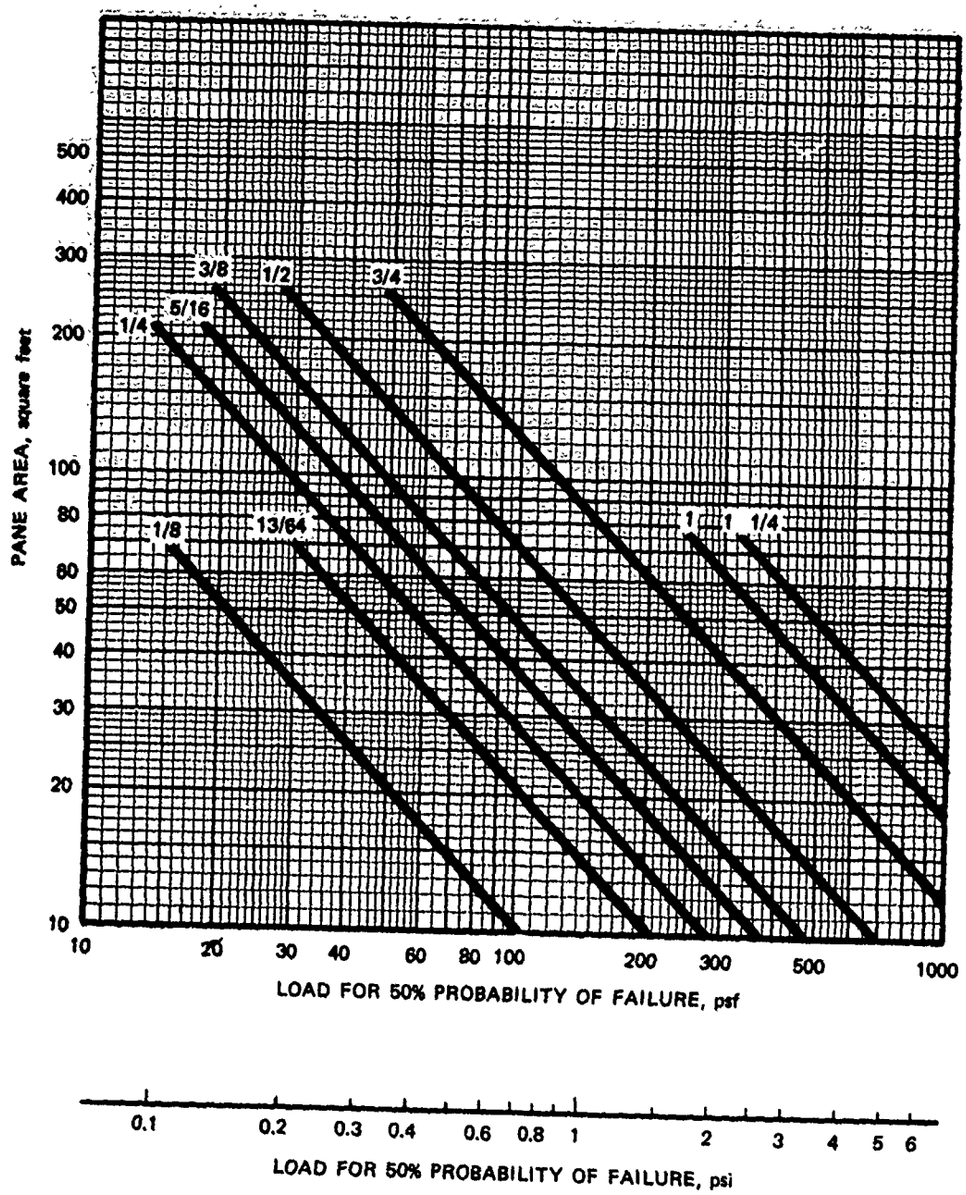


SOURCE: Adapted from Ref. 22.

FIG. 2 PLATE GLASS FAILURE LOADS FOR TIME TO FAILURE OF 60 SECONDS

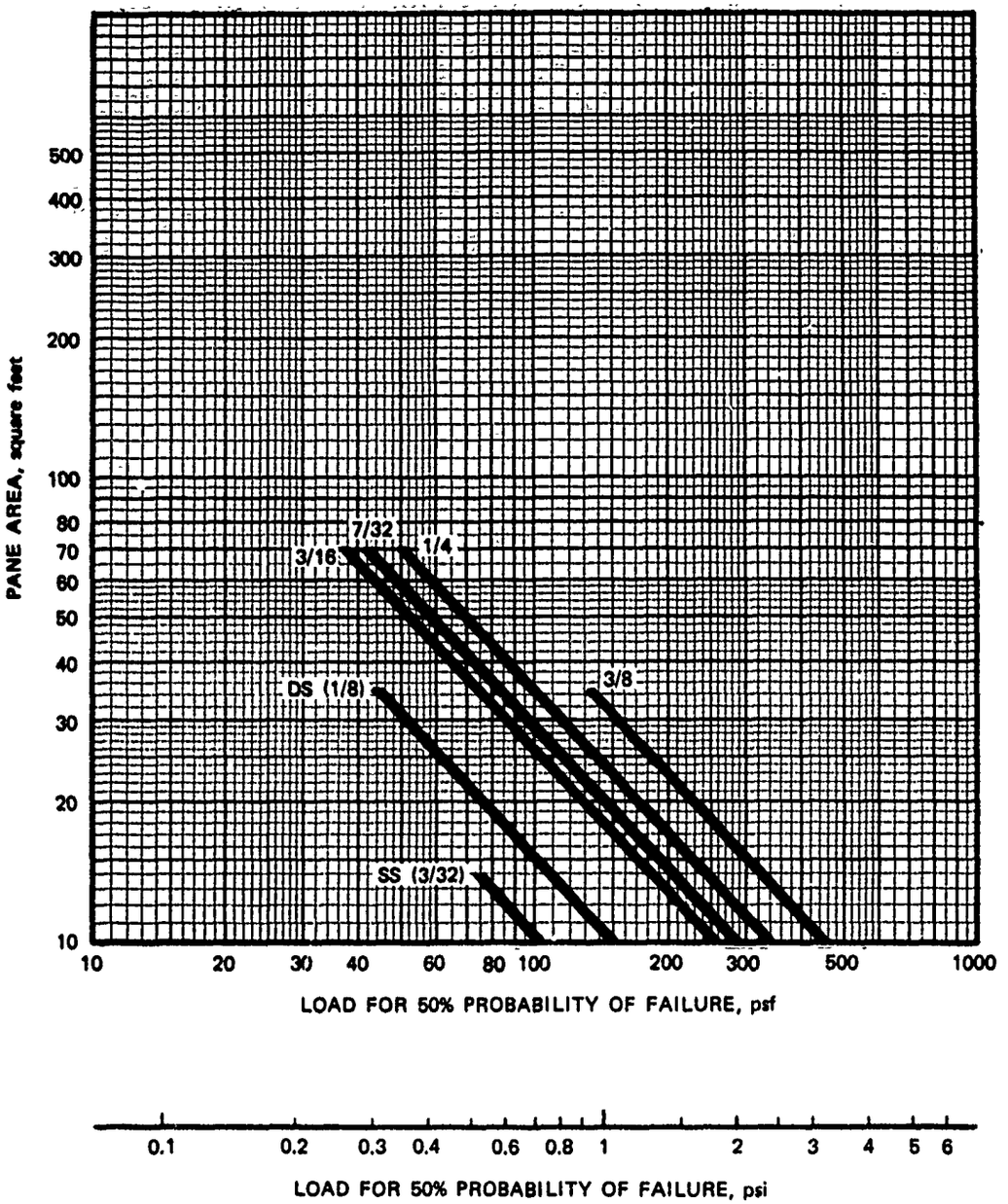


SOURCE: Adapted from Ref. 22.

FIG. 3 SHEET GLASS FAILURE LOADS FOR TIME TO FAILURE OF 60 SECONDS

- All load values were multiplied by 2.5 to remove the factor of safety, thus providing the load for 50 percent probability of failure

The figures in their original form were developed empirically to represent the behavior of plate and sheet glass as it exists in service. Orr's results were used for values in the size range above 10 square feet. U.S. Bureau of Standards' data (similar to those shown in Appendix C) were used for points associated with a glass area of 0.1 square foot. Data from the two sources with like thicknesses were connected by smooth curves and then "adjusted rationally to conform to data and to experience available in the intermediate area."[23]

Curve fitting procedures were applied in this study to obtain equations describing the information shown graphically in Figures 2 and 3. For plate glass (Figure 2)

$$q_{sf} = \frac{18,300}{A} h^{1.38} \qquad (7)^*$$

and for sheet glass (Figure 3)

$$q_{sf} = \frac{2.5}{A} (-336 + 8530\ h - 7710\ h^2). \qquad (8)^*$$

Equations 7 and 8 were used to predict the 50 percent probable static failure loads to be used in conjunction with the response curve shown in Figure 1.

## Transition from Static to Dynamic Response

The fact that the ultimate tensile strength of glass is inversely proportional to the length of time that the load is acting has been

---

* The computer program routinely provided six significant figures that were used in subsequent and related calculations. After all such work was completed, values to be shown in the report were rounded to three significant figures, arbitrarily and not to imply any specific degree of accuracy in predicting glass pane behavior.

studied before.[24] The relationship developed between strength and time duration of load was based on tests[6] of 1/4-in. glass rods. In glass plates, ". . . a failure always originates at some form of imperfection on the surface or on the cut edge. The larger the plate, or the greater the area stressed, the greater the possibility of an imperfection being present and the lower the stress required to cause failure."[15] On this basis, it was decided that an extrapolation of 1/4-in. glass rod strength to glass pane strength was unwarranted for this study.

Data relating breaking stress to various loading rates[22] were used to develop Figure 4. The breaking stress values were normalized to the stress corresponding to a 60-second time to failure since Equations 7 and 8 were based on that time to failure. It was assumed that the relationship between load and stress is such that a factor selected from Figure 4 could be applied directly to Equations 7 and 8. Thus, the increased load carrying capacity of glass panes subjected to dynamic instead of static loads could be taken into consideration. The curve fitting equation of the six types tried that best fits the data was

$$\frac{\sigma}{\sigma_o} = 1.37\ t^{-0.0653} \qquad (9)$$

where $\sigma_o$ indicates the stress with a time to failure of 60 seconds.

Use of the computer program described later in this chapter revealed a time to incipient failure of between 10 and 40 milliseconds for most windows. Very large panes with thicknesses greater than 1/4 in. had higher times to incipient failure. However, using 10 to 40 milliseconds as the predominant range of interest led to selection of 1.8 as the ratio of dynamic to static breaking strength for use in this study. Thus, Equation 7 for plate glass becomes

$$q_{df} = \frac{33,000}{A}\ h^{1.38} \qquad (10)^*$$

---

* The footnote appearing on page 18 applies to this equation also.

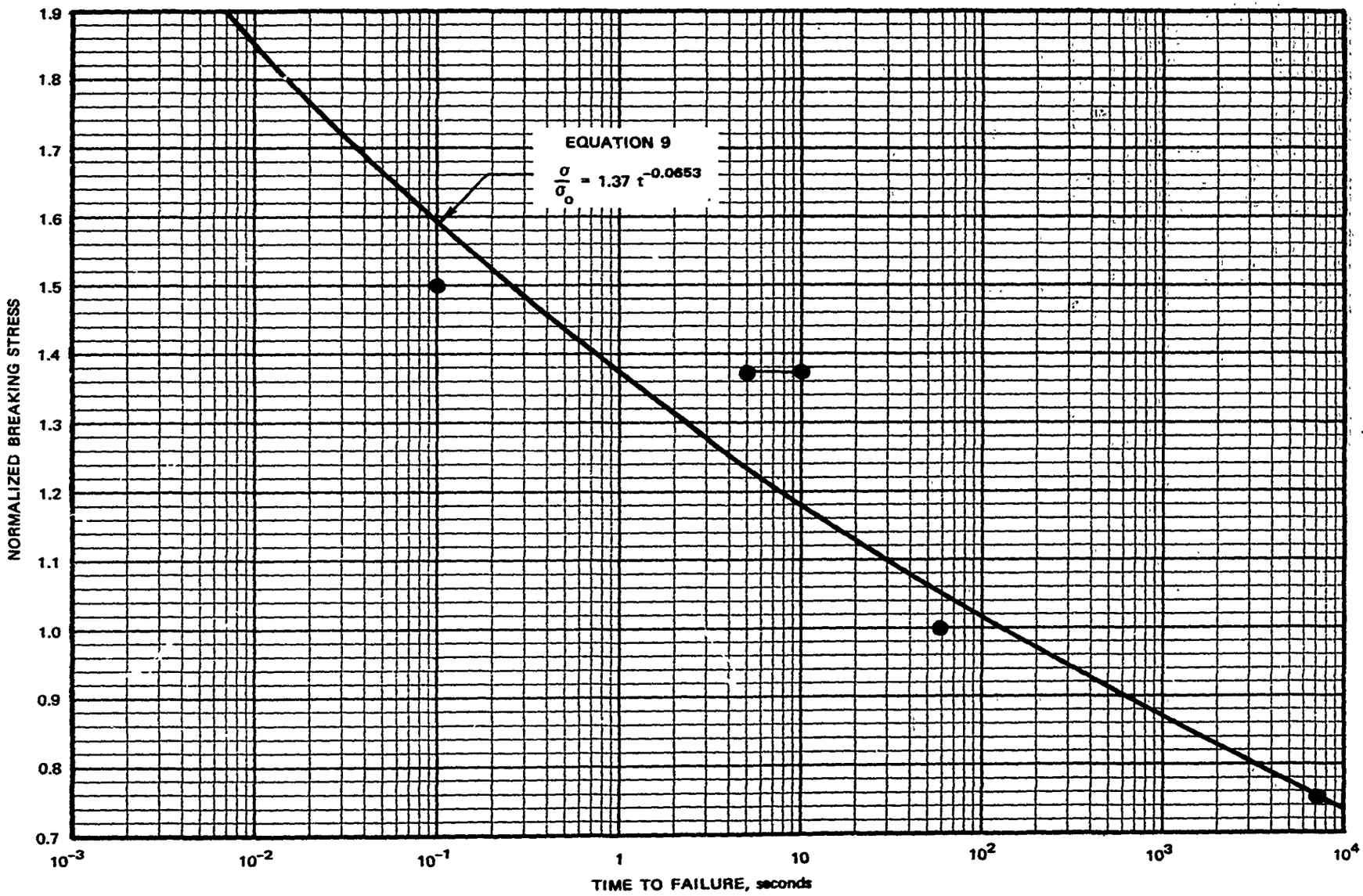


FIG. 4 EFFECT OF LOADING RATE ON NORMALIZED BREAKING STRESS

and Equation 8 for sheet glass becomes

$$q_{df} = \frac{4.5}{A} (-336 + 8530\,h - 7710\,h^2). \qquad (11)^*$$

It became possible at this point to describe the dynamic response of windows to air blast loading by using Equation 6 with the failure loads provided by Equations 10 and 11.

## Air Blast Loading

The loading function selected was the pressure-time relationship shown in Figure 5, which describes the interaction of a nuclear blast wave with the front face of a closed rectangular structure. Even though windows are located randomly and overpressures vary with location on a wall, this average front-face loading was chosen as the pressure felt by any window in a wall facing an explosion. The equations describing front-face loading are:[25]

$$p_r = 2\,p_{so}\left(\frac{7\,P_o + 4\,p_{so}}{7\,P_o + p_{so}}\right) \qquad (12)$$

$$p_{do} = \frac{5}{2}\left(\frac{p_{so}^2}{7\,P_o + p_{so}}\right) \qquad (13)$$

$$p_s = p_{so}\left(1 - \frac{t}{t_o}\right) e^{-t/t_o} \qquad (14)$$

$$p_d = p_{do}\left(1 - \frac{t}{t_u}\right)^2 e^{-2t/t_u} \qquad (15)$$

$$U = c_o\left(1 + \frac{6\,p_{so}}{7\,P_o}\right)^{1/2} \qquad (16)$$

$$t_c = \frac{3\,S}{U} \qquad (17)$$

---

* The footnote appearing on page 18 applies to this equation also.

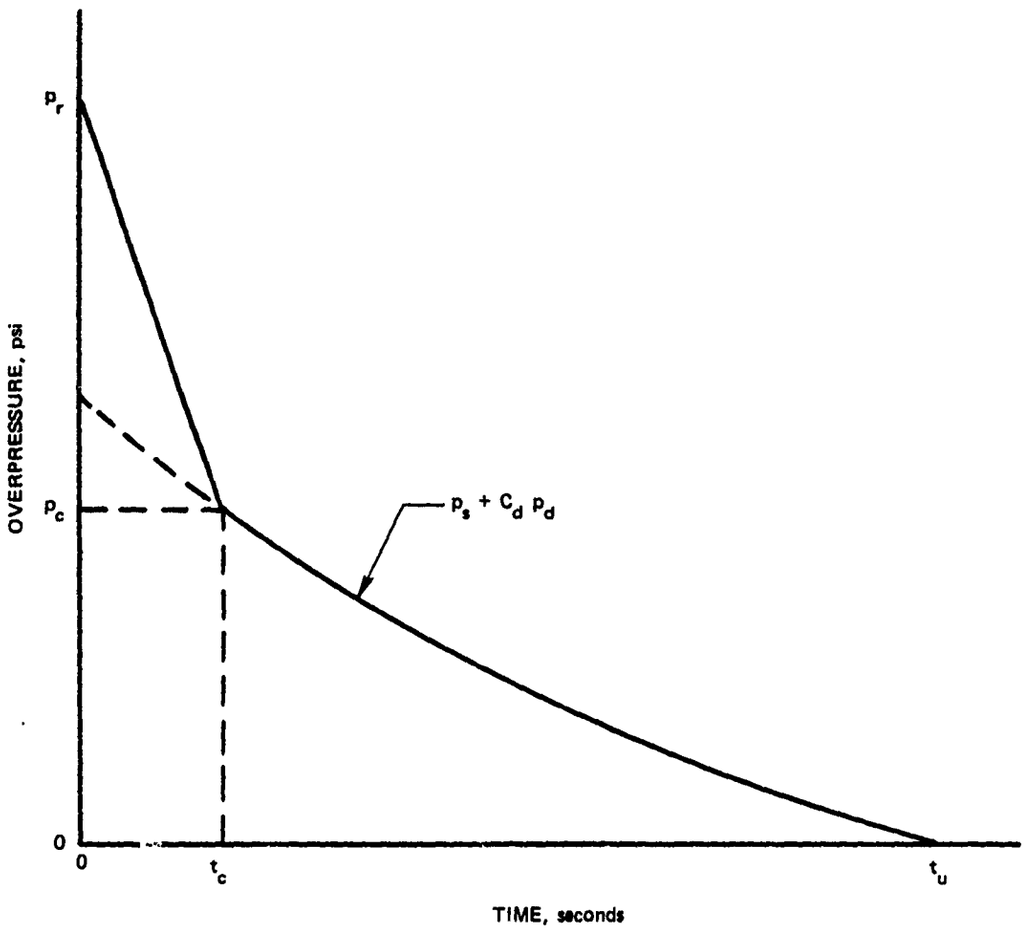


FIG. 5 FRONT-FACE AIR BLAST LOADING

$$p_c = p_s + C_d p_d \tag{18}$$

$$t_o = \frac{W^{1/3}}{(2.2399 + 0.1886\ p_{so})} \cdot \tag{19}*$$

The following assumptions were made concerning the loading:

- A linear decay from peak reflected pressure to stagnation pressure
- No back-iace loading
- $t_u = t_o$
- $C_d = 1.0$

The equations describing the loading function shown in Figure 5 are:

$$p(t) = \frac{t_c - t}{t_c}(p_r - p_c) + p_c \qquad 0 \le t \le t_c \tag{20}$$

$$p(t) = p_s + C_d p_d \qquad t_c \le t \le t_o \tag{21}$$

$$p(t) = 0 \qquad t \ge t_o \cdot \tag{22}$$

The loading function for windows parallel to a blast wave (windows in side walls) was obtained by letting S = 0, leading to $t_c = 0$ (Equation 17), thus causing Equation 20 to be eliminated from any computations. Because of the negligible effect of the stagnation term, $C_d p_d$ (Equation 21), at very low overpressures, the drag coefficient, $C_d$, was not changed[25] from 1.0 to -0.4 in loading calculations for windows in side walls.

Window Pane Response to Nuclear Blast Wave Loading

A computer program was developed to solve Equation 1 for the incipient failure pressure of a square pane of either sheet or plate glass subjected to nuclear blast wave loading. A flow chart and the FORTRAN program

---

* Equation 19 was taken from Reference 26.

are presented in Figure 6 and Table 6, respectively.* The resistance-displacement subroutine combines Equation 6 with either Equation 10 or 11 depending on an input statement specifying glass type. Thus, the R(x) portion of Equation 1 is provided. The F(t) portion of Equation 1 is contained in the applied force-time subroutine for which Equations 12 through 22 were used to create a load-time function (Figure 5) given weapon yield, ambient pressure, speed of sound, and clearing distance.

Rather than attempting an exact solution, Equation 1 is solved numerically within the program by applying the Newmark $\beta$ Method.[27] The method entails solving the differential equation in short time increments using the values at the end of one increment for the start of the next increment. The program was developed using a value for $\beta$ that results in a linear variation of acceleration within each increment. The incipient failure pressure is found by an interval halving routine that narrows the size of the interval between a load that causes failure and one that does not.

## Incipient Failure Prediction Results

A 1 Mt weapon was selected to determine the blast wave positive phase duration; however, pane incipient failure pressures were found to be insensitive to positive phase duration over an examined weapon yield range of 1 kt to 100 Mt. Other parameters fixed in solving for incipient failure pressures were an ambient atmospheric pressure of 14.7 psi and a speed of sound in undisturbed air of 1120 feet per second. A clearing

---

* The computer program was originally developed by a colleague, J. L. Bockholt, for another OCD project involving the analysis of walls. Program modifications for use herein were made by Bockholt.

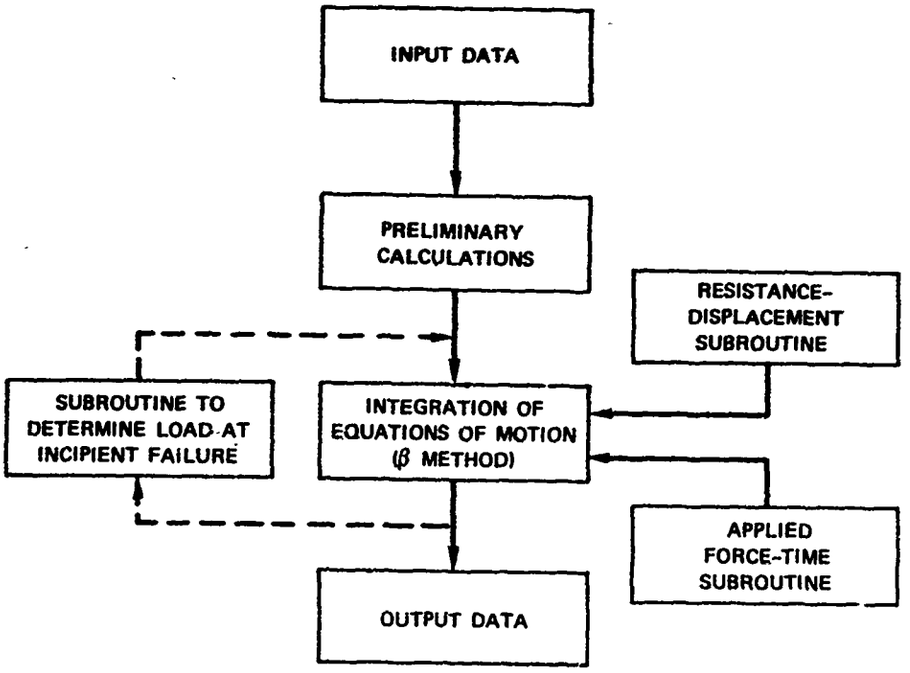


FIG. 6 COMPUTER PROGRAM FLOW CHART

Table 6

COMPUTER PROGRAM

```
100* ANALYSIS ØF WINDØWS SUBJECTED TØ DYNAMIC LATERAL LØADS
105*
110 60 FØRMAT("0INPUT SIDE,H,GLASSTYPE")
115 61 FØRMAT("0GLASSTYPE NØT RECØGNIZED -- RETYPE")
120 62 FØRMAT("0PRØPERTIES ØF THE WINDØW BEING ANALYZED ARE AS FØLLØWS:"
125 & /,5X,"LENGTH ØF SIDE =",F7.2," INCHES    THICKNESS =",F7.4,
130 & " INCHES",/,5X,"TYPE ØF GLASS =",2A4,11X,"STATIC STRENGTH =",
135 & F6.3," PSI")
140 65 FØRMAT(F6.3,F7.3,F12.2,F12.3,F14.5)
145 66 FØRMAT("0IS TIME HISTØRY ØF THE WINDØW DESIRED (YES=1,NØ=0)")
150 68 FØRMAT("0THE TIME HISTØRY ØF THE WINDØW IS AS FØLLØWS:",//,
155 &" TIME   LØAD   ACCELERATIØN   VELØCITY   DISPLACEMENT")
160 70 FØRMAT("0IS SPECIFIC LØAD, INCLUDING PRESSURE, TØ BE GIVEN (INPUT
165 & 0)"/" ØR IS INCIPIENT CØLLAPSE PRESSURE TØ BE FØUND (INPUT 1)")
170 71 FØRMAT("0THE VALUES ØF THE PARAMETERS AT THE FINAL TIME INTERVAL
175 & ARE:"/"  T =",F6.3," SECØNDS            P =",F7.3," LB/IN."
180 &      /"  A =",F9.2," IN./SEC/SEC    V =",F9.3," IN./SEC"
185 &     /"  Y =",F7.4," IN.")
190 72 FØRMAT(1HØ,7("----------"))
195 73 FØRMAT("0WINDØW DID NØT FAIL - MAXIMUM DEFLECTIØN REACHED AT",
200 & F6.3," SECØNDS")
205 74 FØRMAT("0WINDØW FAILED AT",F7.3," SECØNDS")
210*
215 CØMMØN YI,QT,ADH4,E,AREA,PF,TIME,P,L1
220 DIMENSIØN A(100),V(100),Y(100),T(100),PL(100)
225 REAL MASS
230 ALPHA GLASSTYPE,LETTER
235*
240*  INPUT DATA
245 5 PRINT 60
250 INPUT,SIDE,H,GLASSTYPE
255 PRINT 70
260 INPUT,L1
265 CALL FØRCE(2)
270*
275*  DETERMINE VALUES ØF ØFTEN USED VARIABLES
280 E=10000000.0
285 DELTA=0.001
290 AREA=SIDE*SIDE
295 MASS=0.09*AREA*H/386.07
300 ZKLM=0.67
305 PFMAX=0; PFMIN=0
310 ADH4=(SIDE/H)**4
315 13 IF(GLASSTYPE.EQ."HEET")GØTØ 10
320 IF(GLASSTYPE.EQ."LATE")GØTØ 9
325 PRINT 61; INPUT,GLASSTYPE; GØ TØ 13
```

Table 6 (Continued)

```
330*
335 9 PFSTAT=18309.1*H**1.37849/AREA
340 LETTER="   P"; GØTØ 25
345*
350* PLATE GLASS
355 10 PFSTAT=2.5*(-336.532+8532.32*H-7706.59*H*H)/AREA
360 LETTER="   S"
365 25 PRINT 62,SIDE,H,LETTER,GLASSTYPE,PFSTAT
370*  80% INCREASE IN DYNAMIC STRENGTH ØVER STATIC STRENGTH
375 PFDYN=1.8*PFSTAT
380 IF(L1.EQ.0)GØTØ 23
385*  INITIAL VALUES FØR DETERMINING INCIPIENT CØLLAPSE PRESSURE
390 PF=PFDYN
395 GØ TØ 20
400 16 PF=(PFMAX+PFMIN)/2.0
405 20 CALL FØRCE(3)
410*
415*  INITIALIZE VALUES FØR BETA METHØD (BETA=1/6)
420 23 TIME=0
425 T(1)=0
430 I=1
435 DELTA=0.001
440 CALL FØRCE(1)
445 PL(1)=P
450 PT=P*AREA
455 Y(1)=0; V(1)=0
460 V(1)=0
465 A(1)=PT/(MASS*ZKLM)
470*
475*  PRØCEDURE FØR ALL SUBSEQUENT INTERVALS
480 1 I=I+1
485 TIME=TIME+DELTA
490 8 T(I)=TIME
495 11 KØUNT=0
500 A(I)=A(I-1)
505 Y(I)=Y(I-1)+DELTA*V(I-1)+DELTA*DELTA*A(I-1)/2.0
510 XI=Y(I)/H
515 CALL FØRCE (1)
520 PL(I)=P
525 PT=P*AREA
530 2 CALL RESIST
535*
540* SAFEGUARD TØ PRØTECT AGAINST ANY IRREGULARITIES IN PRØGRAM
545 KØUNT=KØUNT+1
550 IF(KØUNT.LE.10)GØTØ4
555 DELTA=DELTA/2.0
560 TIME=TIME-DELTA
```

Table 6 (Continued)

```
565 ICHECK=ICHECK+1
570 IF(ICHECK.GT.3)GØTØ 999
575 GØTØ 8
580*
585 4 ANEW=(PT-QT)/(MASS*ZKLM)
590 ADELTA=ANEW-A(I)
595 Y(I)=Y(I)+DELTA*DELTA*ADELTA/6.0
600 XI=Y(I)/H
605 A(I)=ANEW
610* CHECK TØ SEE IF ASSUMED VALUE ØF ACCELRATIØN IS WITHIN
615*  DESIRED ACCURACY ØF CALCULATED VALUE
620 IF(ABS(ADELTA/ANEW).GT.0.01)GØTØ 2
625 3 V(I)=V(I-1)+DELTA*(A(I)+A(I-1))/2.0
630* CHECK TØ DETERMINE IF MAXIMUM DEFLECTIØN HAS BEEN REACHED
635* IF SØ WALL DID NØT FAIL
640 15 IF(Y(I).LE.Y(I-1))GØTØ 6
645* CHECK TØ SEE IF WALL STILL HAS RESISTANCE- IF NØT,WALL FAILED
650 IF(PFDYN*AREA-QT)7,7,1
655*
660* INTERVAL HALVING PRØCEDURE TØ FIND LØAD CAUSING INCIPIENT FAILURE
665* WALL DID NØT FAIL - SET PFMIN TØ PF
670 6 IFAIL=0
675 IF(L1.EQ.0)GØTØ 18
680 PFMIN=PF
685 IF(PFMAX)19,19,17
690 19 PF=2.0*PF
695 GØTØ 20
700* WALL FAILED - SET PFMAX TØ PF
705 7 IFAIL=1
710 IF(L1.EQ.0)GØTØ 18
715 PFMAX=PF
720* CHECK TØ SEE IF INTERVAL IS WITHIN DESIRED ACCURACY
725 17 IF((PFMAX-PFMIN)/PFMAX.GT.0.01)GØTØ 16
730*
735* ØUTPUT DATA
740 18 CALL FØRCE(4)
745 IF(IFAIL.EQ.0)PRINT 73,TIME
750 IF(IFAIL.EQ.1)PRINT 74,TIME
755 PRINT 66
760 INPUT,M
765 IF(M)22,22,21
770 21 PRINT 68
775 PRINT 65,(T(J),PL(J),A(J),V(J),Y(J),J=1,I)
780 GØTØ 12
785 22 PRINT 71,T(I),PL(I),A(I),V(I),Y(I)
790 12 PRINT 72
```

Table 6 (Continued)

```
795 GØTØ 5
800 999 STØP; END
1000*
1005 SUBRØUTINE RESIST
1010*  THIS SUBRØUTINE DETERMINES THE DYNAMIC RESISTANCE ØF THE WINDØW
1015 CØMMØN XI,QT,ADH4,E,AREA,PR,TIME,P,L1
1020 QT=AREA*(E/ADH4)*(21.7*X1+2.8*XI**3)
1025 RETURN; END
1030*
2000 SUBRØUTINE FØRCE (IENTRY)
2005*  THIS SUBRØUTINE DETERMINES THE LØAD ACTING ØN THE WINDØW
2010 CØMMØN XI,QT,ADH4,E,AREA,PR,TIME,P,L1
2015 GØTØ(1,2,3,4),IENTRY
2020*
2025* DETERMINE LØAD ACTING ØN THE WALL
2030 1 IF(TIME-TC)101,102,102
2035 101 P=PC+(TC-TIME)*(PR-PC)/TC
2040 RETURN
2045 102 IF(TIME-TØ)103,104,104
2050 103 P=PSØ*(1-TIME/TØ)*EXP(-TIME/TØ)+PDØ*(1-TIME/TØ)**2
2055 &      *EXP(-2*TIME/TØ)
2060 RETURN
2065 104 P=0
2070 RETURN
2075*
2080*  INPUT LØAD DATA
2085 2 PRINT 630
2090 IF(L1.EQ.0)GØTØ 205
2095 INPUT, W,PØ,CØ,S
2100 RETURN
2105 205 PRINT 655
2110 INPUT,W,PØ,CØ,S,PSØ
2115 PR=2.0*PSØ*(7.0*PØ+4.0*PSØ)/(7.0*PØ+PSØ)
2120 IF(S.EQ.0)PR=PSØ
2125 GØTØ 305
2130*
2135*  DETERMINE LØAD PRØPERTIES FØR GIVEN PEAK PRESSURE
2140 3 PSØ=(PR-14.0*PØ+SQRT(196.0*PØ*PØ+196.0*PØ*PR+PR*PR))/16.0
2145 302 IF(S.EQ.0)PSØ=PR
2150 305 PDØ=2.5*PSØ*PSØ/(7.0*PØ+PSØ)
2155 U=CØ*SQRT(1.0+6.0*PSØ/(7.0*PØ))
2160 TC=3.0*S/U
2165 TØ=W**0.3333/(2.2399+0.1886*PSØ)
2170 PC=PSØ*(1.0-TC/TØ)*EXP(-TC/TØ)+PDØ*(1.0-TC/TØ)**2*EXP(-2.0*TC/TØ)
2175 RETURN
2180*
```

Table 6 (Concluded)

```
2185*  0UTPUT L0AD DATA F0R L0AD ACTING 0N WALL
2190 4 IF(L1.EQ.0)G0T0 390
2195 PRINT 660
2200 G0T0 395
2205 390 PRINT 665
2210 395 C0NTINUE
2215 400 PRINT 600, W,P0,C0,S,U,T0,PR,PS0,PD0,TC
2220 RETURN
2225*
2230 600 F0RMAT(10X,"W =",F8.1," KT   P0 =",F6.2," PSI     C0 =",F6.1,
2235 &" FPS",/,10X,"S =",F6.1," FT     U =",F7.1," FPS    T0 =",F6.3,
2240 &" SEC",/,9X,"PR =",F7.3," PSI  PS0 =",F7.3," PSI   PD0 =",F7.3,
2245 &" PSI",/,9X,"TC =",F7.4," SEC")
2250 630 F0RMAT(" INPUT W,P0,C0,S")
2255 655 F0RMAT("&,PS0")
2260 660 F0RMAT("0L0AD CAUSING INCIPIENT FAILURE IS AS F0LL0WS:")
2265 65 F0RMAT("0PR0PERTIES 0F L0AD ACTING 0N WIND0W ARE AS F0LL0WS:")
2270 777 RETURN; END
```

distance of 20 feet was used in calculating front-face loading. That distance was established from a series of computer runs demonstrating that the incipient failure overpressure was influenced very little when the clearing distance exceeded 20 feet. Incipient failure predictions, using the above-mentioned parameters, are presented in Figures 7 and 8 for plate glass and Figures 9 and 10 for sheet glass. Figures 7 and 9 relate to side-wall loading and Figures 8 and 10 relate to front-face loading.

A statistically normal strength distribution and a coefficient of variation of 25 percent were assumed in Reference 22 from which Figures 2 and 3 were prepared. The 50 percent probability of failure stated in conjunction with those figures has been carried through to Figures 7 through 10. The maximum pane areas shown in Figures 7 through 10 were limited to those allowed by the Uniform Building Code[28] when designing for the least wind load, i.e., 15 pounds per square foot. More information on allowable pane sizes is found in Appendix A.

The development in this chapter leading to Figures 7 through 10 was for square panes. It is believed that use of the figures is valid for panes with aspect ratios as low as 1/3. The strongest argument in support of this statement is that the information used in preparing Figures 2 and 3 is valid for any pane with an aspect ratio exceeding 1/3. Furthermore, extensive development of an analytical method for rectangular panes did not seem warranted. The membrane term for square panes was shown to be significantly changed by applying test data to the analytical equations. Insufficient test data were available to make a similar comparison had the development herein been for rectangular panes. Finally, the data in Table 5, which include some rectangular pane data, plotted well in Figure 1.

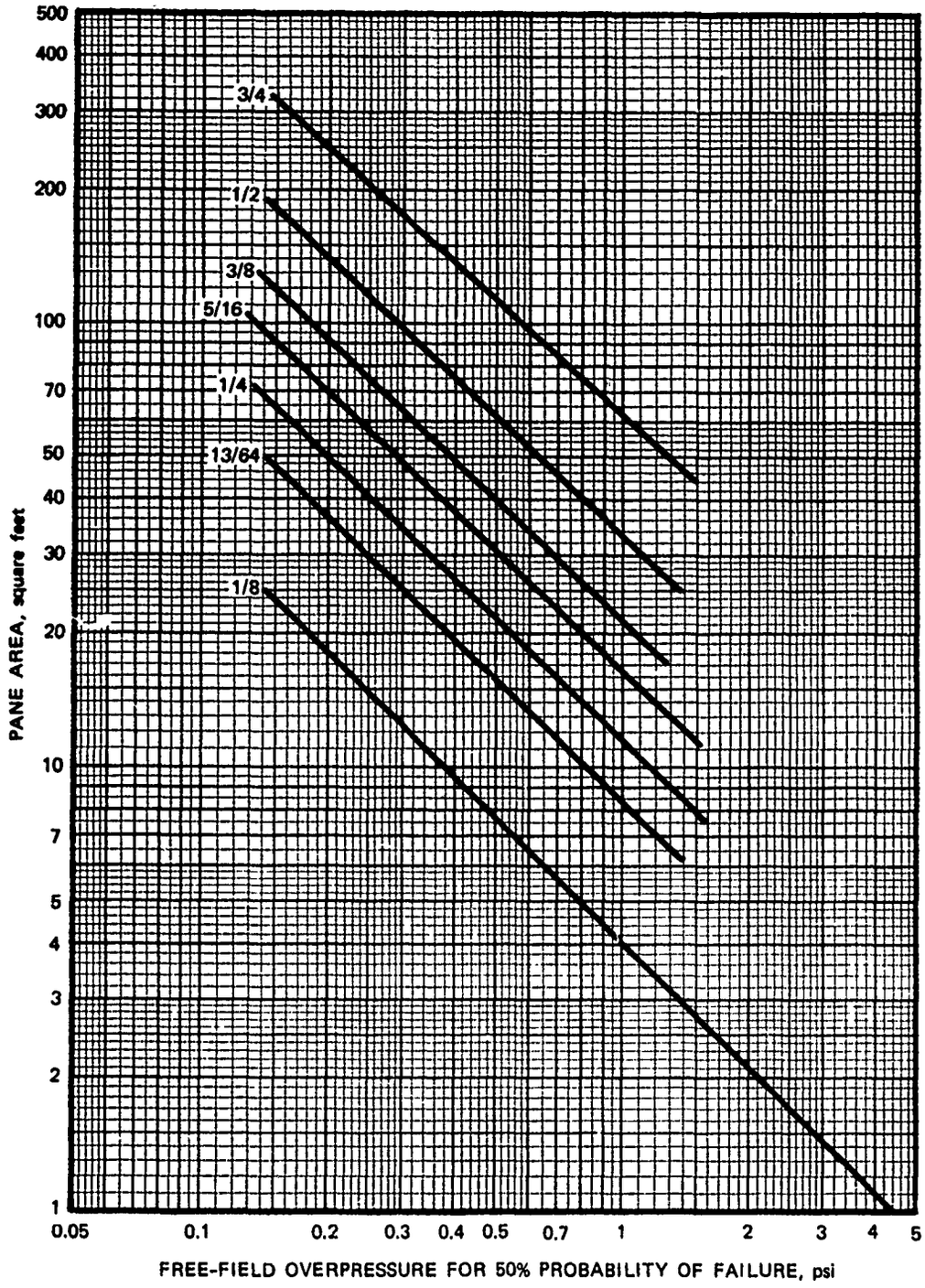


FIG. 7 PLATE GLASS INCIPIENT FAILURE PRESSURES FOR SIDE-WALL LOADING AS A FUNCTION OF PANE AREA AND THICKNESS

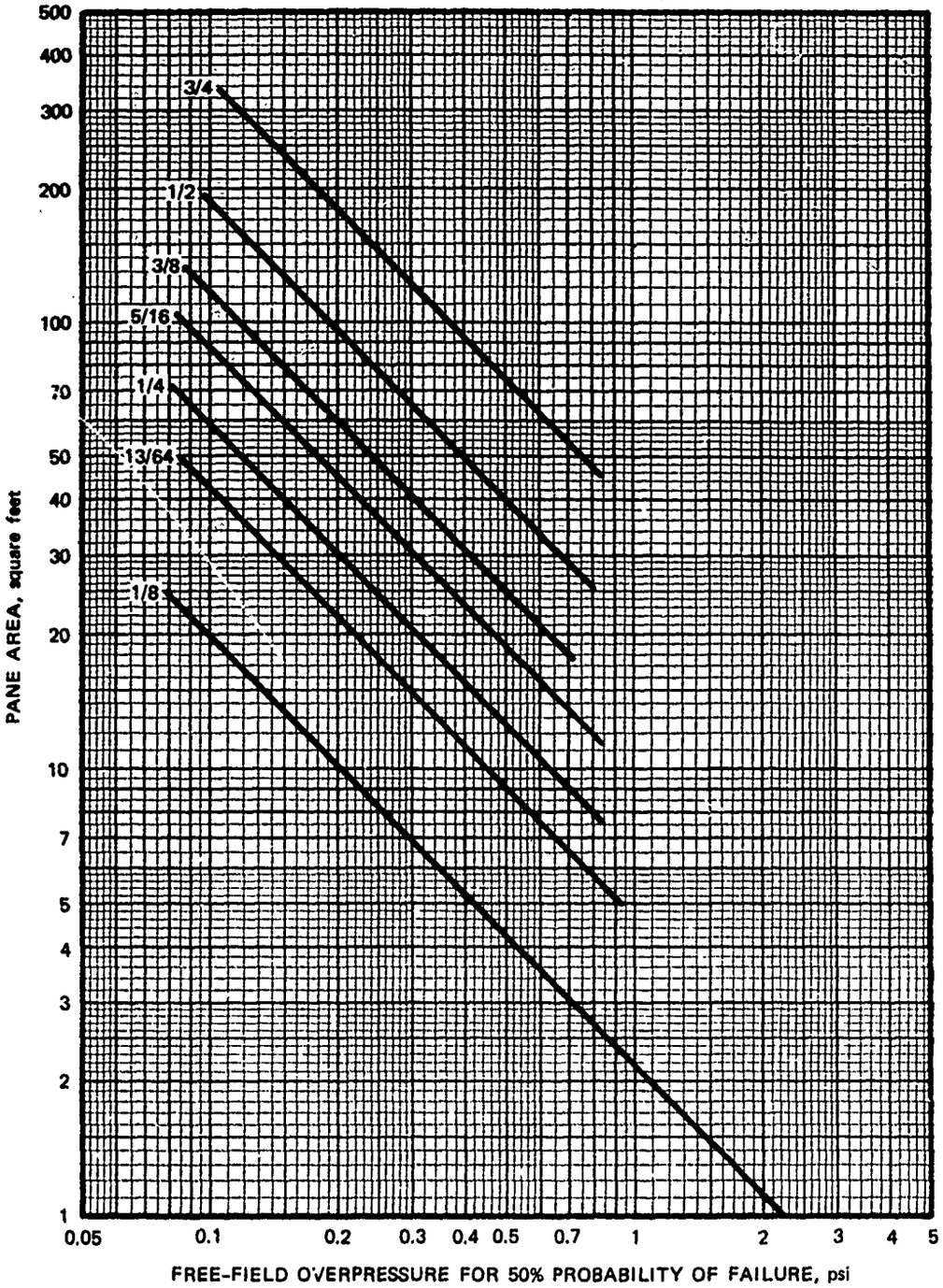


FIG. 8 PLATE GLASS INCIPIENT FAILURE PRESSURES FOR FRONT-FACE LOADING AS A FUNCTION OF PANE AREA AND THICKNESS

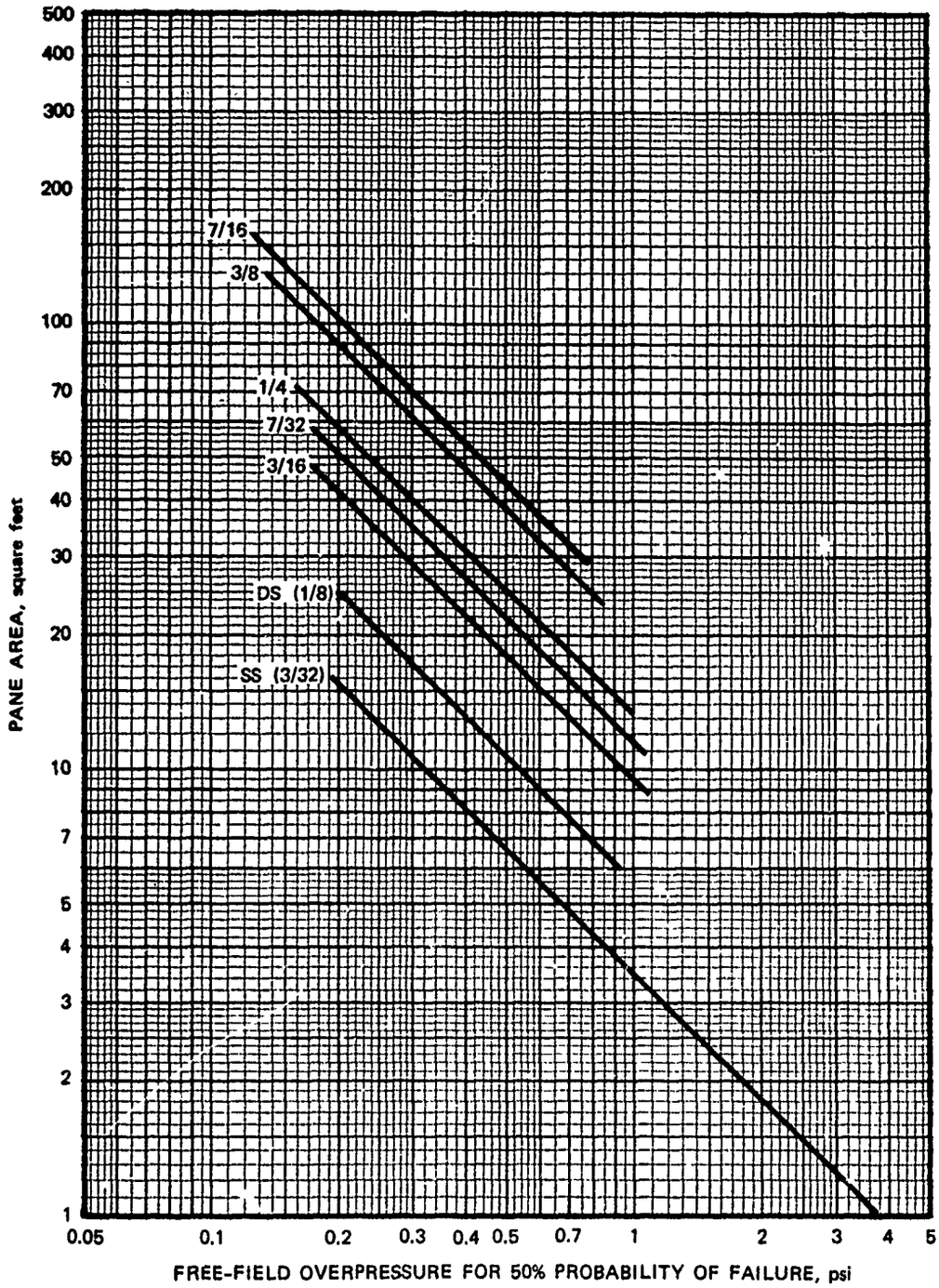


FIG. 9 SHEET GLASS INCIPIENT FAILURE PRESSURES FOR SIDE-WALL LOADING AS A FUNCTION OF PANE AREA AND THICKNESS

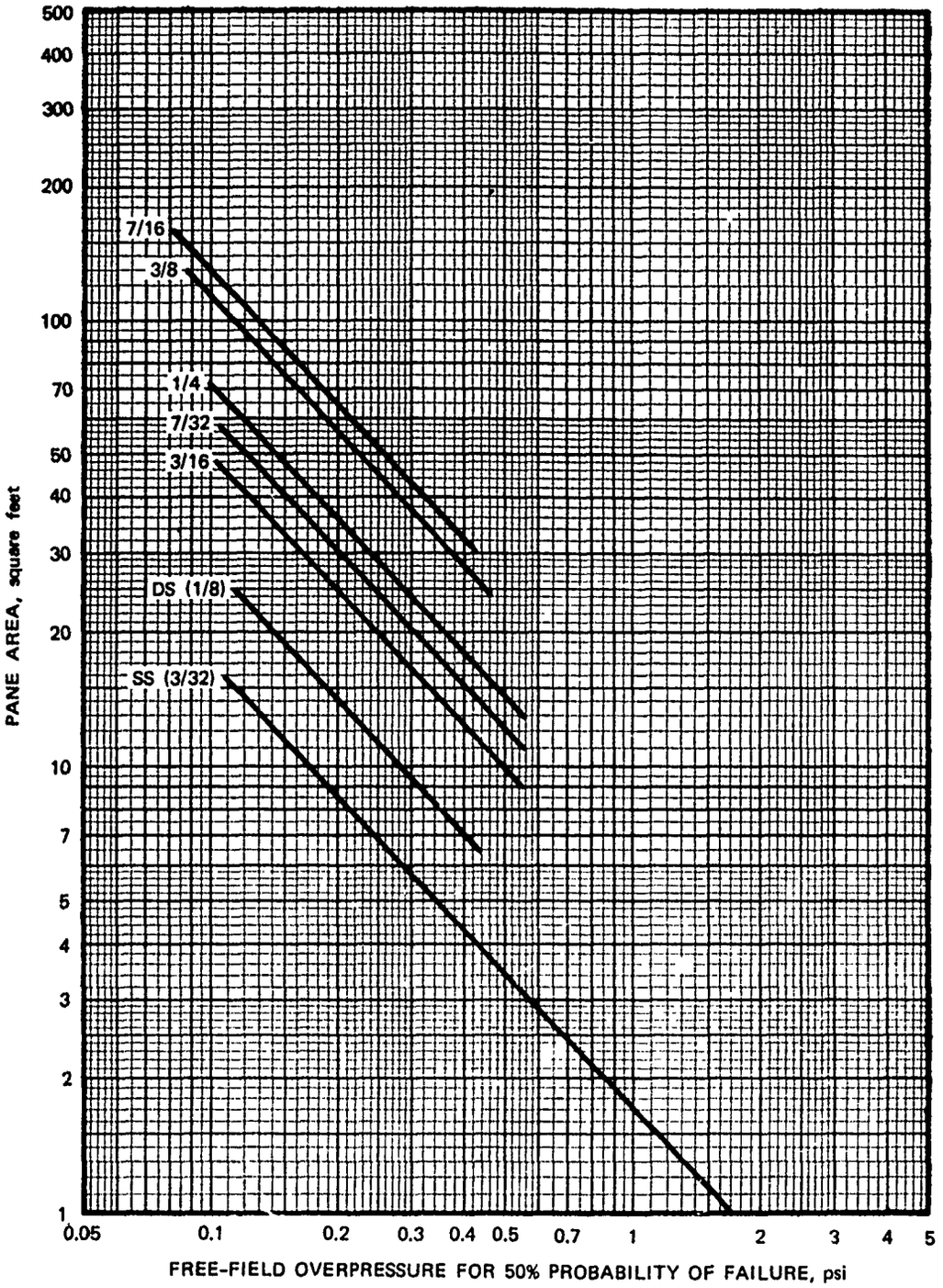


FIG. 10 SHEET GLASS INCIPIENT FAILURE PRESSURES FOR FRONT-FACE LOADING AS A FUNCTION OF PANE AREA AND THICKNESS

In multipane windows, the premature failure of muntins* too weak to withstand the pressures distributed to them by the glass panes was not analyzed in this investigation. However, to obtain an approximate incipient failure overpressure, it is suggested that all thin, weak muntins be ignored; thus the area within substantial frame members, considered as a pane area, is then used in the appropriate one of the Figures 7 through 10. For example, approximate results for the window types shown in Figure B-1 could be found as follows: type 1, two pane areas (upper and lower); types 2, 3, and 8, two pane areas each (right and left) with a third pane area for the vent in type 8; types 4 and 5, the greatest area (and thus the lowest incipient failure pressure) within substantial frame members is found by considering the entire movable portion as one pane area; types 6 and 7, four pane areas each; and type 9, one pane area equal to the area of the large, center pane (assuming all frame members are strong).

Some full scale test data concerning window response to dynamic loadings are contained in Appendix D. A shatter pressure prediction equation is given in Appendix D as Equation D-1. The table accompanying the equation indicates that the shatter pressure should be adjusted for various aspect ratios. For reasons stated previously in this section, application of the table to methods discussed in this chapter is not recommended.

The option of specifying an overpressure in the input data to the computer program was employed in developing figures indicating time to failure in Appendix E.

---

* A muntin is a thin member separating panes of glass within a window frame.

# III WEIGHT, NUMBER, AND SPATIAL DENSITY OF GLASS FRAGMENTS

## Introduction

Data on mass,* velocity, and spatial density of glass missiles resulting from window failure caused by a nuclear explosion were first taken during Operation Teapot.[29] Glass missiles emanating from multipane windows with either steel or wood frames were trapped in Styrofoam absorbers. The same data were analyzed further with consideration given to biological implications.[30] Then a model[31] that predicted the velocity of glass fragments was developed using drag characteristics determined in drop tests.[32] Further testing was done during Operation Plumbbob[33,34] with one of the objectives being a comparison of missile velocities predicted by the model and those measured in the field. A discussion of the translation model and its use in predicting the velocity of glass fragments is presented in Chapter IV. Since the test procedures, data collected, and discussions of results are already well documented, this chapter is limited to providing methods based on the Operation Teapot data for predicting the fragment weight distribution, the probable number of fragments, and the spatial distribution of fragments.

In the Teapot tests, houses were located at 4,700, 5,500, and 10,500 feet from a nuclear explosion with a yield of nearly 30 kt, which caused peak overpressures of 5.0, 3.8, and 1.9 psi, respectively, at the

---

* All nuclear test data consistently report mass in grams, using mass in the lay sense, i.e., synonymous with weight. The term weight is used in this report. Weights in grams found herein may be converted to the English system of weights by using 454 grams per pound.

three distances. Only data from windows facing ground zero and mounted in houses were selected for use in this chapter. Data from windows mounted in house side or rear walls with respect to ground zero and from windows mounted in the open were not used.

## Fragment Weight

Data[29] from 13 traps located behind seven different house front windows are presented in Table 7. The data are grouped by overpressure and glass thickness. Both the geometric mean fragment weight and the average fragment weight are shown in the table. The former provides the best indication of the most probable fragment weight to expect since it is changed very little by the presence of a few heavy pieces. The latter is useful in calculations of the total number and spatial density of fragments. Values summarizing the data for each window were calculated and added to the tabulated field data.

Figure 11, prepared from information contained in Table 7, is presented as a means of predicting both average and geometric mean fragment weights. Because of the limited data found in the literature, predictions for single and double strength glass thicknesses only are given; however, these two thicknesses make up most of the glass installed in windows today.

An additional scale has been provided for use if the window in question is in a side wall with respect to ground zero. It was believed that reflected pressures cause window failures in front walls. Since no reflection occurs on side walls, the free-field overpressure for side walls must be approximately equal to the reflected pressure for front walls, so that the peak pressure load causing window failure will be nearly the same in each case. Thus, the front-face $p_{so}$ values were placed on the lower scale, the corresponding $p_r$ values were placed on the upper scale, and the upper scale was labeled as $p_{so}$ for side windows. It was realized

Table 7

WINDOW GLASS FRAGMENT WEIGHT DATA*

| Free-Field Overpressure, $P_{so}$ (psi) | Trap Designation | Average Thickness of Panes h (in.) | Number of Fragments Caught in Traps† | Geometric Mean Weight, $M_{50}$ (gm) | Average Weight, $\bar{M}$ (gm) | Distance from Window to Trap, x (ft) | Size of Individual Panes (in.) | Number of Panes per Window | Frame Material |
|---|---|---|---|---|---|---|---|---|---|
| 5.0 | 2A | .092 | 254 | .140 | .226 | 8.83 | 12 x 12 | 16 | Wood‡ |
| 5.0 | 2C | .096 | 423 | .140 | .282 | 13.50 | 12 x 16 | 20 | Steel |
| 5.0 | $2D_1$ | .094 | 247 | .113 | .307 | 9.00 | 12 x 16 | 12 | Steel |
| 5.0 | $2D_2$ | .089 | 231 | .095 | .140 | 9.00 | | | |
| | | | 478 | .104 | .226 | | | | |
| 5.0 | $2E_1$ | .124 | 242 | .153 | .415 | 10.50 | 12 x 23.5 | 9 | Steel§ |
| 5.0 | $2E_2$ | .122 | 732 | .142 | .241 | 10.50 | | | |
| | | | 974 | .145 | .284 | | | | |
| 3.8 | $3C_1$ | .120 | 61 | .810 | 1.275 | 7.00 | 12 x 12 | 16 | Wood§ |
| 3.8 | $3C_2$ | .118 | 259 | .540 | .993 | 7.00 | | | |
| | | | 320 | .580 | 1.047 | | | | |
| 1.9 | $4B_1$ | .124 | 1 | 2.125 | 2.125 | 10.67 | 15 x 18 | 20 | Steel‡ |
| 1.9 | $4B_2$ | .123 | 11 | 1.322 | 1.677 | 10.67 | | | |
| 1.9 | $4B_3$ | .124 | 5 | 1.596 | 1.704 | 10.67 | | | |
| 1.9 | $4B_4$ | .124 | 5 | 4.407 | 5.260 | 10.67 | | | |
| | | | 22 | 1.854 | 2.518 | | | | |
| 1.9 | 4D | .088 | 15 | .694 | 1.312 | 13.50 | 12 x 16 | 20 | Steel‡ |

* All data were taken from 13 traps located behind 7 windows mounted in house walls that faced ground zero. In cases of more than one trap per window, data from traps have been combined to provide results for each window as well as each trap.

† The number of fragments given is limited to the number for which the velocity could be calculated.

‡ Window covered with venetian blinds.

§ Window covered with curtains.

Source: Reference 29.

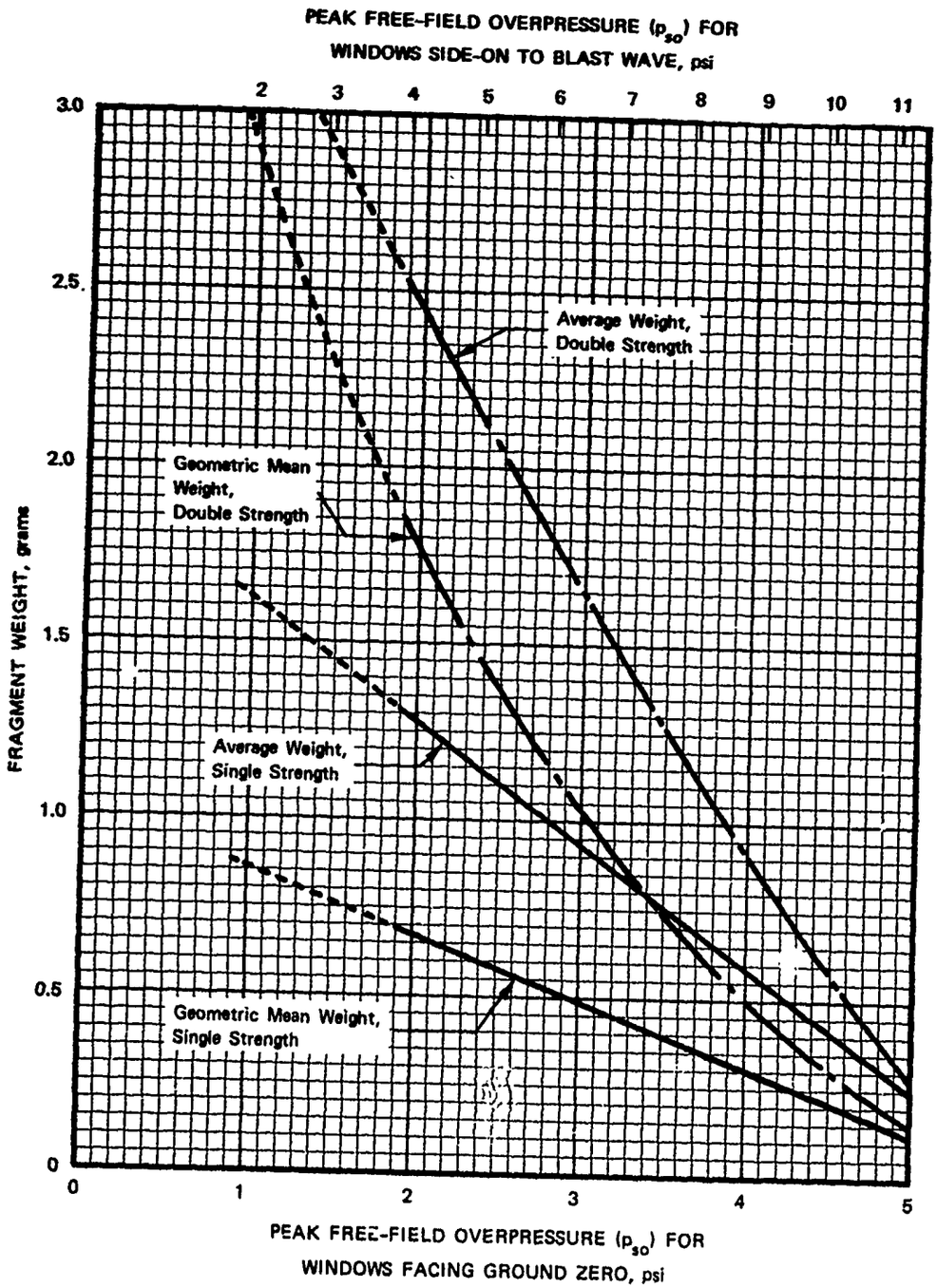


SOURCE: Based on data in Table 7.

FIG. 11 FRAGMENT WEIGHT PREDICTIONS

that drag loading for front and side walls is not the same; however, the differences introduced by accounting for drag loading at these low overpressures were neglected since they were so small.

## Number of Fragments

The total number of glass fragments originating from a window can be estimated if it is assumed that the average weight of fragments caught in a trap or traps behind the window is indicative of the average weight of all of the fragments produced by the window.[29] Accepting that assumption, it follows that:

$$N = \frac{A h \gamma}{\overline{M}} \quad . \tag{23}$$

Equation 23 accounts for the fact that the number of fragments depends on overpressure as well as pane properties since $\overline{M}$ is taken from Figure 11.

## Spatial Density of Fragments

The spatial density of fragments very close to a window can be estimated by dividing the total number of fragments by the window area:[29]

$$N_o = \frac{N}{A} = \frac{h\gamma}{\overline{M}} \quad . \tag{24}$$

Equation 2· was used in preparing Table 8.

The spatial density data presented in Table 8 were grouped only by overpressure. Further grouping by thickness as was done for the fragment weight data in Table 7 was not done here since:

- The spatial density versus overpressure curve reaches a maximum at 3.8 psi and no single strength data were available at that pressure

Table 8

WINDOW GLASS SPATIAL DENSITY DATA

| Free-Field Overpressure, $p_{so}$ (psi) | Trap Designation | Distance from Window to Trap, x (ft) | Average Spatial Density per Trap, $N_x$ (fragments per sq ft) | Average $N_x$ per Window (fragments per sq ft) | Average $N_x$ per Window Times 2.5 (fragments per sq ft) | Average Spatial Density at Window, $N_o$ (fragments per sq ft) | Percent of $N_o$ Remaining After Approximately 10 Feet of Travel | |
|---|---|---|---|---|---|---|---|---|
| | | | | | | | $\frac{N_x}{N_o} \times 100\%$ | $\frac{2.5\ N_x}{N_o} \times 100\%$ |
| 5.0 | 2A | 8.83 | 72.1 | 72.1 | 180 | 2393 | 3.0% | 7.5% |
| 5.0 | 2C | 13.50 | 120.1 | 120.1 | 300 | 2001 | 6.0 | 15.0 |
| 5.0 | $2D_1$ | 9.00 | 70.1 | 68.0 | 170 | 2380 | 2.8 | 7.1 |
| 5.0 | $2D_2$ | 9.00 | 65.6 | | | | | |
| 5.0 | $2E_1$ | 10.50 | 68.7 | 138.5 | 346 | 2546 | 5.4 | 13.6 |
| 5.0 | $2E_2$ | 10.50 | 207.9 | | | | | |
| | | | 100.8 | 99.7 | 249 | 2330 | 4.3% | 10.7% |
| 3.8 | $3C_1$ | 7.00 | 17.3 | 45.5 | 114 | 668 | 6.8 | 17.0 |
| 3.8 | $3C_2$ | 7.00 | 73.6 | | | | | |
| | | | 45.5 | | | | | |
| 1.9 | $4B_1$ | 10.67 | 0.3 | 1.56 | 3.9 | 289 | 0.5 | 1.4 |
| 1.9 | $4B_2$ | 10.67 | 3.1 | | | | | |
| 1.9 | $4B_3$ | 10.67 | 1.4 | | | | | |
| 1.9 | $4B_4$ | 10.67 | 1.4 | | | | | |
| 1.9 | 4D | 13.50 | 4.3 | 4.3 | 10.8 | 394 | 1.1 | 2.7 |
| | | | 2.1 | 2.93 | 7.35 | 342 | 0.8% | 2.1% |

Source: Columns 1-4 represent data found in Reference 29. The remaining columns represent calculations performed in this investigation using these data and the data in Table 7.

- The $N_x$ values at 1.9 and 5.0 psi appear to be fairly insensitive to glass thickness
- It seemed desirable to maintain a correlation between this work and the biological considerations presented in Chapter V herein

Average spatial densities, $N_x$, in fragments per square foot, found by dividing the number of missiles in a trap by the surface area of the trap, are presented in the fourth column of Table 8. The $N_x$ values

> . . . are based on the missiles whose velocities were computed. Judging from the appearance of the front of the first cells* of several traps, it was estimated that about 60 per cent of the missiles striking a trap arrived in such a way that their velocities could not be computed. Missiles striking the trap at low velocities failed to embed themselves in the Styrofoam. Other missiles entered holes already made by previous missiles, and some missiles were lost because their trajectories stopped at the boundary between cells. . . . the impact of large objects made gross deformations in the Styrofoam, making it impossible to evaluate the velocities for smaller glass missiles which were already present. . . . Consideration should be given to the fact that these traps were estimated to have an efficiency of about 40 per cent in catching missiles.[29]

The calculated values shown in Table 8 are plotted in Figure 12. Points were connected by straight lines since no intermediate values were available to suggest a different curve. The curves are based on multipane, single or double strength windows with total glass areas of between 2,300 and 5,400 sq in. The upper curve accounts for the 40 percent efficiency of the traps while the lower curve is representative of the actual number of missiles caught.

The upper curve in Figure 12 is recommended for use in predicting fragment spatial density approximately 10 feet behind a window. $N_{10}$ can

---

* Several layers of Styrofoam were used in each trap, each thickness being referred to as a cell.

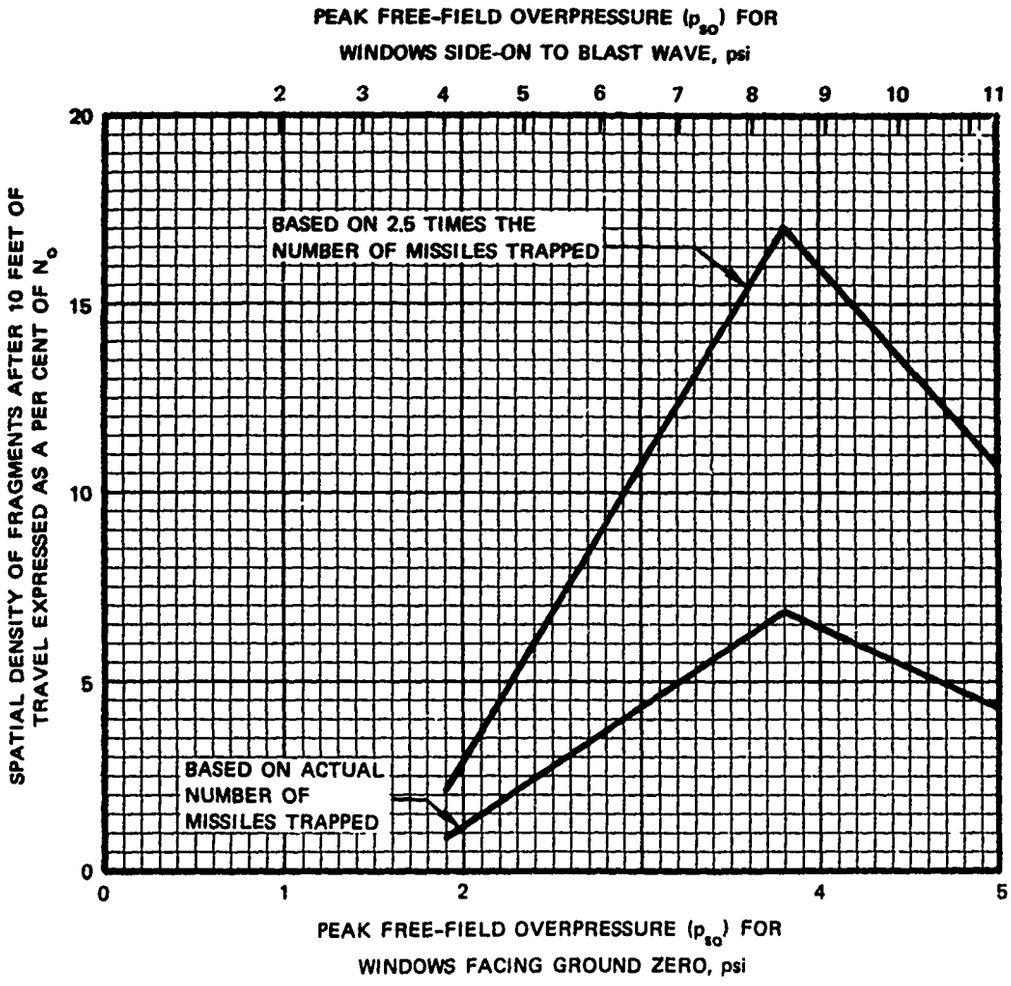


SOURCE: Based on data in Table 8.

FIG. 12 SPATIAL DENSITY PREDICTIONS AFTER 10 FEET OF TRAVEL AS A FUNCTION OF OVERPRESSURE

be found by multiplying the percentage obtained from Figure 12 by $N_o$, which is found by using Equation 24. Since no other data were found, it is suggested that Figure 12 serve as a rough guide to spatial densities for windows both larger and smaller than the size range tested.

It was believed that spatial density depended on the pressure causing window failure, which is reflected pressure for front windows and free-field overpressure for side windows. Therefore, an additional overpressure scale for side windows has been provided across the top of Figure 12 following the same procedure described previously in this chapter for the scale at the top of Figure 11.

# IV FRAGMENT TRANSLATION MODEL

Bowen's translation model[31] is an available method for estimating distance, velocity, and acceleration data at various times for glass missiles. The model is applicable to a classical blast wave ". . . not appreciably modified by terrain effects and possessing a well-defined shock front." Five assumptions were made in creating the model:

1. No surface friction existed. Glass fragment translation through air satisfies this assumption perfectly.

2. No energy gain or loss resulted from ". . . moving with or against gravity. The kinetic energy that is lost during lofting would be regained as the object fell to its original elevation, thus mitigating somewhat the error in the predicted motion."

3. ". . . only the propelling force of the wind was considered." This assumption means that the initial velocity of a fragment was taken as zero, i.e., a fragment is treated as though it is suspended motionless in space and then operated on by the blast winds only. The validity of this assumption pertaining to glass fragments is questionable.

4. ". . . the properties of an object which governed acceleration (area presented to the wind, drag coefficient, and mass) . . ." were assumed constant throughout acceleration.

5. ". . . no allowance was made for the fact that a displaced object may be moved to a lower overpressure region and thus be acted upon by correspondingly weaker blast winds."

Table 9 is a presentation of the results obtained by Bowen based on the foregoing discussion. Five blast wave parameters are needed to use the model, namely, $P_o$, $c_o$, $p_{so}$, $t_o$, and $t_u$. Values for $t_o$ for standard conditions can be found with sufficient accuracy using Equation 19. Values for $t_u$ can be found by multiplying $t_o$ by an appropriate factor selected from Figure 13. A fragment acceleration coefficient, which accounts for the fragment area presented to the wind, the weight, and the drag coefficient of the fragment, is also required:*

$$\alpha = \frac{A_f}{m} C_d. \tag{25}$$

The results of tests[32] performed to determine $\alpha$ for pieces of 0.125-in. thick window glass and 0.225-in. thick plate glass, dropped both flat and edge first, are presented in Figure 14.

The above blast and fragment parameters are combined into the following nondimensional terms for use in Table 9:

$$P = p_{so}/P_o \tag{26}$$

$$A = \alpha P_o t_u g/ c_o \tag{27}$$

$$T = t/t_o \tag{28}$$

$$V(n) = (v/c_o) \times 10^n \tag{29}$$

$$D(n) = (x/t_u c_o) \times 10^n \tag{30}$$

$$\dot{V}(n) = (\dot{v} t_u/c_o) \times 10^n . \tag{31}$$

The decimal point location is indicated in Table 9 by the letter n. For example, if P = 0.10, A = 1000, and T = 0.120, V(6) is found to be 55677,

---

* $\alpha$ is defined[31,32] as the presented area divided by the fragment mass and then reported in $ft^2/lb$. On the basis of the footnote on page 36, $\alpha$ is considered herein as area/unit weight, retaining the units $ft^2/lb$ in all usages.

Table 9

## COMPUTED MOTION PARAMETERS FOR OBJECTS DISPLACED BY CLASSICAL BLAST WAVES

| P | A | T: | 0 | .002 | .004 | .008 | .015 | .030 | .060 | .120 | .250 | .500 | .750 | 1.000 | Final | $T_{final}$ |
|---|---|---|---|---|---|---|---|---|---|---|---|---|---|---|---|---|
| | | V (7): | 0 | 88 | 175 | 345 | 635 | 1218 | 2253 | 3912 | 6333 | 8820 | 9941 | 10296 | 10312 | |
| .068 | 3 | D (8): | 0 | 1 | 3 | 12 | 44 | 169 | 641 | 2327 | 8439 | 25850 | 47142 | 70020 | 78517 | 1.092 |
| | | V̇ (7): | 49066 | 48500 | 47950 | 46860 | 45040 | 41460 | 35410 | 26640 | 16090 | 7350 | 2990 | 450 | 0 | |
| | | V (7): | 0 | 293 | 582 | 1149 | 2109 | 4038 | 7433 | 12801 | 20435 | 27852 | 30821 | | 31449 | |
| | 10 | D (7): | 0 | | 1 | 4 | 14 | 56 | 212 | 766 | 2750 | 8303 | 14963 | | 22561 | 1.020 |
| | | V̇ (6): | 16355 | 16155 | 15958 | 15573 | 14930 | 13670 | 11560 | 8541 | 4970 | 2080 | 693 | | 0 | |
| | | V (7): | 0 | 877 | 1741 | 3433 | 6278 | 11930 | 21674 | 36500 | 56161 | 72687 | 77374 | | 77687 | |
| | 30 | D (7): | 0 | 1 | 3 | 12 | 43 | 167 | 625 | 2219 | 7761 | 22595 | 39619 | | 49734 | 0.895 |
| | | V̇ (6): | 49066 | 48359 | 47666 | 46319 | 44085 | 39766 | 32709 | 22998 | 12132 | 3979 | 645 | | 0 | |
| | | V (6): | 0 | 291 | 576 | 1127 | 2037 | 3777 | 6578 | 10369 | 14477 | 16736 | | | 16896 | |
| | 100 | D (7): | 0 | 3 | 10 | 41 | 141 | 537 | 1952 | 6613 | 21514 | 57390 | | | 84057 | 0.676 |
| | | V̇ (5): | 16355 | 15998 | 15651 | 14987 | 13915 | 11942 | 8989 | 5442 | 2159 | 293 | | | 0 | |
| | | V (6): | 0 | 864 | 1692 | 3245 | 5674 | 9907 | 15714 | 21879 | 26410 | | | | 27340 | |
| | 300 | D (7): | 0 | 8 | 31 | 120 | 403 | 1468 | 4990 | 15361 | 44252 | | | | 94925 | 0.458 |
| | | V̇ (5): | 49066 | 46971 | 45000 | 41392 | 35994 | 27296 | 16832 | 7547 | 1650 | | | | 0 | |
| | | V (6): | 0 | 2776 | 5253 | 9478 | 15143 | 22942 | 30579 | 35809 | 37497 | | | | 37500 | |
| | 1000 | D (7): | 0 | 25 | 98 | 356 | 1151 | 3772 | 11148 | 29385 | 72750 | | | | 79332 | 0.270 |
| | | V̇ (4): | 16355 | 14546 | 13015 | 10583 | 7675 | 4336 | 1807 | 466 | 5 | | | | 0 | |
| | | V (6): | 0 | 7549 | 13179 | 20999 | 28954 | 36776 | 41926 | 43909 | | | | | 43993 | |
| | 3000 | D (7): | 0 | 71 | 259 | 884 | 2484 | 7005 | 17782 | 41155 | | | | | 56458 | 0.159 |
| | | V̇ (4): | 49066 | 35858 | 27310 | 17282 | 9279 | 3569 | 948 | 75 | | | | | 0 | |
| | | V (6): | 0 | 17670 | 26508 | 35305 | 41625 | 46042 | 47903 | | | | | | 48084 | |
| | 9000 | D (7): | 0 | 175 | 579 | 1712 | 4167 | 10150 | 22914 | | | | | | 36728 | 0.092 |
| | | V̇ (3): | 14720 | 6565 | 3687 | 1618 | 621 | 164 | 20 | | | | | | 0 | |
| | | V (7): | 0 | 186 | 370 | 732 | 1346 | 2586 | 4797 | 8373 | 13662 | 19090 | 21447 | 22143 | 22172 | |
| .10 | 3 | D (7): | 0 | | 1 | 3 | 9 | 35 | 134 | 488 | 1780 | 5484 | 10009 | 14854 | 16451 | 1.081 |
| | | V̇ (6): | 10563 | 10446 | 10331 | 10105 | 9727 | 8981 | 7720 | 5874 | 3592 | 1607 | 617 | 79 | 0 | |
| | | V (7): | 0 | 619 | 1231 | 2433 | 4466 | 8550 | 15748 | 27142 | 43334 | 58605 | 64117 | | 65030 | |
| | 10 | D (7): | 0 | 1 | 2 | 9 | 30 | 117 | 442 | 1596 | 5735 | 17274 | 30974 | | 44789 | 0.991 |
| | | V̇ (6): | 35211 | 34780 | 34357 | 33530 | 32151 | 29451 | 24934 | 18455 | 10662 | 4157 | 1159 | | 0 | |
| | | V (6): | 0 | 186 | 368 | 725 | 1324 | 2507 | 4527 | 7550 | 11421 | 14366 | 14980 | | 14990 | |
| | 30 | D (7): | 0 | 2 | 7 | 26 | 90 | 345 | 1288 | 4545 | 15714 | 44931 | 77637 | | 87959 | 0.828 |
| | | V̇ (5): | 10563 | 10400 | 10240 | 9930 | 9418 | 8437 | 6853 | 4713 | 2352 | 630 | 40 | | 0 | |
| | | V (6): | 0 | 615 | 1214 | 2364 | 4238 | 7745 | 13170 | 20056 | 26737 | 29507 | | | 29549 | |
| | 100 | D (6): | 0 | 1 | 2 | 9 | 29 | 109 | 391 | 1291 | 4051 | 10392 | | | 12684 | 0.588 |
| | | V̇ (5): | 35211 | 34274 | 33371 | 31661 | 28948 | 24111 | 17254 | 9631 | 3229 | 166 | | | 0 | |
| | | V (6): | 0 | 1815 | 3527 | 6674 | 11421 | 19217 | 28969 | 38092 | 43502 | | | | 44039 | |
| | 300 | D (6): | 0 | 2 | 6 | 25 | 81 | 287 | 940 | 2759 | 7546 | | | | 12672 | 0.382 |
| | | V̇ (4): | 10563 | 9957 | 9398 | 8408 | 7002 | 4921 | 2717 | 1042 | 148 | | | | 0 | |
| | | V (6): | 0 | 5730 | 10604 | 18439 | 28080 | 39911 | 49951 | 55677 | | | | | 56779 | |
| | 1000 | D (7): | 0 | 52 | 197 | 717 | 2179 | 6786 | 18945 | 47387 | | | | | 97492 | 0.220 |
| | | V (4): | 35211 | 29769 | 25479 | 19234 | 12654 | 6243 | 2219 | 430 | | | | | 0 | |
| | | V (6): | 0 | 14926 | 24836 | 37145 | 48177 | 57673 | 63035 | 64483 | | | | | 64485 | |
| | 3000 | D (7): | 0 | 140 | 496 | 1613 | 4298 | 11440 | 27641 | 61685 | | | | | 66790 | 0.129 |
| | | V̇ (3): | 10563 | 6740 | 4663 | 2596 | 1225 | 408 | 88 | 1 | | | | | 0 | |
| | | V (6): | 0 | 32061 | 44935 | 56140 | 63298 | 67740 | 69201 | | | | | | 69239 | |
| | 9000 | D (7): | 0 | 323 | 1015 | 2836 | 6574 | 15342 | 33599 | | | | | | 42608 | 0.075 |
| | | V̇ (3): | 31690 | 10438 | 5105 | 1957 | 672 | 153 | 9 | | | | | | 0 | |
| | | V (7): | 0 | 137 | 273 | 540 | 994 | 1916 | 3574 | 6298 | 10428 | 14752 | 16649 | 17259 | 17290 | |
| .15 | 1 | D (7): | 0 | | | 2 | 7 | 26 | 98 | 360 | 1330 | 4146 | 7613 | 11338 | 13067 | 1.114 |
| | | V̇ (7): | 78671 | 77860 | 77070 | 75510 | 72890 | 67720 | 58890 | 45730 | 28730 | 13000 | 5130 | 970 | 0 | |
| | | V (7): | 0 | 411 | 817 | 1617 | 2976 | 5727 | 10648 | 18654 | 30564 | 42539 | 47360 | 48571 | 48610 | |
| | 3 | D (7): | 0 | | 1 | 6 | 20 | 77 | 294 | 1072 | 3927 | 12109 | 22033 | 32571 | 35280 | 1.064 |
| | | V (6): | 23601 | 23347 | 23097 | 22607 | 21787 | 20168 | 17418 | 13352 | 8165 | 3461 | 1188 | 93 | 0 | |
| | | V (6): | 0 | 137 | 272 | 537 | 985 | 1885 | 3466 | 5954 | 9430 | 12492 | 13406 | | 13491 | |
| | 10 | D (7): | 0 | 1 | 5 | 19 | 66 | 255 | 963 | 3469 | 12410 | 36978 | 65553 | | 87180 | 0.934 |
| | | V (6): | 78671 | 77685 | 76716 | 74829 | 71681 | 65535 | 55283 | 40583 | 22700 | 7722 | 1498 | | 0 | |
| | | V (6): | 0 | 409 | 812 | 1595 | 2903 | 5459 | 9741 | 15930 | 23339 | 28069 | | | 28614 | |
| | 30 | D (6): | 0 | | 1 | 6 | 19 | 75 | 276 | 962 | 3251 | 9009 | | | 14907 | 0.737 |
| | | V (5): | 23601 | 23188 | 22784 | 22005 | 20728 | 18311 | 14505 | 9531 | 4283 | 787 | | | 0 | |
| | | V (6): | 0 | 1353 | 2659 | 5140 | 9097 | 16235 | 26597 | 38527 | 48331 | | | | 50886 | |
| | 100 | D (6): | 0 | 1 | 5 | 18 | 62 | 230 | 802 | 2548 | 7610 | | | | 18291 | 0.493 |
| | | V (5): | 78671 | 75942 | 73342 | 68503 | 61051 | 48440 | 32022 | 15799 | 4053 | | | | 0 | |
| | | V (6): | 0 | 3959 | 7601 | 14071 | 23308 | 37233 | 52609 | 64838 | 70129 | | | | 70248 | |
| | 300 | D (6): | 0 | 4 | 14 | 52 | 167 | 572 | 1776 | 4920 | 12715 | | | | 16408 | 0.310 |
| | | V̇ (4): | 23601 | 21681 | 19979 | 17107 | 13344 | 8421 | 4021 | 1251 | 71 | | | | 0 | |
| | | V (6): | 0 | 12152 | 21747 | 35909 | 51461 | 68068 | 80049 | 85424 | | | | | 85866 | |
| | 1000 | D (6): | 0 | 11 | 41 | 143 | 415 | 1215 | 3191 | 7580 | | | | | 11803 | 0.176 |
| | | V̇ (4): | 78671 | 61322 | 49088 | 33388 | 19384 | 8167 | 2417 | 287 | | | | | 0 | |

Source: Ref. 31.

Table 9 (Continued)

| P | A | T: | 0 | .002 | .004 | .008 | .015 | .030 | .060 | .120 | .250 | .500 | .750 | 1.000 | Final | $T_{final}$ |
|---|---|---|---|---|---|---|---|---|---|---|---|---|---|---|---|---|
| | | V (6): | 0 | 29712 | 46419 | 64522 | 78639 | 89205 | 94174 | | | | | | 94913 | |
| .15 | 3000 | D (7): | 0 | 281 | 957 | 2937 | 7384 | 18539 | 42794 | | | | | | 78423 | 0.103 |
| | | V̇ (3): | 23601 | 12265 | 7478 | 3581 | 1471 | 422 | 67 | | | | | | 0 | |
| | | V (5): | 0 | 5724 | 7468 | 8791 | 9543 | 9952 | | | | | | | 10040 | |
| | 9000 | D (7): | 0 | 594 | 1768 | 4656 | 10315 | 23180 | | | | | | | 49210 | 0.060 |
| | | V̇ (3): | 70804 | 15437 | 6494 | 2178 | 671 | 124 | | | | | | | 0 | |
| | | V (8): | 0 | 709 | 1412 | 2797 | 5159 | 9972 | 18694 | 33219 | 55666 | 79530 | 90144 | 93841 | 94326 | |
| .20 | .3 | D (8): | 0 | 1 | 2 | 10 | 34 | 131 | 501 | 1847 | 6879 | 21660 | 39963 | 59715 | 75430 | 1.195 |
| | | V̇ (7): | 41667 | 41270 | 40880 | 40120 | 38830 | 36280 | 31870 | 25160 | 16130 | 7380 | 3000 | 750 | 0 | |
| | | V (7): | 0 | 236 | 470 | 932 | 1718 | 3318 | 6211 | 11005 | 18345 | 25994 | 29258 | 30281 | 30336 | |
| | 1 | D (7): | 0 | | 1 | 3 | 11 | 44 | 167 | 613 | 2275 | 7125 | 13085 | 19477 | 22777 | 1.127 |
| | | V̇ (6): | 13889 | 13754 | 13620 | 13360 | 12921 | 12050 | 10551 | 8277 | 5237 | 2321 | 886 | 169 | 0 | |
| | | V (7): | 0 | 709 | 1410 | 2791 | 5140 | 9905 | 18458 | 32445 | 53308 | 73877 | 81694 | 83460 | 83509 | |
| | 3 | D (7): | 0 | 1 | 2 | 10 | 33 | 130 | 497 | 1818 | 6679 | 20600 | 37382 | 55103 | 59218 | 1.058 |
| | | V̇ (6): | 41667 | 41233 | 40806 | 39970 | 38568 | 35793 | 31048 | 23932 | 14589 | 5913 | 1872 | 108 | 0 | |
| | | V (6): | 0 | 236 | 469 | 926 | 1699 | 3246 | 5958 | 10200 | 16013 | 20819 | 22032 | | 22099 | |
| | 10 | D (6): | 0 | | 1 | 3 | 11 | 43 | 162 | 582 | 2072 | 6108 | 10725 | | 13452 | 0.894 |
| | | V̇ (5): | 13889 | 13711 | 13537 | 13198 | 12632 | 11527 | 9687 | 7043 | 3807 | 1145 | 156 | | 0 | |
| | | V (6): | 0 | 706 | 1397 | 2741 | 4971 | 9290 | 16389 | 26321 | 37483 | 43582 | | | 43974 | |
| | 30 | D (6): | 0 | 1 | 2 | 9 | 33 | 125 | 458 | 1573 | 5210 | 14074 | | | 20710 | 0.677 |
| | | V̇ (5): | 41667 | 40854 | 40063 | 38542 | 36066 | 31440 | 24313 | 15301 | 6234 | 784 | | | 0 | |
| | | V (6): | 0 | 2324 | 4550 | 8730 | 15269 | 26672 | 42325 | 58939 | 70827 | | | | 72901 | |
| | 100 | D (6): | 0 | 2 | 8 | 31 | 103 | 375 | 1277 | 3931 | 11310 | | | | 22876 | 0.437 |
| | | V̇ (4): | 13889 | 13299 | 12743 | 11726 | 10203 | 7746 | 4781 | 2129 | 430 | | | | 0 | |
| | | V (6): | 0 | 6744 | 12803 | 23233 | 37417 | 57327 | 77289 | 91341 | 95988 | | | | 95997 | |
| | 300 | D (6): | 0 | 6 | 23 | 85 | 266 | 888 | 2651 | 7054 | 17590 | | | | 19256 | 0.270 |
| | | V̇ (4): | 41667 | 37336 | 33631 | 27665 | 20384 | 11787 | 5046 | 1336 | 14 | | | | 0 | |
| | | V (5): | 0 | 2017 | 3504 | 5549 | 7607 | 9598 | 10884 | 11356 | | | | | 11371 | |
| | 1000 | D (6): | 0 | 18 | 66 | 223 | 623 | 1747 | 4410 | 10160 | | | | | 13346 | 0.151 |
| | | V̇ (3): | 13889 | 10028 | 7569 | 4729 | 2501 | 946 | 245 | 16 | | | | | 0 | |
| | | V (5): | 0 | 4669 | 6954 | 9200 | 10795 | 11887 | 12336 | | | | | | 12373 | |
| | 3000 | D (7): | 0 | 441 | 1452 | 4268 | 10327 | 25025 | 56278 | | | | | | 87144 | 0.089 |
| | | V̇ (3): | 41667 | 18053 | 9993 | 4311 | 1624 | 423 | 49 | | | | | | 0 | |
| | | V (5): | 0 | 8302 | 10362 | 11795 | 12545 | 12921 | | | | | | | 12976 | |
| | 9000 | D (7): | 0 | 867 | 2491 | 6329 | 13659 | 30061 | | | | | | | 54150 | 0.052 |
| | | V̇ (2): | 12500 | 1959 | 745 | 230 | 67 | 10 | | | | | | | 0 | |
| | | V (7): | 0 | 108 | 215 | 427 | 788 | 1526 | 2869 | 5122 | 8633 | 12351 | 13974 | 14533 | 14611 | |
| .25 | .3 | D (7): | 0 | | | 1 | 5 | 20 | 75 | 279 | 1044 | 3299 | 6089 | 9095 | 11534 | 1.199 |
| | | V̇ (7): | 64655 | 64070 | 63500 | 62370 | 60480 | 56690 | 50100 | 39890 | 25720 | 11590 | 4620 | 1170 | 0 | |
| | | V (7): | 0 | 360 | 717 | 1422 | 2623 | 5074 | 9522 | 16940 | 28356 | 40143 | 45027 | 46504 | 46632 | |
| | 1 | D (7): | 0 | | 1 | 5 | 17 | 65 | 250 | 925 | 3445 | 10810 | 19837 | 29489 | 34777 | 1.135 |
| | | V̇ (6): | 21552 | 21351 | 21154 | 20767 | 20114 | 18813 | 16556 | 13078 | 8287 | 3585 | 1321 | 244 | 0 | |
| | | V (6): | 0 | 108 | 215 | 426 | 784 | 1513 | 2823 | 4971 | 8168 | 11245 | 12346 | 12566 | 12571 | |
| | 3 | D (7): | 0 | 1 | 4 | 14 | 50 | 195 | 745 | 2733 | 10052 | 30943 | 55942 | 82193 | 86992 | 1.045 |
| | | V̇ (6): | 64655 | 63999 | 63352 | 62086 | 59957 | 55734 | 48467 | 37432 | 22617 | 8734 | 2533 | 91 | 0 | |
| | | V (6): | 0 | 360 | 715 | 1411 | 2586 | 4935 | 9034 | 15389 | 23897 | 30479 | 31872 | | 31910 | |
| | 10 | D (6): | 0 | | 1 | 5 | 17 | 64 | 242 | 866 | 3061 | 8918 | 15513 | | 18373 | 0.857 |
| | | V̇ (5): | 21552 | 21268 | 20990 | 20448 | 19546 | 17787 | 14861 | 10662 | 5542 | 1469 | 126 | | 0 | |
| | | V (6): | 0 | 1074 | 2126 | 4161 | 7520 | 13956 | 24332 | 38369 | 53178 | 60127 | | | 60345 | |
| | 30 | D (6): | 0 | 1 | 4 | 14 | 49 | 185 | 674 | 2284 | 7414 | 19566 | | | 26056 | 0.628 |
| | | V̇ (5): | 64655 | 63256 | 61899 | 59300 | 55100 | 47358 | 35710 | 21496 | 7949 | 638 | | | 0 | |
| | | V (6): | 0 | 3528 | 6880 | 13102 | 22646 | 38751 | 59733 | 80440 | 93498 | | | | 95022 | |
| | 100 | D (6): | 0 | 3 | 12 | 45 | 151 | 544 | 1809 | 5419 | 15118 | | | | 26728 | 0.396 |
| | | V̇ (4): | 21552 | 20464 | 19452 | 17631 | 14981 | 10901 | 6316 | 2564 | 406 | | | | 0 | |
| | | V (5): | 0 | 1015 | 1906 | 3393 | 5326 | 7874 | 10230 | 11727 | | | | | 12110 | |
| | 300 | D (6): | 0 | 9 | 33 | 123 | 383 | 1231 | 3559 | 9182 | | | | | 21572 | 0.243 |
| | | V̇ (4): | 64655 | 56495 | 49759 | 39389 | 27546 | 14769 | 5777 | 1323 | | | | | 0 | |
| | | V (5): | 0 | 2959 | 5005 | 7645 | 10121 | 12330 | 13643 | 14043 | | | | | 14045 | |
| | 1000 | D (6): | 0 | 26 | 94 | 310 | 841 | 2279 | 5591 | 12612 | | | | | 14590 | 0.137 |
| | | V̇ (3): | 21552 | 14433 | 10322 | 5995 | 2938 | 1026 | 238 | 6 | | | | | 0 | |
| | | V (5): | 0 | 6521 | 9346 | 11921 | 13615 | 14711 | 15106 | | | | | | 15123 | |
| | 3000 | D (7): | 0 | 617 | 1974 | 5614 | 13207 | 31215 | 68967 | | | | | | 94176 | 0.080 |
| | | V̇ (3): | 64655 | 23671 | 12102 | 4817 | 1713 | 409 | 32 | | | | | | 0 | |
| | | V (5): | 0 | 10886 | 13173 | 14661 | 15394 | 15735 | | | | | | | 15768 | |
| | 9000 | D (7): | 0 | 1144 | 3200 | 7928 | 16810 | 36491 | | | | | | | 58110 | 0.046 |
| | | V̇ (2): | 19397 | 2292 | 807 | 234 | 65 | 8 | | | | | | | 0 | |
| | | V (7): | 0 | 152 | 302 | 600 | 1108 | 2150 | 4054 | 7268 | 12307 | 17623 | 19908 | 20690 | 20804 | |
| .30 | .3 | D (7): | 0 | | | 2 | 7 | 27 | 104 | 388 | 1457 | 4617 | 8524 | 12729 | 16174 | 1.201 |
| | | V̇ (6): | 9247 | 9168 | 9090 | 8937 | 8678 | 8160 | 7249 | 5814 | 3762 | 1673 | 657 | 170 | 0 | |
| | | V (7): | 0 | 506 | 1008 | 1998 | 3690 | 7146 | 13443 | 23996 | 40294 | 56964 | 63694 | 65668 | 65841 | |
| | 1 | D (7): | 0 | | 2 | 7 | 23 | 90 | 347 | 1283 | 4797 | 15073 | 27633 | 41028 | 48756 | 1.142 |
| | | V̇ (6): | 30822 | 30548 | 30277 | 29746 | 28849 | 27054 | 23912 | 18990 | 12031 | 5091 | 1819 | 328 | 0 | |
| | | V (6): | 0 | 152 | 302 | 598 | 1103 | 2128 | 3975 | 7008 | 11505 | 15732 | 17162 | | 17414 | |
| | 3 | D (6): | 0 | | | 2 | 7 | 27 | 103 | 378 | 1391 | 4272 | 7695 | | 11771 | 1.035 |
| | | V̇ (6): | 92446 | 91547 | 90641 | 88868 | 85880 | 79935 | 69639 | 53809 | 32177 | 11873 | 3175 | | 0 | |
| | | V (6): | 0 | 505 | 1003 | 1980 | 3627 | 6911 | 12616 | 21374 | 32820 | 41136 | 42616 | | 42633 | |
| | 10 | D (6): | 0 | | 2 | 7 | 23 | 88 | 332 | 1186 | 4162 | 11986 | 20680 | | 23309 | 0.825 |
| | | V̇ (5): | 30822 | 30404 | 29994 | 29196 | 27868 | 25283 | 20989 | 14847 | 7420 | 1741 | 84 | | 0 | |

## Table 9 (Continued)

| P | A | T: | 0 | .002 | .004 | .008 | .015 | .030 | .060 | .120 | .250 | .500 | .750 | 1.000 | Final | $T_{final}$ |
|---|---|---|---|---|---|---|---|---|---|---|---|---|---|---|---|---|
| | | V (6): | 0 | 1507 | 2979 | 5820 | 10481 | 19319 | 33295 | 51603 | 69808 | 77210 | | | 77317 | |
| .30 | 30 | D (6): | 0 | 1 | 5 | 20 | 67 | 253 | 913 | 3055 | 9739 | 25202 | | | 30955 | 0.590 |
| | | V (5): | 92466 | 90267 | 88139 | 84084 | 77580 | 65751 | 48368 | 27908 | 9431 | 450 | | | 0 | |
| | | V (5): | 0 | 493 | 959 | 1812 | 3097 | 5199 | 7811 | 10227 | 11592 | | | | 11700 | |
| | 100 | D (6): | 0 | 4 | 16 | 62 | 205 | 726 | 2369 | 6931 | 18862 | | | | 30043 | 0.366 |
| | | V (4): | 30822 | 29024 | 27372 | 24446 | 20304 | 14203 | 7778 | 2916 | 362 | | | | 0 | |
| | | V (5): | 0 | 1408 | 2615 | 4574 | 7018 | 10069 | 12707 | 14243 | | | | | 14554 | |
| | 300 | D (6): | 0 | 12 | 45 | 165 | 505 | 1584 | 4456 | 11223 | | | | | 23530 | 0.223 |
| | | V (4): | 92466 | 78821 | 67944 | 51892 | 34628 | 17406 | 6319 | 1269 | | | | | 0 | |
| | | V (5): | 0 | 4007 | 6614 | 9801 | 12613 | 14977 | 16288 | 16622 | | | | | 16623 | |
| | 1000 | D (6): | 0 | 35 | 124 | 400 | 1057 | 2791 | 6701 | 14888 | | | | | 15638 | 0.125 |
| | | V (3): | 30822 | 19210 | 13089 | 7141 | 3298 | 1080 | 227 | 1 | | | | | 0 | |
| | | V (5): | 0 | 8452 | 11745 | 14572 | 16324 | 17411 | 17755 | | | | | | 17762 | |
| | 3000 | D (6): | 0 | 80 | 250 | 692 | 1593 | 3697 | 8066 | | | | | | 10009 | 0.073 |
| | | V (3): | 92466 | 29055 | 13911 | 5196 | 1770 | 393 | 19 | | | | | | 0 | |
| | | V (5): | 0 | 13411 | 15882 | 17400 | 18113 | 18421 | | | | | | | 18440 | |
| | 9000 | D (7): | 0 | 1523 | 3982 | 9527 | 19826 | 42498 | | | | | | | 61565 | 0.043 |
| | | V (2): | 27740 | 2584 | 852 | 236 | 63 | 6 | | | | | | | 0 | |
| | | V (7): | 0 | 200 | 399 | 792 | 1465 | 2845 | 5380 | 9689 | 16489 | 23665 | 26730 | 27787 | 27954 | |
| .35 | .3 | D (7): | 0 | | 1 | 3 | 9 | 35 | 135 | 503 | 1898 | 6037 | 11155 | 16664 | 21476 | 1.214 |
| | | V (6): | 12500 | 12399 | 12300 | 12104 | 11773 | 11105 | 9919 | 8014 | 5213 | 2304 | 902 | 244 | 0 | |
| | | V (7): | 0 | 668 | 1330 | 2638 | 4874 | 9455 | 17828 | 31936 | 53819 | 76087 | 84941 | 87520 | 87766 | |
| | 1 | D (7): | 0 | 1 | 2 | 9 | 30 | 117 | 448 | 1662 | 6236 | 19633 | 35989 | 53412 | 64400 | 1.156 |
| | | V (6): | 41667 | 41314 | 40965 | 40280 | 39119 | 36786 | 32661 | 26086 | 16555 | 6909 | 2433 | 451 | 0 | |
| | | V (6): | 0 | 200 | 399 | 790 | 1456 | 2812 | 5259 | 9284 | 15239 | 20735 | 22522 | | 22817 | |
| | 3 | D (6): | 0 | | 1 | 3 | 9 | 35 | 133 | 488 | 1798 | 5512 | 9904 | | 15059 | 1.032 |
| | | V (5): | 12500 | 12379 | 12260 | 12026 | 11631 | 10842 | 9465 | 7321 | 4343 | 1549 | 392 | | 0 | |
| | | V (6): | 0 | 666 | 1323 | 2610 | 4778 | 9094 | 16560 | 27922 | 42468 | 52503 | 54045 | | 54051 | |
| | 10 | D (6): | 0 | 1 | 2 | 8 | 29 | 114 | 426 | 1517 | 5291 | 15092 | 25877 | | 28159 | 0.802 |
| | | V (5): | 41667 | 41088 | 40520 | 39416 | 37577 | 34002 | 28070 | 19607 | 9475 | 2010 | 54 | | 0 | |
| | | V (6): | 0 | 1986 | 3922 | 7647 | 13727 | 25146 | 42895 | 65500 | 86877 | 94593 | | | 94626 | |
| | 30 | D (6): | 0 | 2 | 6 | 25 | 86 | 322 | 1156 | 3827 | 12011 | 30607 | | | 35439 | 0.563 |
| | | V (4): | 12500 | 12178 | 11867 | 11278 | 10338 | 8651 | 6225 | 3462 | 1084 | 29 | | | 0 | |
| | | V (5): | 0 | 648 | 1255 | 2356 | 3986 | 6582 | 9678 | 12393 | 13795 | | | | 13873 | |
| | 100 | D (6): | 0 | 5 | 21 | 79 | 259 | 908 | 2912 | 8356 | 22309 | | | | 32959 | 0.345 |
| | | V (4): | 41667 | 38931 | 36446 | 32114 | 26131 | 17658 | 9221 | 3240 | 321 | | | | 0 | |
| | | V (5): | 0 | 1836 | 3376 | 5812 | 8748 | 12247 | 15113 | 16674 | | | | | 16934 | |
| | 300 | D (6): | 0 | 15 | 57 | 207 | 623 | 1917 | 5281 | 13059 | | | | | 25233 | 0.210 |
| | | V (3): | 12500 | 10412 | 8801 | 6512 | 4174 | 1991 | 683 | 123 | | | | | 0 | |
| | | V (5): | 0 | 5110 | 8261 | 11945 | 15031 | 17522 | 18828 | | | | | | 19114 | |
| | 1000 | D (6): | 0 | 44 | 153 | 485 | 1257 | 3251 | 7681 | | | | | | 16550 | 0.118 |
| | | V (3): | 41667 | 24324 | 15896 | 8237 | 3639 | 1133 | 220 | | | | | | 0 | |
| | | V (5): | 0 | 10385 | 14091 | 17125 | 18918 | 19993 | 20302 | | | | | | 20305 | |
| | 3000 | D (6): | 0 | 97 | 298 | 809 | 1834 | 4200 | 9082 | | | | | | 10523 | 0.069 |
| | | V (2): | 12500 | 3439 | 1561 | 555 | 183 | 39 | 1 | | | | | | 0 | |
| | | V (5): | 0 | 15854 | 18478 | 20011 | 20716 | 20998 | | | | | | | 21011 | |
| | 9000 | D (7): | 0 | 1799 | 4610 | 10861 | 22381 | 47630 | | | | | | | 64499 | 0.040 |
| | | V (2): | 37500 | 2863 | 897 | 242 | 61 | 5 | | | | | | | 0 | |
| | | V (7): | 0 | 85 | 170 | 338 | 625 | 1216 | 2308 | 4176 | 7152 | 10315 | 11679 | 12169 | 12276 | |
| .40 | .1 | D (8): | 0 | 1 | 3 | 11 | 38 | 147 | 569 | 2126 | 8072 | 25810 | 47818 | 71554 | 99719 | 1.290 |
| | | V (6): | 5405 | 5365 | 5324 | 5245 | 5110 | 4837 | 4346 | 3542 | 2326 | 1035 | 413 | 124 | 0 | |
| | | V (7): | 0 | 256 | 510 | 1013 | 1874 | 3646 | 6909 | 12481 | 21305 | 30570 | 34470 | 35803 | 36019 | |
| | .3 | D (7): | 0 | | 1 | 3 | 11 | 44 | 170 | 636 | 2410 | 7679 | 14187 | 21181 | 27648 | 1.227 |
| | | V (6): | 16216 | 16092 | 15969 | 15727 | 15315 | 14481 | 12986 | 10544 | 6866 | 2996 | 1157 | 314 | 0 | |
| | | V (6): | 0 | 85 | 170 | 337 | 624 | 1211 | 2287 | 4107 | 6931 | 9775 | 10879 | 11191 | 11220 | |
| | 1 | D (7): | 0 | 1 | 3 | 11 | 37 | 147 | 565 | 2102 | 7902 | 24880 | 45545 | 67506 | 81618 | 1.159 |
| | | V (6): | 54054 | 53613 | 53177 | 52320 | 50864 | 47924 | 42680 | 34193 | 21638 | 8843 | 3026 | 542 | 0 | |
| | | V (6): | 0 | 256 | 509 | 1009 | 1861 | 3596 | 6730 | 11882 | 19456 | 26282 | 28390 | | 28705 | |
| | 3 | D (6): | 0 | | 1 | 3 | 11 | 44 | 167 | 615 | 2265 | 6918 | 12385 | | 18505 | 1.020 |
| | | V (5): | 16216 | 16062 | 15909 | 15609 | 15102 | 14087 | 12304 | 9501 | 5565 | 1900 | 445 | | 0 | |
| | | V (6): | 0 | 851 | 1690 | 3332 | 6095 | 11580 | 21018 | 35224 | 52969 | 64529 | 66013 | | 66017 | |
| | 10 | D (6): | 0 | 1 | 3 | 11 | 37 | 143 | 534 | 1893 | 6554 | 18495 | 31501 | | 32888 | 0.776 |
| | | V (5): | 54054 | 53278 | 52516 | 51035 | 48573 | 43790 | 35884 | 24677 | 11475 | 2164 | 17 | | 0 | |
| | | V (5): | 0 | 254 | 500 | 973 | 1740 | 3167 | 5343 | 8033 | 10449 | 11215 | | | 11216 | |
| | 30 | D (6): | 0 | 2 | 8 | 31 | 107 | 402 | 1429 | 4678 | 14454 | 36285 | | | 39581 | 0.537 |
| | | V (4): | 16216 | 15763 | 15327 | 14503 | 13201 | 10894 | 7656 | 4095 | 1183 | 13 | | | 0 | |
| | | V (5): | 0 | 825 | 1591 | 2966 | 4966 | 8064 | 11617 | 14573 | 15964 | | | | 16015 | |
| | 100 | D (6) | 0 | 7 | 26 | 99 | 321 | 1109 | 3499 | 9858 | 25862 | | | | 35565 | 0.326 |
| | | V (4). | 54054 | 50090 | 46531 | 40426 | 32208 | 21021 | 10478 | 3453 | 261 | | | | 0 | |
| | | V (5) | 0 | 2318 | 4220 | 7151 | 10567 | 14457 | 17496 | 19044 | | | | | 19255 | |
| | 300 | D (6). | 0 | 19 | 71 | 254 | 753 | 2271 | 6139 | 14938 | | | | | 26743 | 0.198 |
| | | V (3): | 16216 | 13187 | 10925 | 7832 | 4828 | 2196 | 713 | 114 | | | | | 0 | |
| | | V (5) | 0 | 6310 | 9999 | 14135 | 17440 | 20014 | 21289 | | | | | | 21529 | |
| | 1000 | D (6). | 0 | 54 | 185 | 576 | 1465 | 3724 | 8678 | | | | | | 17359 | 0.111 |
| | | V (3) | 54054 | 29529 | 18538 | 9154 | 3887 | 1155 | 207 | | | | | | 0 | |
| | | V (5): | 0 | 12379 | 16446 | 19635 | 21444 | 22492 | 22762 | | | | | | 22763 | |
| | 3000 | D (6): | 0 | 116 | 349 | 930 | 2080 | 4739 | 10108 | | | | | | 10979 | 0.065 |
| | | V (2) | 16216 | 3921 | 1695 | 576 | 185 | 37 | | | | | | | 0 | |

## Table 9 (Continued)

| P | A | T: | 0 | .002 | .004 | .008 | .015 | .030 | .060 | .120 | .250 | .500 | .750 | 1.000 | Final | $T_{final}$ |
|---|---|---|---|---|---|---|---|---|---|---|---|---|---|---|---|---|
| | | V (5): | 0 | 18272 | 21013 | 22542 | 23232 | 23486 | | | | | | | 23493 | |
| .40 | 9000 | D (7): | 0 | 2086 | 5253 | 12216 | 24965 | 52810 | | | | | | | 67114 | 0.038 |
| | | V̇ (2): | 48649 | 3081 | 919 | 243 | 59 | 3 | | | | | | | 0 | |
| | | V (7): | 0 | 126 | 252 | 500 | 926 | 1808 | 3445 | 6279 | 10842 | 15700 | 17784 | 18546 | 18737 | |
| .50 | .1 | D (7): | 0 | | | 2 | 5 | 21 | 81 | 305 | 1166 | 3750 | 6962 | 10427 | 14825 | 1.310 |
| | | V̇ (6): | 8333 | 8277 | 8222 | 8112 | 7925 | 7541 | 6835 | 5637 | 3733 | 1652 | 660 | 209 | 0 | |
| | | V (7): | 0 | 379 | 755 | 1499 | 2777 | 5416 | 10310 | 18748 | 32238 | 46383 | 52281 | 54316 | 54742 | |
| | .3 | D (7): | 0 | | 1 | 5 | 16 | 63 | 243 | 912 | 3477 | 11134 | 20596 | 30763 | 42156 | 1.274 |
| | | V̇ (6): | 25000 | 24828 | 24657 | 24321 | 23745 | 22564 | 20403 | 16744 | 10974 | 4744 | 1823 | 521 | 0 | |
| | | V (6): | 0 | 126 | 251 | 499 | 924 | 1797 | 3407 | 6149 | 10422 | 14680 | 16291 | 16739 | 16786 | |
| | 1 | D (6): | 0 | | | 2 | 5 | 21 | 81 | 301 | 1135 | 3582 | 6551 | 9701 | 11991 | 1.180 |
| | | V̇ (6): | 83333 | 82710 | 82092 | 80874 | 78794 | 74546 | 66825 | 53929 | 34108 | 13611 | 4542 | 837 | 0 | |
| | | V (6): | 0 | 378 | 753 | 1492 | 2754 | 5325 | 9979 | 17633 | 28792 | 38517 | 41321 | | 41691 | |
| | 3 | D (6): | 0 | | 1 | 5 | 16 | 62 | 238 | 875 | 3219 | 9784 | 17431 | | 25665 | 1.010 |
| | | V̇ (5): | 25000 | 24770 | 24543 | 24096 | 23338 | 21806 | 19081 | 14709 | 8459 | 2720 | 577 | | 0 | |
| | | V (6): | 0 | 1257 | 2495 | 4916 | 8978 | 17010 | 30702 | 50930 | 75199 | 89664 | | | 91114 | |
| | 10 | D (6): | 0 | 1 | 4 | 15 | 52 | 201 | 751 | 2643 | 9037 | 25084 | | | 41899 | 0.744 |
| | | V̇ (5): | 83333 | 82071 | 80833 | 78427 | 74431 | 66692 | 53969 | 36155 | 15816 | 2500 | | | 0 | |
| | | V (5): | 0 | 374 | 736 | 1426 | 2536 | 4560 | 7550 | 11068 | 13977 | | | | 14736 | |
| | 30 | D (6): | 0 | 3 | 11 | 44 | 150 | 559 | 1962 | 6299 | 18986 | | | | 46961 | 0.503 |
| | | V̇ (4): | 25000 | 24203 | 23440 | 22011 | 19783 | 15935 | 10756 | 5400 | 1377 | | | | 0 | |
| | | V (5): | 0 | 1210 | 2316 | 4266 | 7015 | 11082 | 15453 | 18806 | 20176 | | | | 20198 | |
| | 100 | D (6): | 0 | 9 | 36 | 137 | 440 | 1491 | 4579 | 12540 | 32074 | | | | 40074 | 0.302 |
| | | V̇ (4): | 83333 | 76067 | 69685 | 59047 | 45357 | 27936 | 12931 | 3867 | 175 | | | | 0 | |
| | | V (5): | 0 | 3350 | 5992 | 9889 | 14180 | 18740 | 22055 | 23584 | | | | | 23731 | |
| | 300 | D (6): | 0 | 26 | 98 | 343 | 993 | 2907 | 7632 | 18145 | | | | | 29349 | 0.182 |
| | | V̇ (3): | 25000 | 19466 | 15572 | 10581 | 6127 | 2588 | 775 | 101 | | | | | 0 | |
| | | V (5): | 0 | 8772 | 13461 | 18387 | 22041 | 24735 | 25977 | | | | | | 26158 | |
| | 1000 | D (6): | 0 | 73 | 245 | 739 | 1829 | 4528 | 10350 | | | | | | 18758 | 0.102 |
| | | V̇ (3): | 83333 | 40540 | 23831 | 10903 | 4371 | 1220 | 191 | | | | | | 0 | |
| | | V (5): | 0 | 16256 | 20959 | 24368 | 26234 | 27243 | | | | | | | 27462 | |
| | 3000 | D (6): | 0 | 156 | 445 | 1144 | 2500 | 5564 | | | | | | | 11778 | 0.060 |
| | | V̇ (2): | 25000 | 4890 | 1951 | 629 | 191 | 35 | | | | | | | 0 | |
| | | V (5): | 0 | 22867 | 25819 | 27343 | 28009 | 28228 | | | | | | | 28230 | |
| | 9000 | D (7): | 0 | 2584 | 6340 | 14474 | 29240 | 61350 | | | | | | | 71606 | 0.035 |
| | | V̇ (2): | 75000 | 3527 | 973 | 249 | 57 | 2 | | | | | | | 0 | |
| | | V (7): | 0 | 175 | 348 | 693 | 1285 | 2512 | 4805 | 8800 | 15268 | 22113 | 25002 | 26050 | 26325 | |
| .60 | .1 | D (7): | 0 | | 1 | 2 | 7 | 28 | 110 | 415 | 1594 | 5139 | 9539 | 14279 | 20689 | 1.330 |
| | | V̇ (6): | 11842 | 11770 | 11699 | 11557 | 11314 | 10807 | 9858 | 8189 | 5434 | 2368 | 933 | 299 | 0 | |
| | | V (7): | 0 | 524 | 1045 | 2077 | 3852 | 7525 | 14372 | 26250 | 45311 | 65121 | 73208 | 75953 | 76552 | |
| | .3 | D (7): | 0 | | 2 | 6 | 22 | 85 | 329 | 1239 | 4746 | 15223 | 28139 | 41990 | 58498 | 1.292 |
| | | V̇ (6): | 35526 | 35304 | 35082 | 34643 | 33888 | 32322 | 29394 | 24275 | 15905 | 6741 | 2536 | 724 | 0 | |
| | | V (6): | 0 | 175 | 348 | 691 | 1280 | 2495 | 4741 | 8580 | 14555 | 20398 | 22528 | 23091 | 23148 | |
| | 1 | D (6): | 0 | | 1 | 2 | 7 | 28 | 109 | 408 | 1543 | 4861 | 8868 | 13102 | 16217 | 1.182 |
| | | V̇ (5): | 11842 | 11759 | 11677 | 11514 | 11235 | 10659 | 9593 | 7763 | 4872 | 1879 | 600 | 104 | 0 | |
| | | V (6): | 0 | 523 | 1042 | 2065 | 3812 | 7374 | 13817 | 24382 | 39565 | 52265 | 55616 | | 55989 | |
| | 3 | D (6): | 0 | | 2 | 6 | 21 | 84 | 321 | 1179 | 4325 | 13048 | 23105 | | 32969 | 0.988 |
| | | V̇ (5): | 35526 | 35205 | 34887 | 34260 | 33192 | 31022 | 27119 | 20772 | 11645 | 3485 | 649 | | 0 | |
| | | V (5): | 0 | 174 | 345 | 679 | 1238 | 2336 | 4187 | 6863 | 9934 | 11600 | | | 11724 | |
| | 10 | D (6): | 0 | 1 | 5 | 20 | 70 | 270 | 1002 | 3497 | 11793 | 32183 | | | 50288 | 0.709 |
| | | V̇ (4): | 11842 | 11651 | 11463 | 11098 | 10495 | 9331 | 7435 | 4832 | 1979 | 255 | | | 0 | |
| | | V (5): | 0 | 516 | 1014 | 1957 | 3456 | 6138 | 9973 | 14261 | 17542 | | | | 18240 | |
| | 30 | D (6): | 0 | 4 | 15 | 59 | 200 | 739 | 2558 | 8057 | 23730 | | | | 53438 | 0.472 |
| | | V̇ (4): | 35526 | 34242 | 33021 | 30752 | 27269 | 21412 | 13869 | 6545 | 1468 | | | | 0 | |
| | | V (5): | 0 | 1661 | 3157 | 5741 | 9278 | 14280 | 19338 | 22955 | 24240 | | | | 24247 | |
| | 100 | D (6): | 0 | 12 | 48 | 181 | 575 | 1907 | 5716 | 15274 | 38258 | | | | 43920 | 0.282 |
| | | V̇ (3): | 11842 | 10641 | 9609 | 7939 | 5883 | 3430 | 1487 | 406 | 9 | | | | 0 | |
| | | V (5): | 0 | 4532 | 7966 | 12826 | 17890 | 22992 | 26456 | 27914 | | | | | 28011 | |
| | 300 | D (6): | 0 | 35 | 128 | 441 | 1250 | 3562 | 9130 | 21309 | | | | | 31570 | 0.170 |
| | | V̇ (3): | 35526 | 26463 | 20454 | 13213 | 7247 | 2864 | 801 | 84 | | | | | 0 | |
| | | V (5): | 0 | 11430 | 17048 | 22631 | 26516 | 29252 | 30426 | | | | | | 30558 | |
| | 1000 | D (6): | 0 | 94 | 308 | 907 | 2196 | 5324 | 11988 | | | | | | 19952 | 0.095 |
| | | V̇ (2): | 11842 | 5146 | 2850 | 1219 | 466 | 123 | 17 | | | | | | 0 | |
| | | V (5): | 0 | 20161 | 25382 | 28914 | 30780 | 31741 | | | | | | | 31917 | |
| | 3000 | D (6): | 0 | 194 | 538 | 1353 | 2909 | 6393 | | | | | | | 12456 | 0.056 |
| | | V̇ (2): | 35526 | 5718 | 2124 | 656 | 192 | 32 | | | | | | | 0 | |
| | | V (5): | 0 | 27313 | 30406 | 31899 | 32525 | 32714 | | | | | | | 32714 | |
| | 9000 | D (7): | 0 | 3083 | 7414 | 16684 | 33410 | 69669 | | | | | | | 75464 | 0.032 |
| | | V (1): | 10658 | 384 | 99 | 25 | 5 | | | | | | | | 0 | |
| | | V (7): | 0 | 228 | 455 | 905 | 1678 | 3280 | 6264 | 11447 | 19774 | 28472 | 32092 | 33402 | 33790 | |
| .70 | .1 | D (7): | 0 | | 1 | 3 | 9 | 36 | 140 | 526 | 20.4 | 6467 | 11968 | 17885 | 27204 | 1.384 |
| | | V̇ (6): | 15909 | 15810 | 15711 | 15516 | 15179 | 14481 | 13175 | 10889 | 7151 | 3065 | 1196 | 388 | 0 | |
| | | V (7): | 0 | 685 | 1366 | 2714 | 5030 | 9821 | 18729 | 34116 | 58594 | 83649 | 93707 | 97100 | 97878 | |
| | .3 | D (7): | 0 | | 2 | 8 | 27 | 108 | 418 | 1570 | 5992 | 19123 | 35233 | 52470 | 74779 | 1.317 |
| | | V̇ (6): | 47727 | 47418 | 47111 | 46502 | 45455 | 43288 | 39247 | 32221 | 20859 | 8669 | 3220 | 930 | 0 | |
| | | V (6): | 0 | 228 | 455 | 903 | 1672 | 3254 | 6169 | 11118 | 18726 | 26006 | 28589 | 29257 | 29325 | |
| | 1 | D (6): | 0 | | 1 | 3 | 9 | 36 | 138 | 515 | 1941 | 6073 | 11030 | 16253 | 20284 | 1.191 |
| | | V̇ (5): | 15909 | 15793 | 15677 | 15449 | 15057 | 14252 | 12767 | 10242 | 6318 | 2366 | 736 | 127 | 0 | |

## Table 9 (Continued)

| P | A | T: | 0 | .002 | .004 | .008 | .015 | .030 | .060 | .120 | .250 | .500 | .750 | 1.000 | Final | $T_{final}$ |
|---|---|---|---|---|---|---|---|---|---|---|---|---|---|---|---|---|
| | | V (6): | 0 | 684 | 1361 | 2696 | 4970 | 9593 | 17900 | 31353 | 50269 | 65532 | 69320 | | 69708 | |
| .70 | 3 | D (6): | 0 | | 2 | 8 | 27 | 106 | 405 | 1483 | 5392 | 16090 | 28317 | | 39757 | 0.978 |
| | | V̂ (5): | 47727 | 47265 | 46807 | 45907 | 44377 | 41283 | 35773 | 26965 | 14672 | 4164 | 718 | | 0 | |
| | | V (5): | 0 | 227 | 500 | 884 | 1607 | 3016 | 5352 | 8641 | 12259 | 14091 | | | 14200 | |
| | 10 | D (6): | 0 | 2 | 7 | 26 | 89 | 340 | 1254 | 4332 | 14375 | 38619 | | | 57995 | 0.690 |
| | | V̂ (4): | 15909 | 15624 | 15344 | 14805 | 13917 | 12228 | 9544 | 5997 | 2323 | 259 | | | 0 | |
| | | V (5): | 0 | 673 | 1319 | 2534 | 4441 | 7786 | 12411 | 17350 | 20895 | | | | 21555 | |
| | 30 | D (6): | 0 | 5 | 19 | 75 | 252 | 920 | 3142 | 9713 | 28030 | | | | 59489 | 0.454 |
| | | V̂ (4): | 47727 | 45771 | 43925 | 40531 | 35415 | 27071 | 16841 | 7529 | 1538 | | | | 0 | |
| | | V (5): | 0 | 2154 | 4065 | 7302 | 11612 | 17452 | 23080 | 26882 | 28088 | | | | 28091 | |
| | 100 | D (6): | 0 | 16 | 61 | 226 | 709 | 2309 | 6775 | 17747 | 43749 | | | | 47593 | 0.269 |
| | | V̂ (3): | 15909 | 14071 | 12528 | 10101 | 7237 | 4024 | 1650 | 420 | 4 | | | | 0 | |
| | | V (5): | 0 | 5796 | 10027 | 15800 | 21532 | 27050 | 30624 | 32019 | | | | | 32087 | |
| | 300 | D (6): | 0 | 44 | 159 | 537 | 1494 | 4166 | 10478 | 24117 | | | | | 33687 | 0.161 |
| | | V̂ (3): | 47727 | 34077 | 25521 | 15762 | 8262 | 3105 | 822 | 71 | | | | | 0 | |
| | | V (5): | 0 | 14136 | 20600 | 26691 | 30787 | 33526 | 34651 | | | | | | 34753 | |
| | 1000 | D (6): | 0 | 114 | 369 | 1064 | 2529 | 6035 | 13437 | | | | | | 21070 | 0.091 |
| | | V̂ (2): | 15909 | 6241 | 3284 | 1339 | 489 | 125 | 15 | | | | | | 0 | |
| | | V (5): | 0 | 23956 | 29627 | 33241 | 35085 | 36019 | | | | | | | 36162 | |
| | 3000 | D (6): | 0 | 230 | 624 | 1540 | 3271 | 7126 | | | | | | | 13080 | 0.053 |
| | | V̂ (2): | 47727 | 6498 | 2269 | 678 | 195 | 30 | | | | | | | 0 | |
| | | V (5): | 0 | 31560 | 34768 | 36223 | 36821 | | | | | | | | 36985 | |
| | 9000 | D (7): | 0 | 3537 | 8371 | 18637 | 37083 | | | | | | | | 79003 | 0.031 |
| | | V̂ (1): | 14318 | 412 | 100 | 25 | 5 | | | | | | | | 0 | |
| | | V (7): | 0 | 290 | 579 | 1150 | 2132 | 4163 | 7939 | 14462 | 24841 | 35480 | 39802 | 41337 | 41793 | |
| .80 | .1 | D (7): | 0 | | 1 | 3 | 11 | 45 | 175 | 656 | 2505 | 7995 | 14738 | 21965 | 33526 | 1.391 |
| | | V̂ (6): | 20513 | 20380 | 20248 | 19987 | 19538 | 18608 | 16872 | 13853 | 8970 | 3748 | 1429 | 458 | 0 | |
| | | V (6): | 0 | 87 | 174 | 345 | 639 | 1246 | 2372 | 4306 | 7349 | 10399 | 11590 | 11982 | 12070 | |
| | .3 | D (7): | 0 | 1 | 2 | 10 | 34 | 135 | 522 | 1959 | 7443 | 23602 | 43295 | 64289 | 92126 | 1.325 |
| | | V̂ (6): | 61538 | 61124 | 60712 | 59896 | 58494 | 55596 | 50212 | 40913 | 26071 | 10530 | 3806 | 1075 | 0 | |
| | | V (6): | 0 | 290 | 578 | 1147 | 2122 | 4125 | 7801 | 13991 | 23363 | 32088 | 35065 | 35794 | 35862 | |
| | 1 | D (6): | 0 | | 1 | 3 | 11 | 45 | 173 | 642 | 2402 | 7453 | 13464 | 19772 | 24478 | 1.185 |
| | | V̂ (5): | 20513 | 20355 | 20198 | 19889 | 19359 | 18271 | 16277 | 12921 | 7802 | 2810 | 835 | 133 | 0 | |
| | | V (6): | 0 | 869 | 1730 | 3423 | 6303 | 12133 | 22531 | 39141 | 61924 | 79544 | 83588 | | 83939 | |
| | 3 | D (6): | 0 | 1 | 2 | 10 | 34 | 133 | 505 | 1836 | 6612 | 19496 | 34073 | | 46544 | 0.959 |
| | | V̂ (5): | 61538 | 60897 | 60263 | 59017 | 56907 | 52663 | 45184 | 33452 | 17594 | 4678 | 714 | | 0 | |
| | | V (5): | 0 | 288 | 571 | 1120 | 2029 | 3784 | 6644 | 10560 | 14678 | 16607 | | | 16697 | |
| | 10 | D (6): | 0 | 2 | 8 | 32 | 111 | 423 | 1547 | 5281 | 17241 | 45592 | | | 65299 | 0.666 |
| | | V̂ (4): | 20513 | 20105 | 19708 | 18943 | 17694 | 15350 | 11719 | 7106 | 2594 | 242 | | | 0 | |
| | | V (5): | 0 | 853 | 1668 | 3189 | 5547 | 9594 | 15004 | 20524 | 24235 | | | | 24822 | |
| | 30 | D (6): | 0 | 6 | 24 | 93 | 312 | 1129 | 3798 | 11531 | 32641 | | | | 65051 | 0.435 |
| | | V̂ (4): | 61538 | 58697 | 56037 | 51202 | 44050 | 32749 | 19558 | 8281 | 1524 | | | | 0 | |
| | | V (5): | 0 | 2716 | 5086 | 9024 | 14120 | 20743 | 26829 | 30720 | | | | | 31823 | |
| | 100 | D (6): | 0 | 20 | 75 | 278 | 860 | 2754 | 7921 | 20371 | | | | | 50915 | 0.256 |
| | | V̂ (3): | 20513 | 17840 | 15650 | 12305 | 8522 | 4524 | 1762 | 418 | | | | | 0 | |
| | | V (5): | 0 | 7202 | 12261 | 18922 | 25237 | 31069 | 34673 | 35976 | | | | | 36017 | |
| | 300 | D (6): | 0 | 54 | 194 | 645 | 1760 | 4812 | 11900 | 27053 | | | | | 35593 | 0.153 |
| | | V̂ (3): | 61538 | 42031 | 30491 | 18019 | 9051 | 3245 | 815 | 55 | | | | | 0 | |
| | | V (5): | 0 | 16984 | 24234 | 30726 | 34938 | 37657 | 38709 | | | | | | 38782 | |
| | 1000 | D (6): | 0 | 141 | 440 | 1235 | 2885 | 6784 | 14955 | | | | | | 22077 | 0.086 |
| | | V̂ (2): | 20513 | 7263 | 3636 | 1418 | 500 | 123 | 13 | | | | | | 0 | |
| | | V (5): | 0 | 27759 | 33804 | 37438 | 39233 | 40117 | | | | | | | 40233 | |
| | 3000 | D (6): | 0 | 268 | 715 | 1736 | 3651 | 7891 | | | | | | | 13640 | 0.050 |
| | | V̂ (2): | 61538 | 7122 | 2340 | 678 | 192 | 27 | | | | | | | 0 | |
| | | V (5): | 0 | 35709 | 38955 | 40364 | 40940 | | | | | | | | 41077 | |
| | 9000 | D (7): | 0 | 4015 | 9374 | 20681 | 40924 | | | | | | | | 82115 | 0.02 |
| | | V̂ (1): | 18462 | 428 | 99 | 24 | 5 | | | | | | | | 0 | |
| | | V (7): | 0 | 420 | 838 | 1665 | 3085 | 6019 | 11460 | 20815 | 35558 | 50433 | 56385 | 58504 | 59207 | |
| 1.00 | .1 | D (7): | 0 | | 1 | 5 | 16 | 62 | 240 | 900 | 3421 | 10863 | 19957 | 29685 | 47541 | 1.448 |
| | | V̂ (6): | 31250 | 31041 | 30833 | 30421 | 29714 | 28251 | 25530 | 20826 | 13312 | 5454 | 2063 | 679 | 0 | |
| | | V (6): | 0 | 126 | 251 | 499 | 924 | 1801 | 3422 | 6188 | 10491 | 14723 | 16345 | 16876 | 17013 | |
| | .3 | D (6): | 0 | | | 1 | 5 | 19 | 72 | 268 | 1015 | 3197 | 5842 | 8654 | 12941 | 1.374 |
| | | V̂ (6): | 93750 | 93091 | 92437 | 91141 | 88918 | 84333 | 75847 | 61310 | 38463 | 15169 | 5416 | 1571 | 0 | |
| | | V (6): | 0 | 420 | 837 | 1660 | 3068 | 5953 | 11219 | 20000 | 33058 | 44873 | 48773 | 49711 | 49804 | |
| | 1 | D (6): | 0 | | 1 | 5 | 16 | 62 | 236 | 876 | 3254 | 10002 | 17968 | 26300 | 33134 | 1.203 |
| | | V̂ (5): | 31250 | 30994 | 30740 | 30238 | 29381 | 27629 | 24443 | 19154 | 11289 | 3917 | 1133 | 185 | 0 | |
| | | V (5): | 0 | 126 | 250 | 495 | 909 | 1743 | 3215 | 5520 | 8579 | 10830 | 11315 | | 11352 | |
| | 3 | D (6): | 0 | 1 | 3 | 13 | 47 | 182 | 688 | 2482 | 8821 | 25618 | 44422 | | 59773 | 0.950 |
| | | V̂ (5): | 93750 | 92669 | 91602 | 89512 | 85987 | 78958 | 66779 | 48217 | 24295 | 6047 | 837 | | 0 | |
| | | V (5): | 0 | 417 | 824 | 1612 | 2905 | 5365 | 9265 | 14384 | 19458 | 21628 | | | 21702 | |
| | 10 | D (6): | 0 | 3 | 11 | 44 | 151 | 573 | 2075 | 6959 | 22201 | 57530 | | | 78883 | 0.646 |
| | | V̂ (4): | 31250 | 30529 | 29830 | 28495 | 26343 | 22397 | 16526 | 9523 | 3219 | 244 | | | 0 | |
| | | V (5): | 0 | 1230 | 2394 | 4540 | 7798 | 13202 | 20060 | 26600 | 30664 | | | | 31195 | |
| | 30 | D (6): | 0 | 8 | 33 | 127 | 421 | 1499 | 4933 | 14586 | 40217 | | | | 75037 | 0.416 |
| | | V̂ (4): | 93750 | 88601 | 83847 | 75368 | 63215 | 44977 | 25272 | 9954 | 1610 | | | | 0 | |
| | | V (5): | 0 | 3876 | 7170 | 12466 | 19001 | 27025 | 33893 | 37976 | | | | | 38982 | |
| | 100 | D (6): | 0 | 27 | 102 | 370 | 1124 | 3501 | 9784 | 24539 | | | | | 56771 | 0.243 |
| | | V̂ (3): | 31250 | 26410 | 22601 | 17060 | 11219 | 5553 | 2014 | 437 | | | | | 0 | |

## Table 9 (Concluded)

| P | A | T: | 0 | .002 | .004 | .008 | .015 | .030 | .060 | .120 | .250 | .500 | .750 | 1.000 | Final | $T_{final}$ |
|---|---|---|---|---|---|---|---|---|---|---|---|---|---|---|---|---|
| | | V (5): | 0 | 10033 | 16653 | 24913 | 32218 | 38567 | 42263 | 43476 | | | | | 43498 | |
| 1.00 | 300 | D (6): | 0 | 72 | 254 | 827 | 2198 | 5839 | 14111 | 31574 | | | | | 38927 | 0.145 |
| | | V (3): | 93750 | 59448 | 40990 | 22619 | 10682 | 3599 | 846 | 39 | | | | | 0 | |
| | | V (5): | 0 | 22441 | 31088 | 38257 | 42633 | 45389 | 46370 | | | | | | 46418 | |
| | 1000 | D (6): | 0 | 182 | 551 | 1504 | 3435 | 7925 | 17252 | | | | | | 23839 | 0.081 |
| | | V (2): | 31250 | 9401 | 4355 | 1595 | 543 | 126 | 10 | | | | | | 0 | |
| | | V (5): | 0 | 34854 | 41589 | 45220 | 47022 | 47849 | | | | | | | 47935 | |
| | 3000 | D (6): | 0 | 331 | 857 | 2038 | 4227 | 9043 | | | | | | | 14623 | 0.047 |
| | | V (2): | 93750 | 8471 | 2520 | 721 | 194 | 25 | | | | | | | 0 | |
| | | V (5): | 0 | 43453 | 46703 | 48152 | 48703 | | | | | | | | 48810 | |
| | 9000 | D (7): | 0 | 4754 | 10898 | 23754 | 46671 | | | | | | | | 87711 | 0.027 |
| | | V (1): | 28125 | 467 | 109 | 25 | 5 | | | | | | | | 0 | |
| | | V (7): | 0 | 644 | 1283 | 2545 | 4706 | 9143 | 17279 | 31000 | 52023 | 72550 | 80561 | 83400 | 84435 | |
| 1.3 | .1 | D (7): | 0 | | 2 | 6 | 23 | 89 | 342 | 1272 | 4768 | 14907 | 27164 | 40221 | 68159 | 1.523 |
| | | V (6): | 50904 | 50500 | 50100 | 49312 | 47968 | 45231 | 40280 | 32103 | 19851 | 7861 | 2931 | 981 | 0 | |
| | | V (6): | 0 | 193 | 385 | 763 | 1410 | 2735 | 5153 | 9199 | 15302 | 21098 | 23258 | 23963 | 24163 | |
| | .3 | D (6): | 0 | | | 2 | 7 | 27 | 102 | 379 | 1411 | 4374 | 7924 | 11684 | 18340 | 1.435 |
| | | V (5): | 15271 | 15144 | 15017 | 14769 | 14345 | 13486 | 11940 | 9413 | 5699 | 2166 | 761 | 226 | 0 | |
| | | V (6): | 0 | 643 | 1280 | 2536 | 4673 | 9018 | 16831 | 29538 | 47752 | 63543 | 68549 | 69768 | 69898 | |
| | 1 | D (6): | 0 | | 2 | 6 | 23 | 88 | 336 | 1230 | 4492 | 13551 | 24115 | 35121 | 45333 | 1.230 |
| | | V (5): | 50904 | 50404 | 49910 | 48940 | 47297 | 43997 | 38182 | 27020 | 16374 | 5421 | 1540 | 261 | 0 | |
| | | V (5): | 0 | 193 | 382 | 754 | 1381 | 2626 | 4774 | 8022 | 12117 | 14960 | 15538 | | 15578 | |
| | 3 | D (6): | 0 | 1 | 5 | 19 | 67 | 259 | 970 | 3446 | 11967 | 33980 | 58322 | | 78039 | 0.949 |
| | | V (4): | 15271 | 15057 | 14847 | 14438 | 13757 | 12428 | 10219 | 7064 | 3353 | 781 | 101 | | 0 | |
| | | V (5): | 0 | 637 | 1256 | 2443 | 4367 | 7936 | 13367 | 20085 | 26277 | 28703 | | | 28770 | |
| | 10 | D (6): | 0 | 4 | 16 | 63 | 215 | 807 | 2867 | 9372 | 28995 | 73370 | | | 97398 | 0.632 |
| | | V (4): | 50904 | 49455 | 48062 | 45435 | 41294 | 33999 | 23848 | 12837 | 3991 | 253 | | | 0 | |
| | | V (5): | 0 | 1872 | 3618 | 6780 | 11439 | 18807 | 27541 | 35259 | 39647 | | | | 40132 | |
| | 30 | D (6): | 0 | 12 | 47 | 180 | 588 | 2052 | 6556 | 18764 | 50225 | | | | 88643 | 0.401 |
| | | V (3): | 15271 | 14232 | 13292 | 11664 | 9434 | 6324 | 3294 | 1194 | 170 | | | | 0 | |
| | | V (5): | 0 | 5816 | 10573 | 17897 | 26386 | 36110 | 43817 | 48061 | | | | | 48968 | |
| | 100 | D (6): | 0 | 38 | 143 | 510 | 1509 | 4547 | 12291 | 30002 | | | | | 64662 | 0.232 |
| | | V (3): | 50904 | 41285 | 34139 | 24405 | 15046 | 6869 | 2306 | 455 | | | | | 0 | |
| | | V (5): | 0 | 14564 | 23417 | 33709 | 42203 | 49042 | 52783 | 53889 | | | | | 53899 | |
| | 300 | D (6): | 0 | 99 | 345 | 1085 | 2797 | 7203 | 16988 | 37403 | | | | | 43367 | 0.137 |
| | | V (2): | 15271 | 8748 | 5652 | 2880 | 1262 | 399 | 88 | 2 | | | | | 0 | |
| | | V (5): | 0 | 30518 | 40988 | 48842 | 53364 | 56088 | 56984 | | | | | | 57012 | |
| | 1000 | D (6): | 0 | 240 | 705 | 1863 | 4153 | 9398 | 20201 | | | | | | 26147 | 0.076 |
| | | V (2): | 50904 | 12461 | 5223 | 1787 | 583 | 128 | 8 | | | | | | 0 | |
| | | V (5): | 0 | 44930 | 52201 | 56004 | 57781 | 58541 | | | | | | | 58603 | |
| | 3000 | D (6): | 0 | 416 | 1044 | 2429 | 4966 | 10518 | | | | | | | 15899 | 0.044 |
| | | V (1): | 15271 | 1017 | 285 | 76 | 20 | 2 | | | | | | | 0 | |
| | | V (5): | 0 | 54258 | 57460 | 58925 | 59432 | | | | | | | | 59514 | |
| | 9000 | D (7): | 0 | 5716 | 12862 | 27692 | 54027 | | | | | | | | 94835 | 0.026 |
| | | V (1): | 45813 | 504 | 117 | 25 | 4 | | | | | | | | 0 | |
| | | V (6): | 0 | 97 | 193 | 382 | 705 | 1364 | 2561 | 4546 | 7516 | 10345 | 11436 | 11827 | 11989 | |
| 1.7 | .1 | D (7): | 0 | 1 | 2 | 9 | 31 | 122 | 469 | 1731 | 6412 | 19799 | 35857 | 52921 | 97502 | 1.638 |
| | | V (6): | 83046 | 82300 | 81562 | 80112 | 77653 | 72698 | 63917 | 49918 | 30033 | 11642 | 4342 | 1502 | 0 | |
| | | V (6): | 0 | 290 | 577 | 1144 | 2110 | 4076 | 7628 | 13462 | 22037 | 29966 | 32887 | 33854 | 34170 | |
| | .3 | D (6): | 0 | | 1 | 3 | 9 | 37 | 140 | 515 | 1893 | 5791 | 10424 | 15318 | 25785 | 1.525 |
| | | V (5): | 24914 | 24677 | 24443 | 23984 | 23206 | 21645 | 18899 | 14575 | 8565 | 3181 | 1119 | 348 | 0 | |
| | | V (6): | 0 | 966 | 1921 | 3800 | 6986 | 13412 | 24807 | 42926 | 68075 | 89200 | 95776 | 97464 | 97673 | |
| | 1 | D (6): | 0 | 1 | 2 | 9 | 31 | 121 | 459 | 1664 | 5981 | 17764 | 31384 | 45548 | 61411 | 1.278 |
| | | V (5): | 83046 | 82106 | 81179 | 79366 | 76320 | 70283 | 59924 | 44304 | 24092 | 7753 | 2232 | 419 | 0 | |
| | | V (5): | 0 | 289 | 573 | 1128 | 2056 | 3880 | 6958 | 11460 | 16885 | 20496 | 21221 | | 21279 | |
| | 3 | D (5): | 0 | | 1 | 3 | 9 | 35 | 132 | 460 | 1565 | 4361 | 7427 | | 10100 | 0.965 |
| | | V (4): | 24914 | 24503 | 24101 | 23324 | 22044 | 19599 | 15682 | 10413 | 4703 | 1062 | 145 | | 0 | |
| | | V (5): | 0 | 955 | 1877 | 3630 | 6431 | 11499 | 18903 | 27570 | 35083 | 37881 | | | 37957 | |
| | 10 | D (5): | 0 | 1 | 2 | 9 | 29 | 109 | 380 | 1213 | 3652 | 9067 | | | 11948 | 0.630 |
| | | V (4): | 83046 | 80201 | 77493 | 72452 | 64688 | 51545 | 34415 | 17426 | 5090 | 305 | | | 0 | |
| | | V (5): | 0 | 2792 | 5357 | 9908 | 16414 | 26200 | 37099 | 46108 | 50917 | | | | 51407 | |
| | 30 | D (5): | 0 | 2 | 6 | 24 | 79 | 269 | 836 | 2324 | 6071 | | | | 10426 | 0.395 |
| | | V (3): | 24914 | 22860 | 21046 | 17997 | 14017 | 8867 | 4309 | 1461 | 193 | | | | 0 | |
| | | V (5): | 0 | 8537 | 15235 | 25108 | 35862 | 47424 | 55988 | 60447 | | | | | 61316 | |
| | 100 | D (6): | 0 | 52 | 192 | 672 | 1940 | 5667 | 14882 | 35525 | | | | | 73475 | 0.226 |
| | | V (3): | 83046 | 64348 | 51304 | 34681 | 20100 | 8534 | 2695 | 498 | | | | | 0 | |
| | | V (5): | 0 | 20626 | 32179 | 44690 | 54292 | 61727 | 65583 | 66639 | | | | | 66643 | |
| | 300 | D (6): | 0 | 134 | 449 | 1367 | 3424 | 8581 | 19838 | 43129 | | | | | 48278 | 0.133 |
| | | V (2): | 24914 | 12805 | 7748 | 3670 | 1526 | 454 | 95 | 2 | | | | | 0 | |
| | | V (5): | 0 | 40614 | 53232 | 61542 | 66335 | 69064 | 69913 | | | | | | 69930 | |
| | 1000 | D (6): | 0 | 305 | 866 | 2225 | 4863 | 10833 | 23058 | | | | | | 28706 | 0.074 |
| | | V (2): | 83046 | 16580 | 6232 | 2076 | 643 | 137 | 7 | | | | | | 0 | |
| | | V (5): | 0 | 57276 | 64994 | 69046 | 70809 | 71537 | | | | | | | 71587 | |
| | 3000 | D (6): | 0 | 503 | 1230 | 2810 | 5681 | 11938 | | | | | | | 17324 | 0.043 |
| | | V (1): | 24914 | 1224 | 333 | 83 | 21 | 2 | | | | | | | 0 | |
| | | V (5): | 0 | 67375 | 70525 | 71957 | 72458 | | | | | | | | 72529 | |
| | 9000 | D (6): | 0 | 666 | 1476 | 3148 | 6108 | | | | | | | | 10285 | 0.025 |
| | | V (1): | 74741 | 543 | 126 | 27 | 4 | | | | | | | | 0 | |

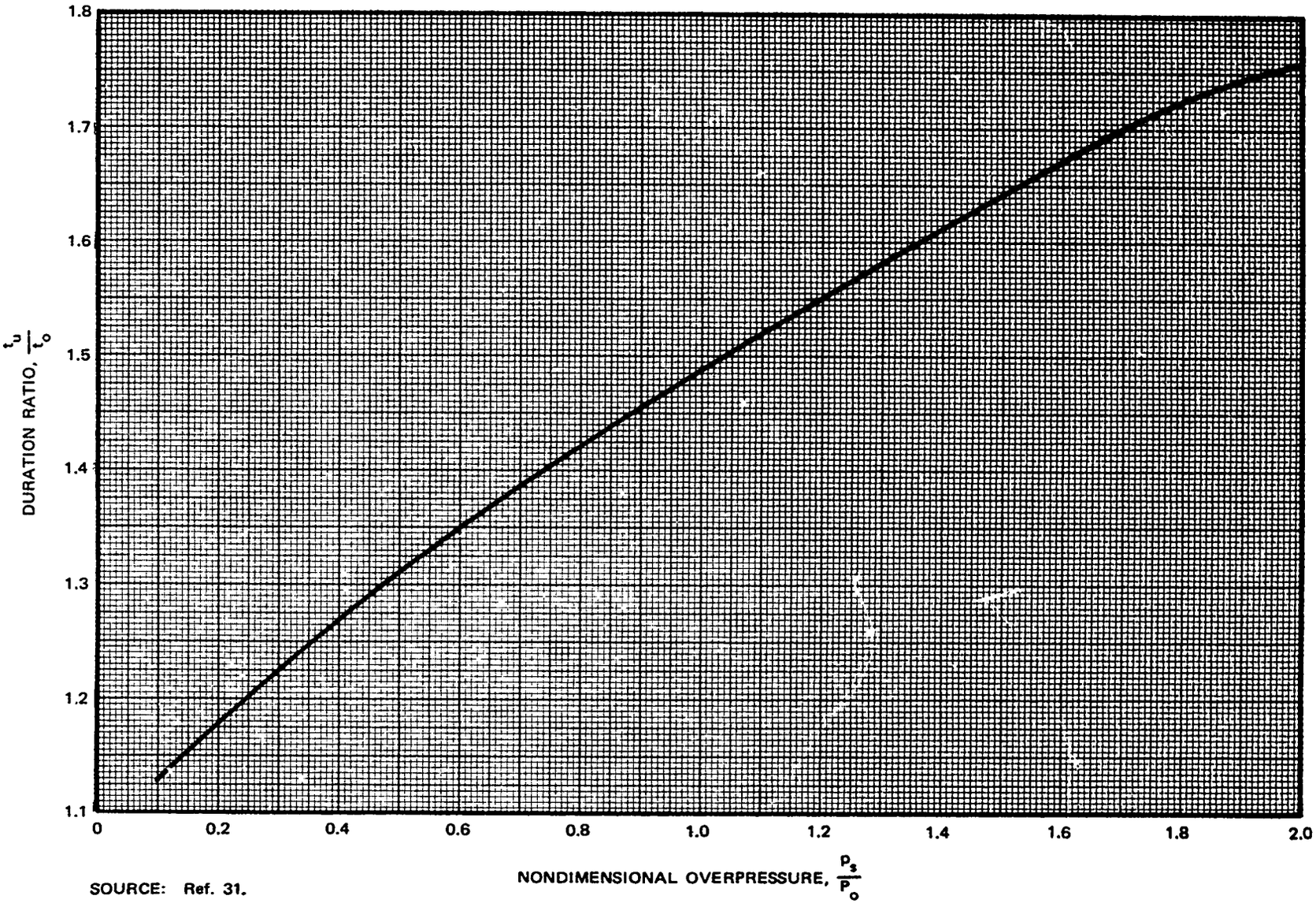


SOURCE: Ref. 31.

FIG. 13 RATIO OF DURATION OF WIND TO POSITIVE PHASE DURATION AS A FUNCTION OF OVERPRESSURE

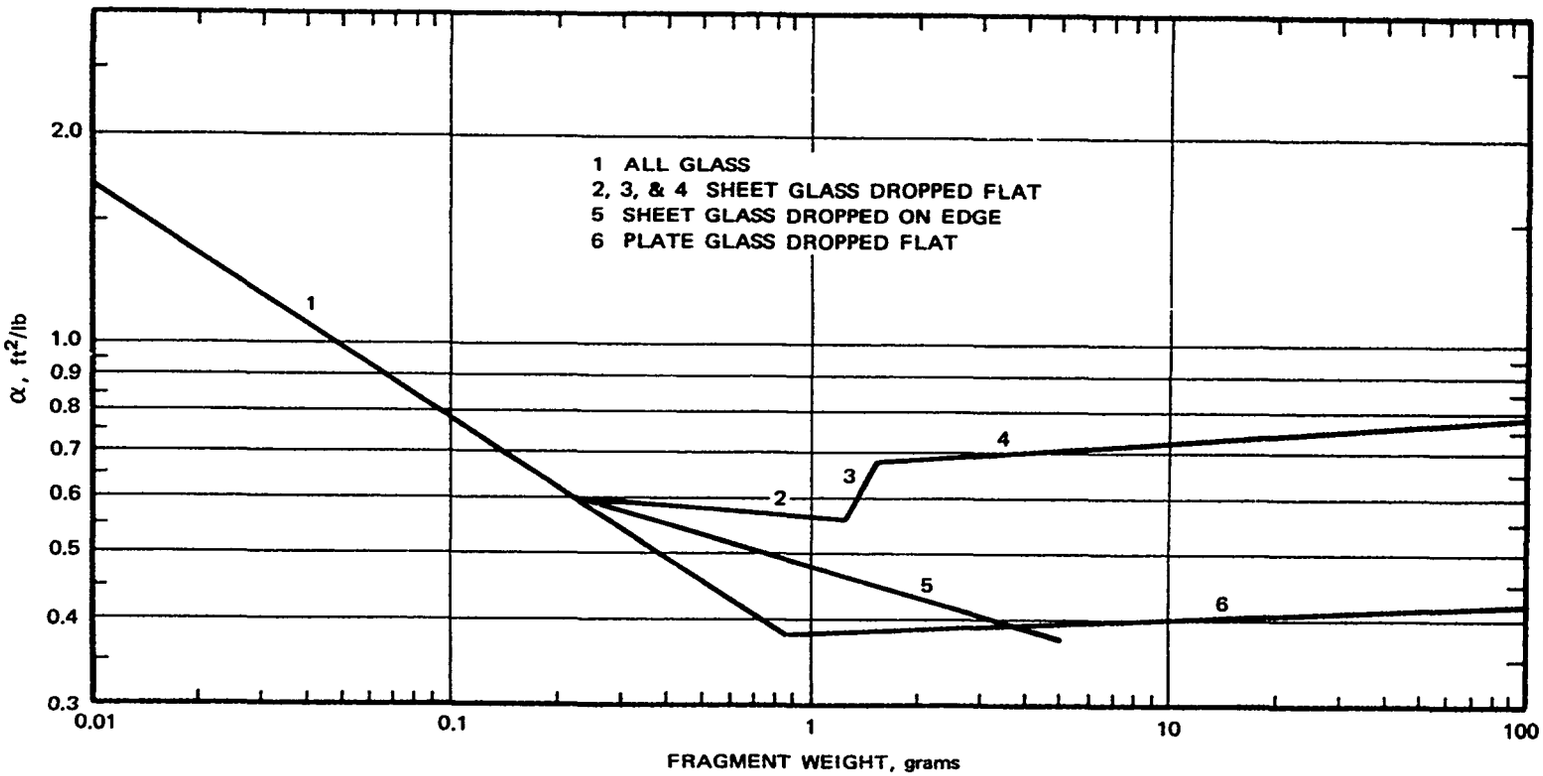


SOURCE: Ref. 32.

FIG. 14 SUMMARY OF ACCELERATION COEFFICIENT DATA FOR GLASS FRAGMENTS

which means that the decimal point has been moved six places to the right. Thus, V is actually 0.055677. $T_{final}$ in Table 9 is the time when the missile velocity and the wind velocity become equal.

Figures 15 through 20 were prepared[31] using Table 9. The figures provide maximum velocity and the corresponding travel distance as a function of $\alpha$ for W = 1, 20, and 1,000 kilotons.

To check the validity of the model, glass missiles emanating from windows in house walls that faced ground zero were trapped during the Operation Plumbbob test series. In general, the model predicted velocities lower than those measured in the field. The results of the tests are discussed in the following extracts from the test report.

> Velocities predicted for glass fragments on the basis of a free-field blast wave ignored any possible modification of the wave . . . by the structure containing the window in the case of the house installations. In some instances . . . the modification noted (as signified by missile velocities) was great enough to suggest that velocities also be computed for a blast wave with a duration the same as that for the free-field wave and with a maximum overpressure equal to the reflected overpressure assuming normal incidence of the free-field blast wave. Although this procedure cannot be rigorously defended by theory, its usefulness as an empirical guide in the prediction of missile velocities is apparent, provided, of course, that it conforms with the experimental evidence available.

It also seems possible that the discrepancies between predicted velocity and measured velocity might be a result of the assumption of zero initial velocity.

> It was observed that the steel window frames used in houses . . . were usually slightly bent in the direction of the blast wave. One frame in a house was actually blown free of its mount. . . . It is doubtful that the frames would have been bent if they had not contained glass. Thus one might suppose that defractive (sic) loading contributed not only to fragmentation of the glass but also to the acquisition of an initial velocity by the window panes before fragmentation was complete. . . .

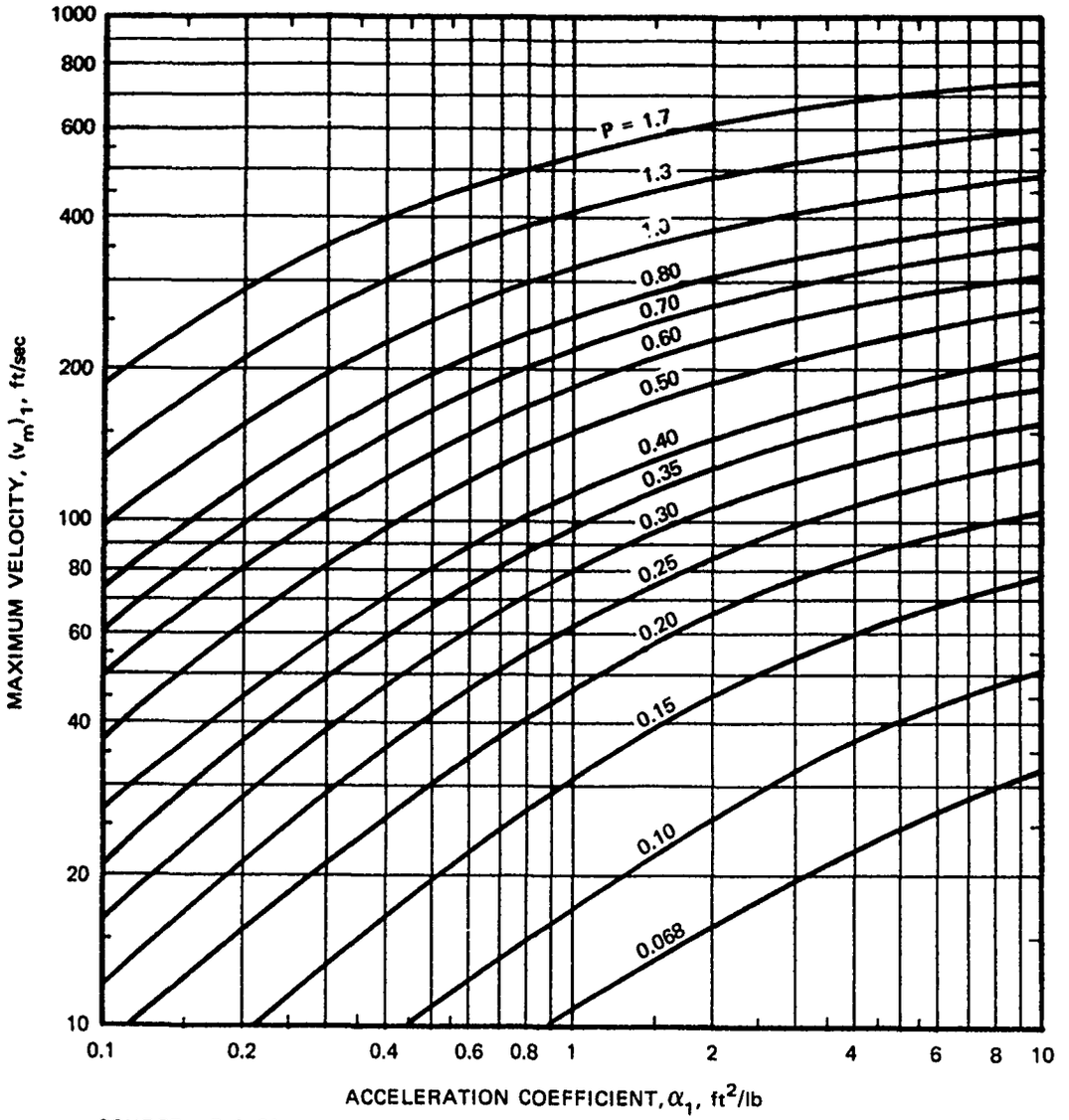


SOURCE: Ref. 31.

FIG. 15 PREDICTED MAXIMUM VELOCITY AS A FUNCTION OF ACCELERATION COEFFICIENT AND NONDIMENSIONAL PEAK OVERPRESSURE
Computed for W = 1 kt, $P_o$ = 14.7 psi, and $c_o$ = 1117 ft/sec
For other conditions, use:

$$\alpha_1 = \alpha\left(\frac{1117}{c_o}\right)^2\left(\frac{P_o}{14.7}\right)^{2/3} W^{1/3}$$

$$v_m = (v_m)_1\left(\frac{c_o}{1117}\right)$$

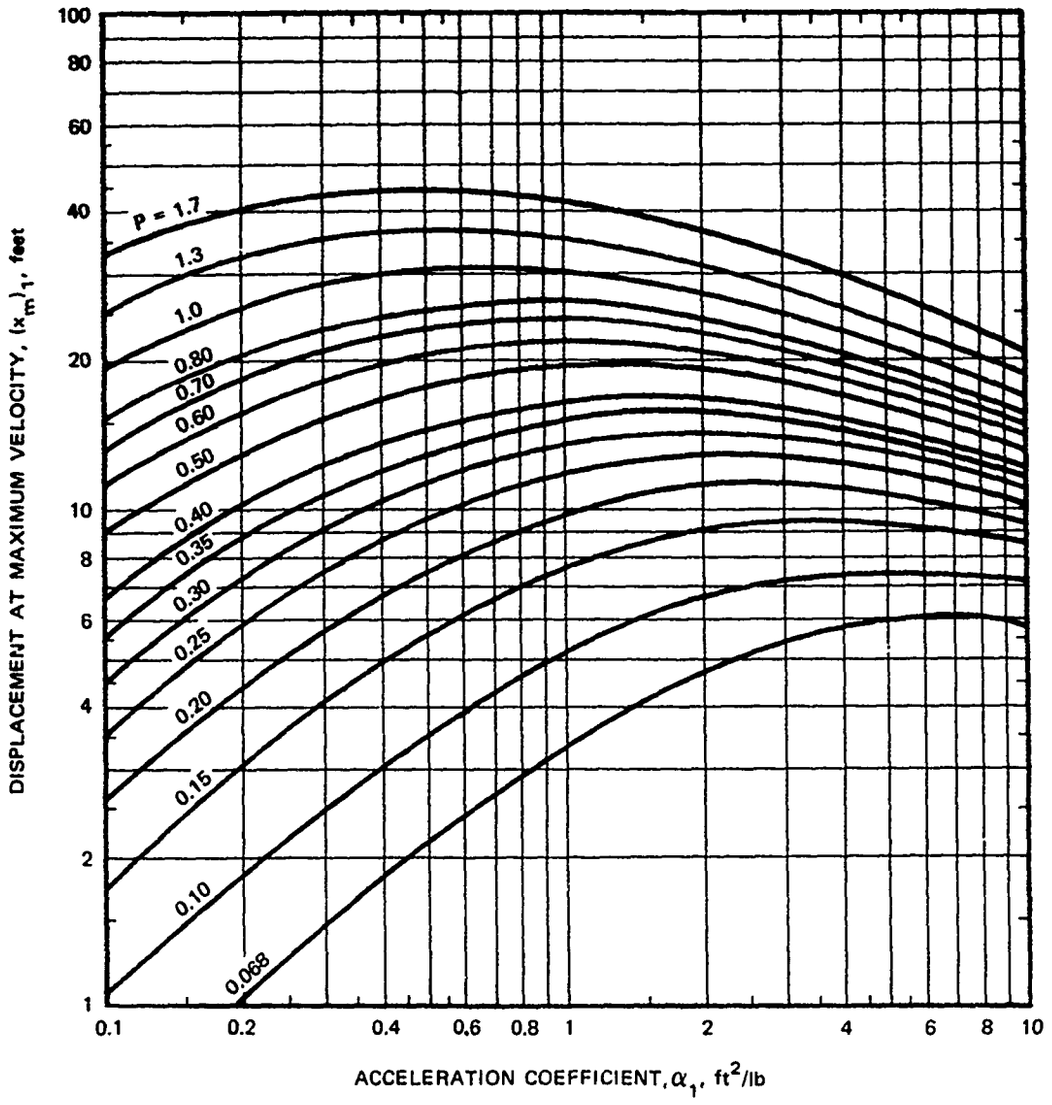


SOURCE: Ref. 31.

FIG. 16 PREDICTED DISPLACEMENT AT MAXIMUM VELOCITY AS A FUNCTION OF ACCELERATION COEFFICIENT AND NONDIMENSIONAL PEAK OVERPRESSURE
Computed for W = 1 kt, $P_o$ = 14.7 psi, and $c_o$ = 1117 ft/sec
For other conditions, use:

$$\alpha_1 = \alpha \left(\frac{1117}{c_o}\right)^2 \left(\frac{P_o}{14.7}\right)^{2/3} W^{1/3}$$

$$x_m = (x_m)_1 \left(\frac{14.7W}{P_o}\right)^{1/3}$$

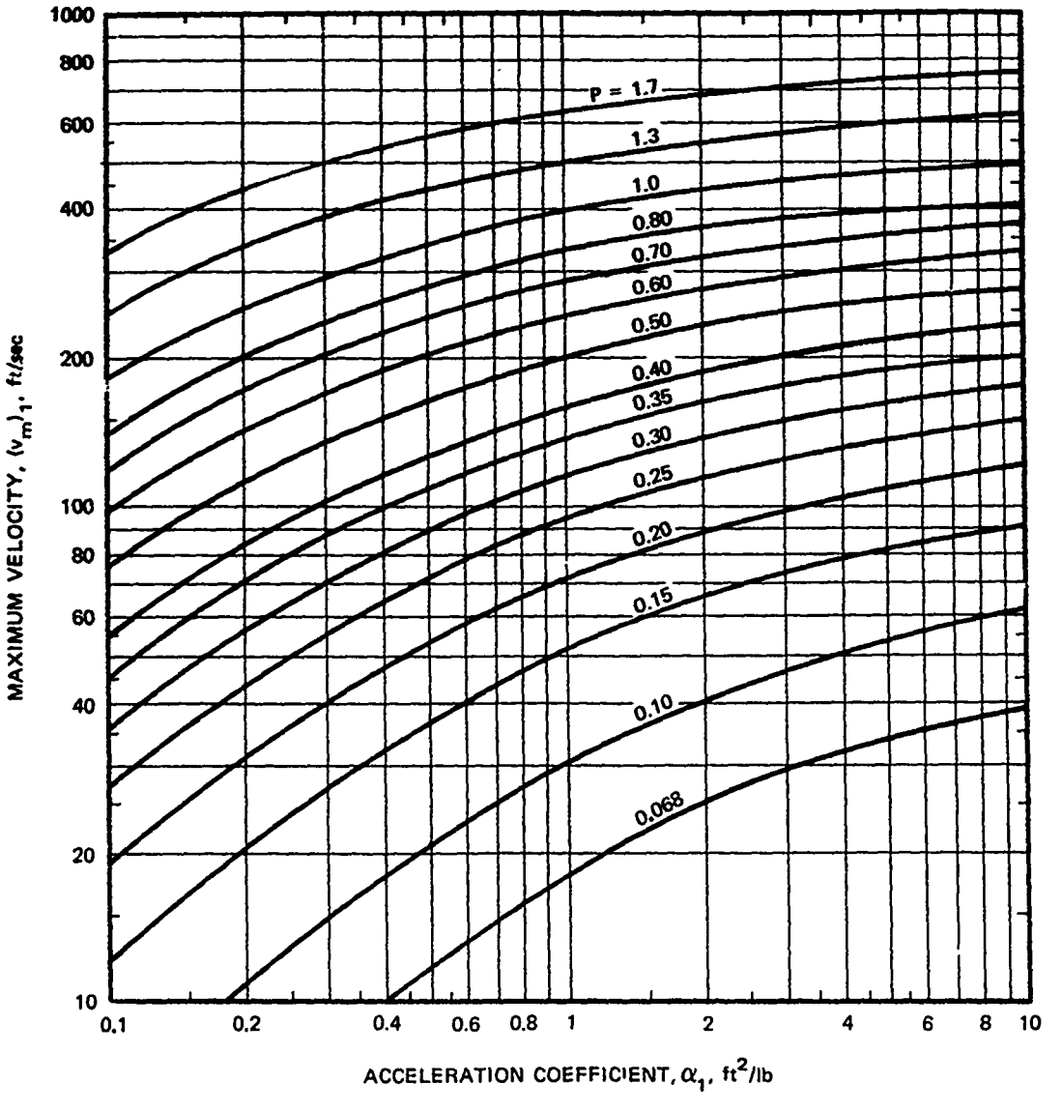


SOURCE: Ref. 31.

FIG. 17 PREDICTED MAXIMUM VELOCITY AS A FUNCTION OF ACCELERATION COEFFICIENT AND NONDIMENSIONAL PEAK OVERPRESSURE
Computed for W = 20 kt, $P_o$ = 14.7 psi, $c_o$ = 1117 ft/sec.
For other conditions, use:

$$\alpha_1 = \alpha\left(\frac{1117}{c_o}\right)^2\left(\frac{P_o}{14.7}\right)^{2/3}\left(\frac{W}{20}\right)^{1/3}$$

$$v_m = (v_m)_1\left(\frac{c_o}{1117}\right)$$

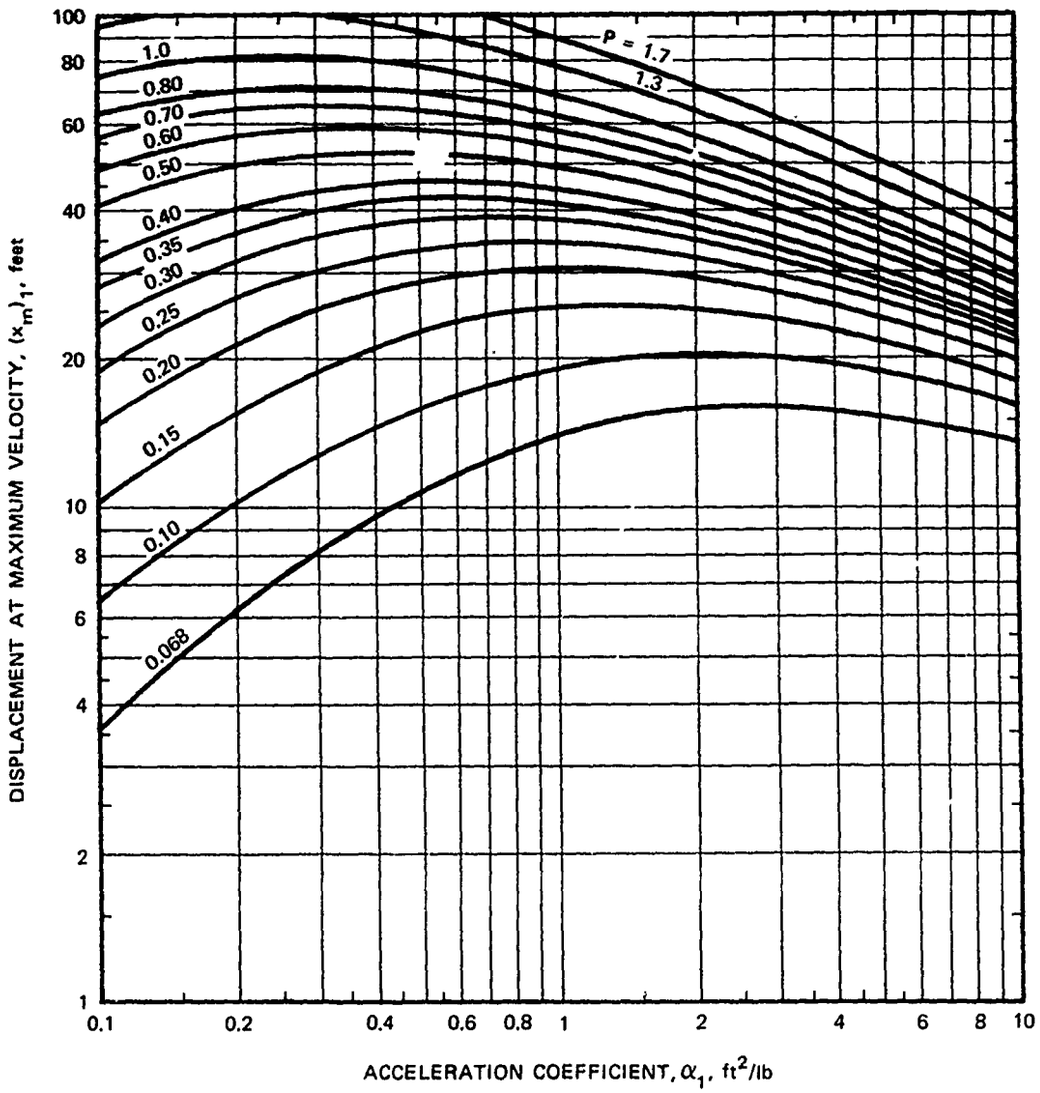


SOURCE: Ref. 31.

FIG. 18 PREDICTED DISPLACEMENT AT MAXIMUM VELOCITY AS A FUNCTION OF ACCELERATION COEFFICIENT AND NONDIMENSIONAL PEAK OVERPRESSURE
Computed for W = 20 kt, $P_o$ = 14.7 psi, and $c_o$ = 1117 ft/sec.
For other conditions, use:

$$\alpha_1 = \alpha\left(\frac{1117}{c_o}\right)^2\left(\frac{P_o}{14.7}\right)^{2/3}\left(\frac{W}{20}\right)^{1/3}$$

$$x_m = (x_m)_1\left(\frac{14.7W}{P_o 20}\right)^{1/3}$$

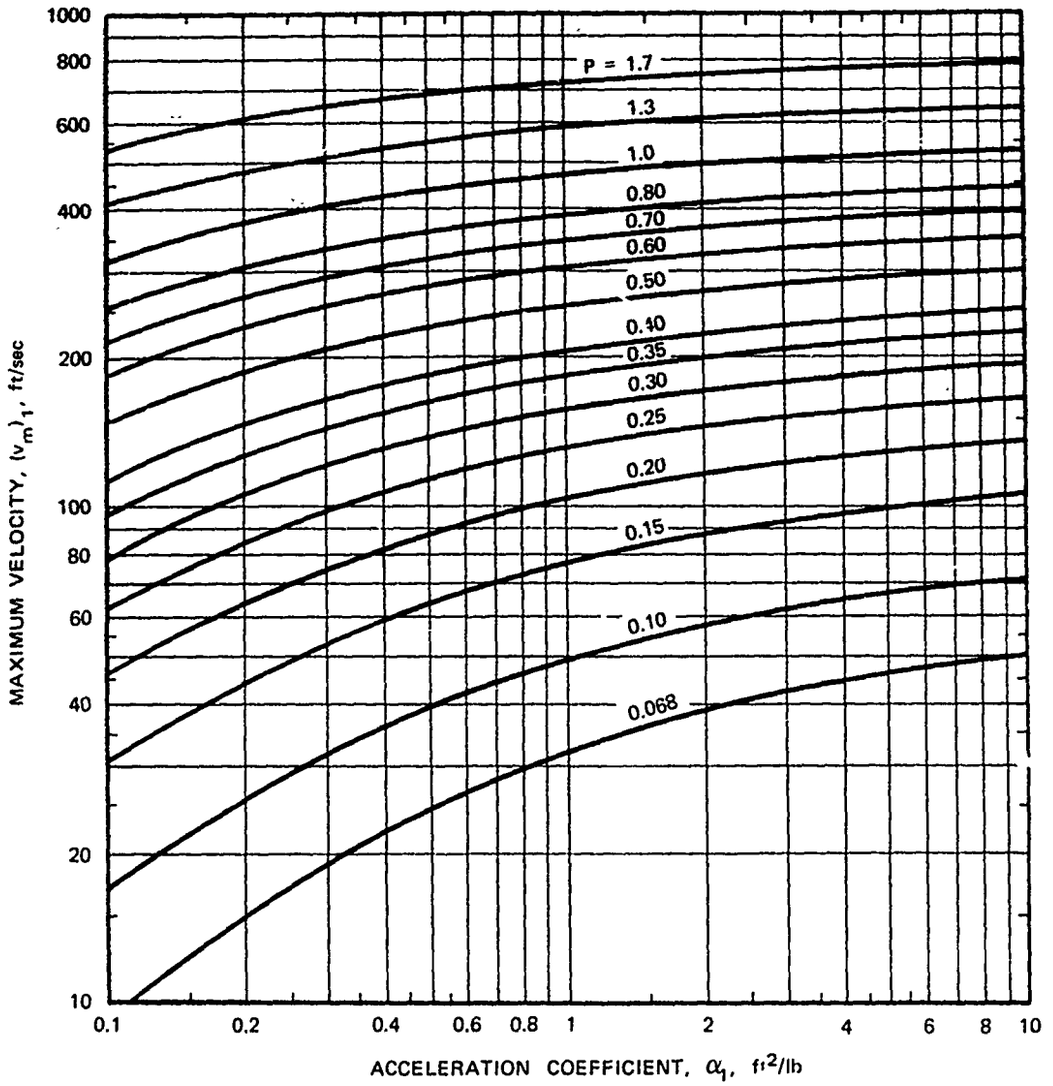


SOURCE: Ref. 31.

FIG. 19 PREDICTED MAXIMUM VELOCITY AS A FUNCTION OF ACCELERATION COEFFICIENT AND NONDIMENSIONAL PEAK OVERPRESSURE

Computed for W = 1 Mt, $P_o$ = 14.7 psi, and $c_o$ = 1117 ft/sec.
For other conditions, use:

$$\alpha_1 = \alpha\left(\frac{1117}{c_o}\right)^2\left(\frac{P_o}{14.7}\right)^{2/3}\left(\frac{W}{1000}\right)^{1/3}$$

$$v_m = (v_m)_1\left(\frac{c_o}{1117}\right)$$

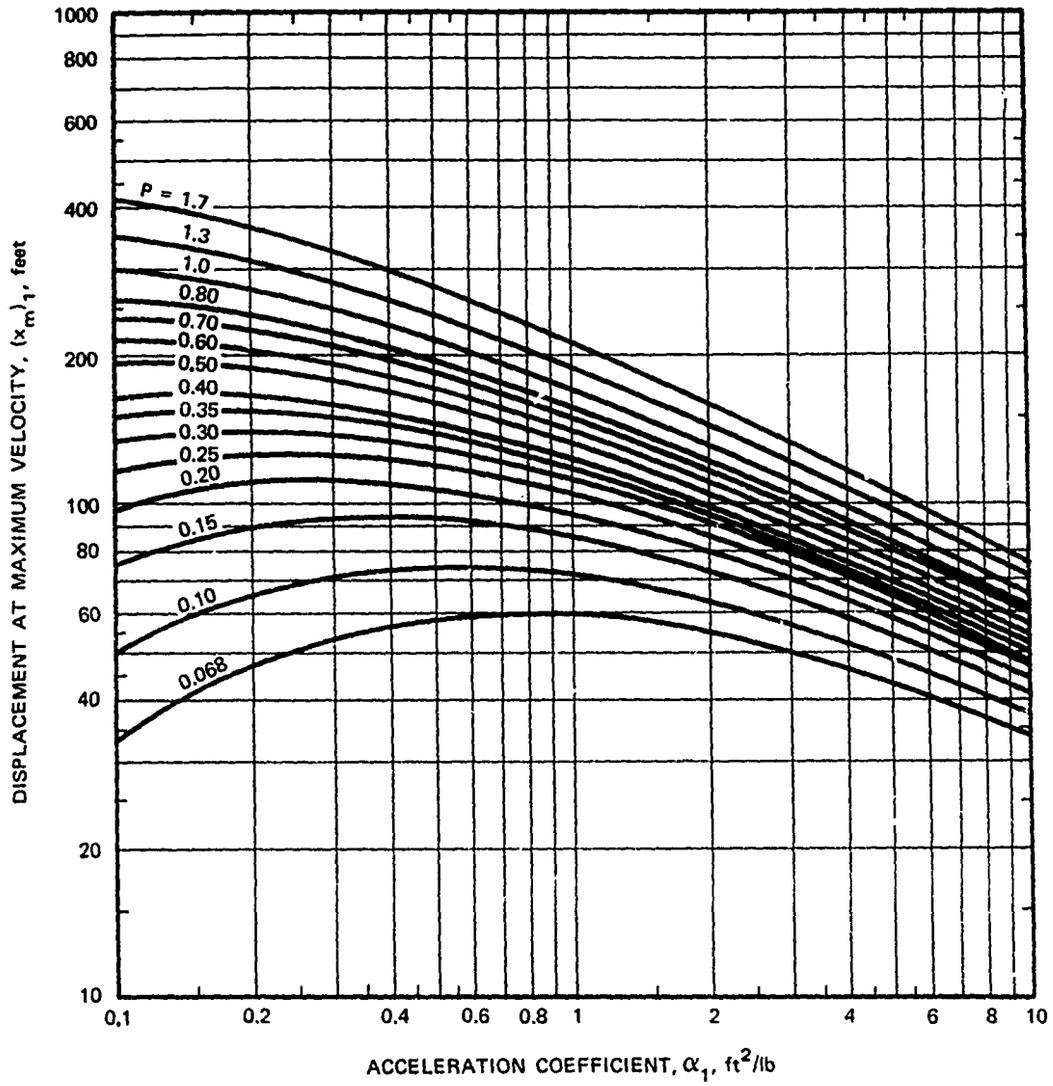


SOURCE: Ref. 31.

FIG. 20 PREDICTED DISPLACEMENT AT MAXIMUM VELOCITY AS A FUNCTION OF ACCELERATION COEFFICIENT AND NONDIMENSIONAL PEAK OVERPRESSURE
Computed for W = 1 Mt, $P_o$ = 14.7 psi, and $c_o$ = 1117 ft/sec
For other conditions, use:

$$\alpha_1 = \alpha\left(\frac{1117}{c_o}\right)^2\left(\frac{P_o}{14.7}\right)^{2/3}\left(\frac{W}{1000}\right)^{1/3}$$

$$x_m = (x_m)_1\left(\frac{14.7W}{P_o\,1000}\right)^{1/3}$$

If a pane supported along its edges is bent, a certain amount of potential and kinetic energy is stored in the pane before actual breakage occurs. Fragments near the center of the pane possessing the greater part of this energy would "pop out" at higher velocities than those near the perimeter. It should be pointed out that the energy thus temporarily stored in each pane is not necessarily derived from the blast winds but is due principally to the sudden increase in pressure existing at the leading edge of a classical blast wave. The defractive (sic) loading effect described above would be enhanced by the process of reflection but would be mitigated provided the blast wave arrived on the lee side of the pane before it shattered. Also, if shattering occurred before appreciable bending had taken place, as might be the case for a relatively strong blast wave, then the defractive (sic) effect would be minimal since the pressure difference between the front and rear of the pane would quickly vanish when the glass is broken.

Further general comments from the test report concerning the glass-fragment data follow:

In comparing the glass-fragment data obtained at all stations, a correspondence was noted between the geometric mean mass of the fragments caught in a trap and the geometric mean velocity. The samples containing the smaller fragments generally were the ones with the higher mean velocities. The variation of acceleration coefficient between small and large glass fragments is not large enough to explain the effect noted. An explanation is quite simple, however, if it is assumed that a relatively strong blast wave not only accelerates the fragments to higher velocities but also fragments the window glass into smaller pieces. . . .

. . . none of the fragments caught in houses impacted with the flat surface against the absorber. . . . Several factors could influence the rotation of a fragment during its travel from the window to the trap. One is missile size - larger fragments have higher moments of inertia and therefore greater resistance to forces tending to cause rotation. Another phenomenon inducing rotation is turbulence of the wind, which is likely to be more pronounced inside houses than in open areas. Still another, but more subtle, phenomenon is the mechanism of breakage of window glass. Results obtained from another study for low (marginal) blast pressures indicate that fragments from the center of the pane break free before those from the perimeter and therefore

acquire correspondingly higher velocities. This sequence of events would not only result in an initial torque tending to cause rotation of many of the fragments but would also help explain the rather large variation in velocities measured in individual samples.

The data discussed above are presented in Figure 21. There were four windows, all with 11.5 in. X 23.5 in. panes of double strength glass mounted in steel frames. Three traps were placed behind each of the two windows that contained nine panes each. Four traps were placed behind each of the other two windows, which contained 20 panes each. These data were taken during Shot Galileo at a distance of 4,700 feet where $p_{so}$ was approximately 3.8 psi. The model, using $p_{so}$, appears to have provided a lower bound for the data; using $p_r$, but retaining the duration calculation for $p_{so}$, it appears nearly to have established an upper bound for the data.

It might be noted that the geometric mean weight of the 2,523 fragments trapped was 0.321 grams, while the predicted weight using the data in Figure 11 was 0.580 grams. This difference is considered within the accuracy ranges encountered in this research.

Data were also collected from windows mounted in the open during Operation Plumbbob; however, such data were not considered indicative of glass entering a room and are not presented herein.

In tests conducted since Teapot and Plumbbob,[35] windows in a two-story house were subjected to a 1.2 psi blast wave caused by exploding five tons of TNT. The translation model again predicted velocities lower than those measured. Apparently, the initial velocity of the fragments must be taken into account to increase the accuracy of the model. A modification of the model to predict velocities more accurately at low overpressures is being considered.[35]

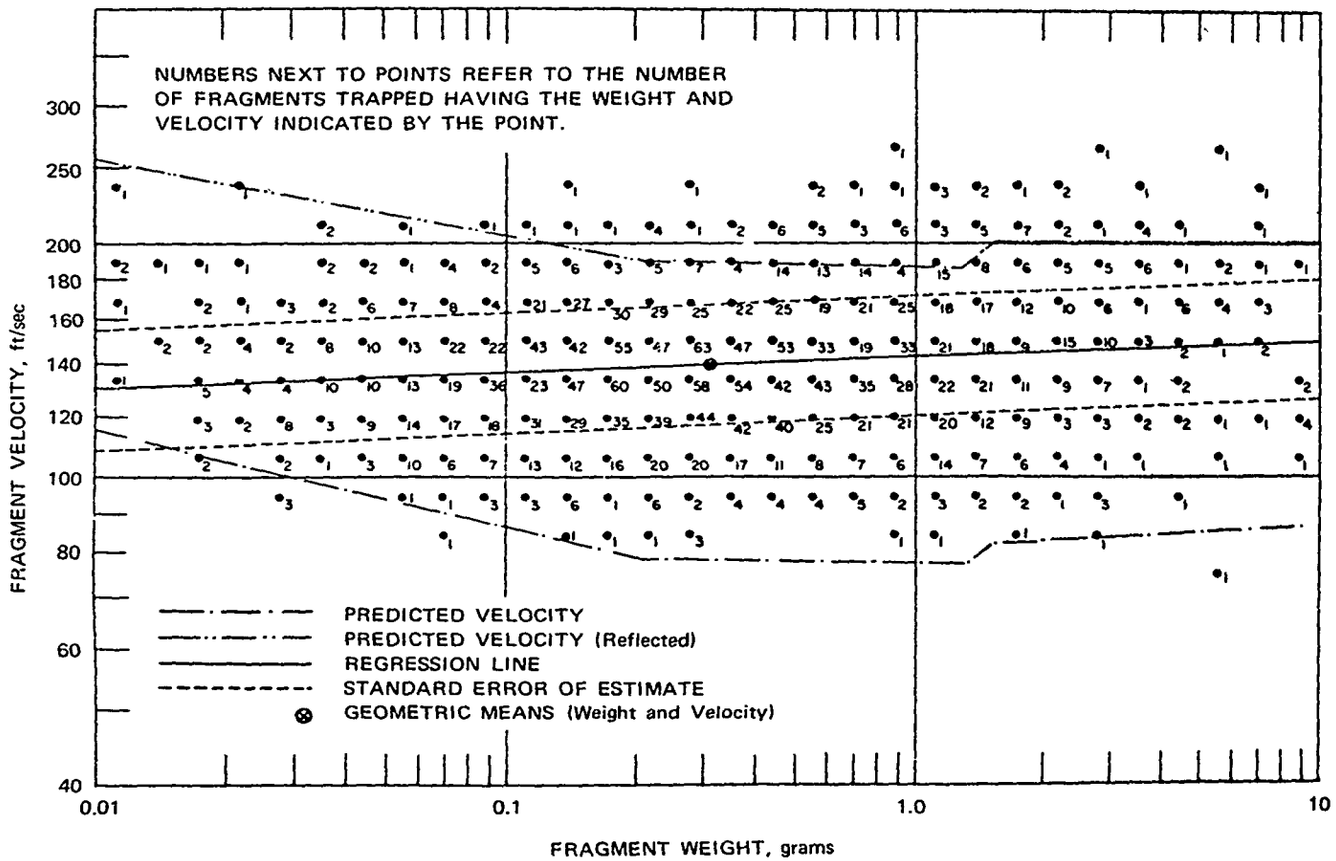


SOURCE: Ref. 33.

FIG. 21 OPERATION PLUMBBOB: ANALYSIS OF WINDOW GLASS FRAGMENTS FROM 14 TRAPS*

*Additional information: windows in house walls which faced ground zero, $p_{so}$ = 3.8 psi, x (average) = 10.3 ft, N = 2523, geometric mean weight = 0.321 grams, geometric mean velocity = 140 ft/sec, all data from two windows with nine 11.5" x 23.5" panes and two windows with twenty 11.5" x 23.5" panes, double strength glass and steel frames.

The following procedure is recommended for estimating fragment velocity:

1. Establish $P_o$, $c_o$, $p_{so}$, $p_r$, W, $t_o$, and $t_u$.
2. Select a fragment weight; $M_{50}$ predicted by Figure 11 is a logical first try.
3. Determine $\alpha$ from Figure 14. The lines depicting window or plate glass dropped flat are recommended.
4. Calculate A using Equation 27.
5. Solve for D(n) using Equation 30 by substituting the desired value for the fragment travel distance, x.
6. If the window is side-on to the blast wave, solve Equation 26 as shown. If the window is facing ground zero, substitute $p_r$ for $p_{so}$ in Equation 26.
7. Enter Table 9 with P, A, and D(n).
8. Read the corresponding V(n).
9. Solve for v using Equation 29.

# V BIOLOGICAL CONSIDERATIONS

The effects of glass fragments on people have been observed at Nagasaki, Hiroshima, and at some accidental, nonnuclear explosions in the United States. The purpose of this chapter is to summarize previously accomplished work concerned with predicting the degree of injury to humans exposed to various glass missile situations. Data found in the literature for predicting injury to humans are based on tests conducted during Operations Teapot and Plumbbob[29,33,34] and subsequent work.[30-32] Injury prediction[30] is based on the penetration of glass missiles fired into the abdominal walls of anesthetized dogs. A word of caution was offered: "The authors are unaware of any reliable data which allows the penetration data obtained on dogs to be applied to the human case. However, the use of the penetration criteria for experimental animals to attempt to predict injury to the civilian and military population will underestimate the damaging potential of glass fragments."[30] Nonetheless, these data are presented in Figure 22 and suggested for use until modified by further research.

The weight and velocity data required to use Figure 22 are derived by methods described in Chapters III and IV. Unfortunately, a precise breakdown of deaths or degree of injuries was not found in the literature; however, Figure 22 delineates the probability of serious injuries. ". . . entry of one of the serous cavities of the body or penetration of the eye can be regarded as a serious wound at least because infections almost always occur. . ."[36] A serious wound has also been defined as "a laceration penetrating the skin wherein the missile either was stopped by bone or passed into the tissues to a depth of 10 mm or more."[34]

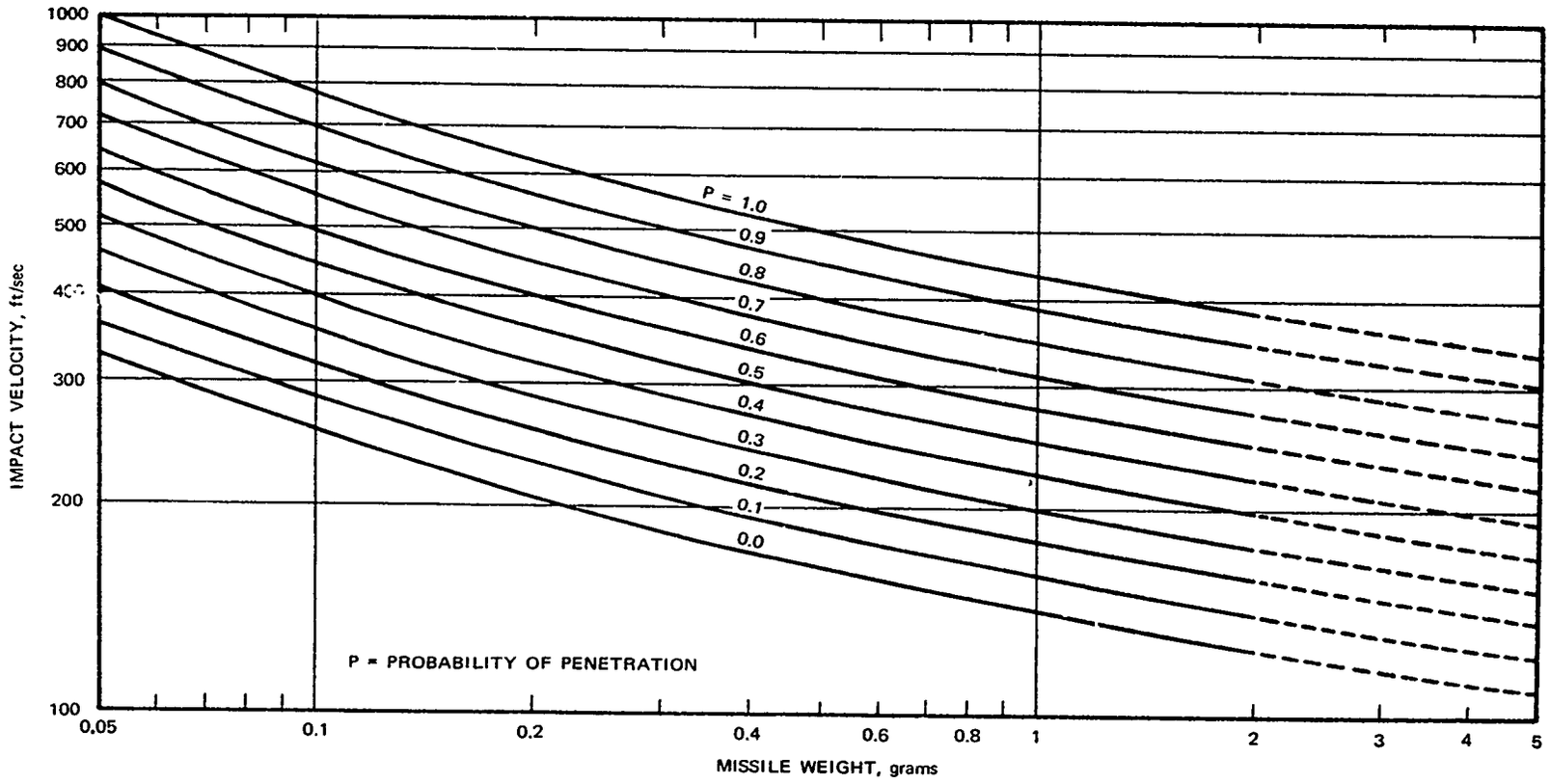


SOURCE: Ref. 30.

FIG. 22 PROBABILITY OF PENETRATION OF GLASS FRAGMENTS INTO THE ABDOMEN OF A DOG AS A FUNCTION OF MISSILE WEIGHT AND IMPACT VELOCITY

The latter quote applies to data taken from full scale field tests in which dogs were stationed approximately 10 feet behind windows exposed to a nuclear explosion.

The number of serious wounds is probably best estimated by using Figure 23. Again from the full scale field test data: ". . . on the average, for every 12 wounds suffered by an animal there was one potentially serious insult . . ."; ". . . in terms of area of the biological target, there were averages of 13.4 total injuries per square foot; the serious injuries numbered about 1.2 per square foot of presented surface area. Assuming a presented area, face-on, for a 160-lb lightly clothed human to be near 6 sq ft in a similar exposure, the above figures might represent a hazard from window glass involving 80 total wounds, of which 7 could be potentially dangerous to life without early surgical care."[34] The preceding quote applies to windows in building walls that faced ground zero, exposed to a free-field overpressure of approximately 2 to 4 psi.

One further set of data,[30,34] widely publicized in the literature, is given in Table 10. The table provides predictions for a 10-gram fragment after ten feet of travel. These data do not seem directly helpful since very few 10-gram fragments were noted in studying the data used to prepare this report.

Table 10

TENTATIVE CRITERIA FOR SECONDARY BLAST EFFECTS

| Injury | Impact Velocity (ft/sec) |
|---|---|
| Skin laceration (threshold) | 50 |
| Serious wound | |
| Threshold | 100 |
| 50% probability | 180 |
| Near 100% probability | 300 |

Source: Reference 36.

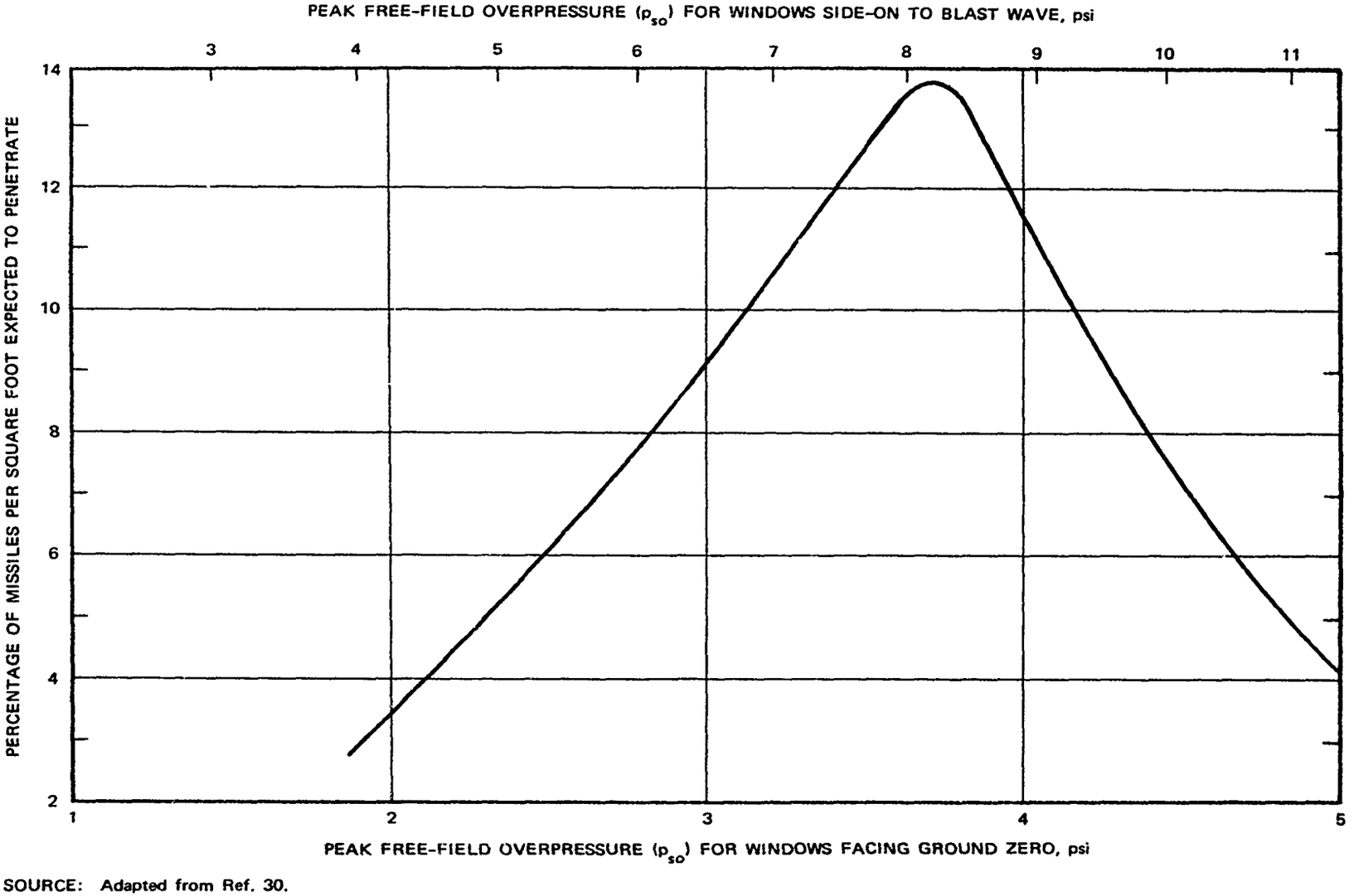


SOURCE: Adapted from Ref. 30.

FIG. 23 EXPECTED FREQUENCY OF PENETRATION AS A FUNCTION OF PEAK OVERPRESSURE*

* Computed for glass missiles occurring about 10 feet behind windows in house walls facing blast. Penetration criterion derived from dog abdomen studies.

The limited information provided by this chapter is intended only to be illustrative, since the subject is beyond the study scope as finally prescribed.

# VI RECOMMENDED ADDITIONAL STUDY

Because modulus of rupture testing of glass laths is apparently not an indication of glass pane response to blast loading, further lath testing does not seem beneficial. However, tests conducted on windows in the shock tunnel operated by URS Corporation at Fort Cronkhite, for example, would be extremely helpful. Meaningful velocity, weight, and spatial density data could possibly be obtained by closing the tunnel with a wall containing a window. A second wall completely covered with the same type of Styrofoam used by Lovelace Foundation in its missile traps could be made movable so that the distance between walls could be varied. In the interest of economy, the same tests could be used to study room-filling phenomena. Also, as a better understanding of room-filling is obtained through work currently being done by a colleague, J. R. Rempel, it appears possible that application of the new knowledge to glass fragment translation might be an improvement over the current approach, which involves translation by the winds associated with a "classical" free-field blast wave.

The failure prediction approach presented in Chapter II is based on membrane and bending action at the center of a square plate. Possibly more attention should be given to determining the amount of error inherent in considering rectangular panes as square panes of the same area. This would not be possible without laboratory testing of rectangular panes in the same manner as the tests made by Bowles and Sugarman[16] on square panes. Another reason for further testing including stress-strain testing all the way to failure is that Orr[15] found that the greatest stress was not at the center. Rather it was some distance away along a diagonal,

and the membrane action was so pronounced in some cases that both surfaces were placed in tension. Further study of the reports by IITRI[37,38] might also be beneficial. IITRI's method of dividing a panel into a grid system allows for checks of failure stresses at locations other than the center. Tests were performed on hydrostone panels to substantiate this work.

As mentioned previously, the computer program presented in Chapter II is already capable of accepting a peak free-field overpressure as input. The results obtained include values for the velocity of the equivalent single-degree-of-freedom system through to failure. It seems possible that this information could be coordinated with Bowen's translation model to provide better estimates of fragment velocity.

# VII APPLICATIONS

The purpose of this chapter is to demonstrate the type of information that can be obtained through the use of procedures presented in this report. Windows to be examined were selected from the 55 structures in the Research Triangle Institute (RTI) San Jose sample[39] of NFSS buildings. Buildings selected for analysis were limited to those with windows in shelter areas on floors above grade. If there were interior walls between windows and designated shelter areas, the windows were excluded from consideration. Buildings with windows meeting these criteria were chosen by studying the RTI report, copies of the original Phase II NFSS Data Collection Forms, and copies of the shelter location sketches required for each shelter space in the NFSS.

Out of the buildings that met the criteria, 14 were chosen for use in this chapter. The data collected for one window from each of the 14 buildings are presented in Table 11. Opening and pane sizes were determined from actual measurements or by scaling from photographs of the buildings. Pane thicknesses were determined by the method described in the footnote on page A-2 of this report.

Predictions of incipient failure overpressures are presented in Table 12 for each of the 14 windows. All of the glass in the 14 windows was found to be sheet glass, thus predictions were made using Figures 9 and 10. The pane area used to predict the incipient failure overpressure for a multipane window was determined from the apparent strength of the window frame. If a frame appeared strong, the area of the largest pane in the window was chosen since the largest pane among panes of equal thickness would fail at the lowest overpressure. If a frame seemed

Table 11

WINDOW FIELD DATA

| RTI Bldg. Number* | Building Name and Address | Wall† | Floor | Opening Size, Width × Height (in.)‡ | Window Frame Type and Material | Number of Panes per Window | Total Glass Area per Window ($ft^2$) | Pane Thickness (in.)§ | Number of Similar Windows on this Floor and Wall |
|---|---|---|---|---|---|---|---|---|---|
| 1 | S.C. County Welfare Building<br>55 West Younger Ave.<br>San Jose | C | 2 | 30 × 74 | Fixed glass, aluminum | 1 | 12.4 | 3/16 | 61 |
| 8 | De Anza Hotel<br>233 West Santa Clara St.<br>San Jose | A | 3 | 46 × 72 | Double-hung wood | 2 | 15.7 | SS | 10 |
| 10 | S.C. County Court House<br>161 North 1st Street<br>San Jose | D | 1 | 54 × 114 | Double-hung wood | 2 | 32.9 | 1/4 | 8 |
| 12 | San Jose State Library<br>4th & San Fernando<br>San Jose | B | 1 | 32.5 × 71 | Projected aluminum | 3 | 12.3 | DS | 39 |
| 15 | San Jose Medical & Dental Bldg.<br>6th & Santa Clara<br>San Jose | A | 8 | 38.5 × 72 | Double-hung wood | 2 | 15.3 | SS | 13 |
| 16 | Commercial Building<br>18-28 North 1st Street<br>San Jose | A | 2 | 39 × 72 | Double-hung wood | 2 | 14.4 | SS | 12 |
| 27 | McLaughlin Hall<br>University of Santa Clara<br>Santa Clara | C | 1 | 72 × 64 | Casement, out-swing, fixed center panes, steel | 15 | 26.1 | DS | 15 |
| 28 | Men's Residence Hall<br>University of Santa Clara<br>Santa Clara | A | 2 | 71 × 62 | Fixed center pane, 2 projected panes, movable vent, aluminum | 9 | 17.7 | DS | 12 |

Table 11 (concluded)

| RTI Bldg. Number* | Building Name and Address | Wall† | Floor | Opening Size, Width × Height (in.) | Window Frame Type and Material | Number of Panes per Window | Total Glass Area per Window ($ft^2$) | Pane Thickness (in.)§ | Number of Similar Windows on this Floor and Wall |
|---|---|---|---|---|---|---|---|---|---|
| 35 | Stern Hall Unit #5<br>Stanford University<br>Palo Alto | D | 2 | 57 × 75 | Projected steel | 6 | 24.3 | DS | 11 |
| 38 | Stauffer Building (Organic Chemistry Research)<br>Stanford University, Palo Alto | C | 1 | 118 × 90 | Fixed steel | 5 | 65.0 | 3/16 | 12 |
| 39 | Escondido Village, Bldg #135<br>Stanford University, Palo Alto | C | 6 | 64 × 96 | Fixed aluminum | 2 | 36.2 | DS | 4 |
| 43 | Bldg #5A, Admissions & Treatment<br>V.A. Hospital<br>Palo Alto | D | 2 | 42 × 74 | Double-hung steel | 2 | 17.5 | DS | 11 |
| 44 | Stern Hall Unit #8<br>Stanford University, Palo Alto | B | 2 | 57 × 75 | Projected steel | 6 | 24.3 | DS | 11 |
| 48 | Law School Library<br>Stanford University, Palo Alto | A | 1 | 55.5 × 108 | Double-hung wood | 2 | 31.3 | DS | 16 |

* Numbers from one to 55 were assigned to selected NFSS buildings in the RTI survey.

† Letters, A, B, C, and D are used as in the NFSS to designate the four sides of a building: A is the address side; B, C, and D continue clockwise from A.

‡ If more than one size window was found in a wall, only the size occurring most often was reported.

§ SS was used for single strength and DS for double strength.

Table 12

INCIPIENT FAILURE OVERPRESSURE PREDICTIONS

| RTI Bldg. Number | Wall | Floor | Incipient Failure, Free-Field Overpressure (psi) Front Facing* | Side Facing* | Remarks |
|---|---|---|---|---|---|
| 1 | C | 2 | 0.4 | 0.7 | Pane area of 12.4 $ft^2$ was used. |
| 8 | A | 3 | 0.2 | 0.4 | Pane area of 7.8 $ft^2$ was used. |
| 10 | D | 1 | 0.4 | 0.8 | Pane area of 16.4 $ft^2$ was used. |
| 12 | B | 1 | 0.4 | 0.8 | Frame appeared adequate; area of largest pane, 6.9 $ft^2$, was used. |
| 15 | A | 8 | 0.2 | 0.4 | Pane area of 7.6 $ft^2$ was used. |
| 16 | A | 2 | 0.2 | 0.5 | Pane area of 7.2 $ft^2$ was used. |
| 27 | C | 1 | 0.3 | 0.6 | Horizontal frame members considered weak; center 5 panes were treated as one 9.5 $ft^2$ pane. |
| 28 | A | 2 | 0.4 | 0.7 | Frame appeared adequate; area of largest pane, 7.3 $ft^2$, was used. |
| 35 | D | 2 | 0.2 | 0.3 | Cross members in projected portion considered weak; the 4 panes in the projected portion were considered as one 16.0 $ft^2$ pane. |
| 38 | C | 1 | 0.2 | 0.3 | Frame appeared adequate; area of largest pane, 29.2 $ft^2$, was used. |
| 39 | C | 6 | 0.2 | 0.3 | Pane area of 18.1 $ft^2$ was used. |
| 43 | D | 2 | 0.3 | 0.6 | Pane area of 8.7 $ft^2$ was used. |
| 44 | B | 2 | 0.2 | 0.3 | Cross members in projected portion considered weak; the 4 panes in the projected portion were considered as one 16.0 $ft^2$ pane. |
| 48 | A | 1 | 0.2 | 0.3 | Pane area of 15.7 $ft^2$ was used. |

* Front facing refers to windows in a wall facing an approaching air blast wave; side facing refers to windows in a wall side-on to an approaching air blast wave.

weak, the areas of small panes adjacent to the weak members were added. This approach may be an overcompensation for the contribution to failure provided by the flexibility of thin muntins. Nevertheless, this approach is recommended until tests are performed that indicate a better method for obtaining the degree of strength reduction resulting from weak frame members.

Three peak overpressures, 2.0, 3.0, and 5.0 psi, which are within the range of available nuclear test data on glass, were selected to demonstrate the estimation of the following fragment characteristics: geometric mean weight, average weight, velocity, number produced, and spatial density.

The nuclear test data presented in Chapter III led to predictions of fragment weights for single and double strength window glass. Since three of the 14 windows are thicker than double strength glass, an extrapolation procedure was required. First, fragment weights for single and double strength glass were recorded in Table 13 using information obtained from Figure 11. It was noted that fragment weights appeared insensitive to thickness at $p_{so}$ = 5.0 psi; therefore, the average and geometric mean fragment weights for double strength glass were used for both 3/16-in. and 1/4-in. thicknesses. Second, at 2.0 psi, the geometric mean fragment weight increased by a factor of 2.76 and the average fragment weight increased by a factor of 1.91 from single to double strength. Because direct use of these factors would have led to an inconsistent situation of geometric mean fragment weight larger than average fragment weight, a single value of 2.3 (the average of the 2.76 and 1.91 factors) was adopted for use in scaling up both geometric mean and average fragment weights. The 2.3 factor was applied in equal steps to thicknesses greater than double strength, because the progression of thickness ratios is so nearly constant, namely double strength to single strength, or 1/8 to 3/32 (ratio 1.33), 3/16 to 1/8 (ratio 1.5), and 1/4 to 3/16 (ratio 1.33):

Table 13

FRAGMENT WEIGHT AND VELOCITY PREDICTIONS
FOR OVERPRESSURES ABOVE INCIPIENT FAILURE

| | Free-Field Overpressure (psi) | | Geometric Mean Fragment Weight $M_{50}$, (gm) | Average Fragment Weight $\bar{M}$, (gm) | Velocity of Geometric Mean Weight Fragment After 10 Feet of Travel (fps)* |
|---|---|---|---|---|---|
| | Front Facing | Side Facing | | | |
| Single strength | 2.0 | 4.2 | 0.67 | 1.27 | 87 |
| | 3.0 | 6.5 | 0.48 | 0.93 | 132 |
| | 5.0 | 11.4 | 0.12 | 0.24 | 238 |
| Double strength | 2.0 | 4.2 | 1.85 | 2.43 | 92 |
| | 3.0 | 6.5 | 1.07 | 1.63 | 130 |
| | 5.0 | 11.4 | 0.14 | 0.28 | 234 |
| 3/16-in. sheet | 2.0 | 4.2 | 4.3 | 5.6 | 93 |
| | 3.0 | 6.5 | 2.1 | 3.3 | 138 |
| | 5.0 | 11.4 | 0.14 | 0.28 | 234 |
| 1/4-in. sheet | 2.0 | 4.2 | 9.8 | 13.0 | 94 |
| | 3.0 | 6.5 | 4.2 | 6.6 | 139 |
| | 5.0 | 11.4 | 0.14 | 0.28 | 234 |

* Velocities are given for a weapon yield of 1 Mt, ambient atmospheric pressures of 14.7 psi, speed of sound in undisturbed air of 1,126 fps, and $\alpha$ based on "dropped flat" curve in Figure 14. Linear interpolation was used in Table 9.

$M_{50}$ for 3/16" = 1.85 grams X 2.3 = 4.3 grams

$M_{50}$ for 1/4" = 1.85 grams X 2.3 X 2.3 = 9.8 grams

$\bar{M}$ for 3/16" = 2.43 grams X 2.3 = 5.6 grams

$\bar{M}$ for 1/4" = 2.43 grams X 2.3 X 2.3 = 13 grams.

An identical procedure, resulting in an average multiplying factor of 2.0, was used for the fragment weights at 3.0 psi. The results are recorded in Table 13. No nuclear test data were available to substantiate the above procedure; however, the procedure is suggested for use until test data become available.

The results of velocity calculations, which are recorded in Table 13, were based on the geometric mean fragment weight since that weight is the most likely to occur. Each velocity was calculated assuming the fragment had traveled 10 feet from the window; however, any distance could have been selected. Other assumptions are shown in the footnote accompanying Table 13. An example of a velocity calculation using the single strength glass data at $p_{so}$ = 2.0 psi and following the steps at the end of Chapter IV, is:

1. The velocity was calculated first for a front-facing window with $P_o$ = 14.7 psi, $c_o$ = 1,126 fps, $p_{so}$ = 2.0 psi, $p_r$ = 4.2 psi (Equation 12), W = 1 Mt = 1,000 kt, and $t_o$ = 3.821 sec (Equation 19). A value of $t_u/t_o$ = 1.145 was obtained by entering Figure 13 with $p_{so}/P_o$ = 2.0/14.7 = 0.136; hence $t_u$ = 4.375 sec.

2. The fragment weight used was $M_{50}$ = 0.67 grams (Table 13).

3. A value of $\alpha$ = 0.57 $ft^2/lb$ was obtained by entering Figure 14 with the selected fragment weight.

4. Using Equation 27,

$$A = \frac{\alpha P_o t_u g}{c_o} = \left(0.57 \frac{ft^2}{lb}\right)\left(14.7 \frac{lb}{in^2}\right)(4.375 \text{ sec})$$
$$\left(386 \frac{in}{sec^2}\right)\left(\frac{1}{1126} \frac{sec}{ft}\right)\left(12 \frac{in}{ft}\right)$$

$A = 151$

5. A value of n = 6 was chosen because D(6) is given in Table 9 for values of interest in this example:

$$D(6) = \frac{10 \text{ ft}}{4.375 \text{ sec} \times 1126 \text{ ft/sec}} \times 10^6 = 2030 .$$

6. Since the window is facing ground zero,

$$P = \frac{p_r}{p_o} = \frac{4.2 \text{ psi}}{14.7 \text{ psi}} = 0.286 .$$

7. From Table 9 using linear interpolation when required:

| | P | A | D(6) | V(6) | Interpolating Between |
|---|---|---|---|---|---|
| a | 0.25 | 100 | 1809 | 59,733 | |
| b | " | " | 5419 | 80,440 | |
| c | " | " | 2030 | 61,001 | a & b |
| d | " | 300 | 1231 | 78,740 | |
| e | " | " | 3559 | 102,300 | |
| f | " | " | 2030 | 86,826 | d & e |
| g | 0.30 | 100 | 726 | 51,990 | |
| h | " | " | 2369 | 78,110 | |
| i | " | " | 2030 | 72,721 | g & h |
| j | " | 300 | 1584 | 100,690 | |
| k | " | " | 4456 | 127,070 | |
| l | " | " | 2030 | 104,787 | j & k |
| m | 0.286 | 100 | " | 69,439 | c & i |
| n | " | 300 | " | 99,758 | f & l |
| o | " | 151 | " | 77,170 | m & n |

8. V(6) = 77,170 from step 7.

9. Using Equation 29, $v = 77,170 \times 1126 \text{ fps} \times 10^{-6} = 87 \text{ fps}$.

The above procedure was repeated for a side-facing window with $p_{so}$ = 4.2 psi. Only values that changed from the previous example are shown below.

1. $p_{so}$ = 4.2 psi, $p_r$ is not applicable, and $t_o$ = 3.298 sec (Equation 19). A value of $t_u/t_o$ = 1.220 was obtained by entering Figure 13 with $p_{so}/P_o$ = 4.2/14.7 = 0.286; hence $t_u$ = 4.024 sec.
2. Same as front facing.
3. Same as front facing.
4. A = 139 (slight difference due to change in $t_u$).
5. D(6) = 2207 (slight difference due to change in $t_u$).
6. Since window is side-facing,

$$P = \frac{p_{so}}{P_o} = \frac{4.2 \text{ psi}}{14.7 \text{ psi}} = 0.286 \ .$$

   Note that the numerical result is the same as for the front-facing example.

7. Again a linear interpolation solution similar to the one given above for the front-facing example was used.
8. V(6) = 77,537 from step 7.
9. v = 87 fps, using Equation 29.

The above calculations demonstrate that velocity is insensitive to small changes in the duration of the winds ($t_u$). This conclusion was found to be true for the other velocities reported in Table 13 as well.

The spatial density of fragments at the window ($N_o$) was calculated for each of the 14 windows using Equation 24. Figure 12 was used to obtain the spatial density 10 feet from each window ($N_{10}$). These values are presented in Table 14.

Table 14

PREDICTIONS OF SPATIAL DENSITY AND NUMBER OF FRAGMENTS FOR OVERPRESSURES ABOVE INCIPIENT FAILURE

| RTI Bldg. Number | Wall | Floor | Free-Field Overpressure (psi) Front Facing | Free-Field Overpressure (psi) Side Facing | Number of Fragments Produced, N | Spatial Density of Fragments (fragments/ft$^2$) At Window, $N_o$ | Spatial Density of Fragments (fragments/ft$^2$) 10 Feet from Window, $N_{10}$ |
|---|---|---|---|---|---|---|---|
| 1 | C | 2 | 2.0 | 4.2 | 2,440 | 197 | 5.91 |
| | | | 3.0 | 6.5 | 4,140 | 334 | 35.7 |
| | | | 5.0 | 11.4 | 48,800 | 3,940 | 422 |
| 8 | A | 3 | 2.0 | 4.2 | 6,750 | 430 | 12.9 |
| | | | 3.0 | 6.5 | 9,230 | 588 | 62.9 |
| | | | 5.0 | 11.4 | 35,800 | 2,280 | 244 |
| 10 | D | 1 | 2.0 | 4.2 | 3,720 | 113 | 3.39 |
| | | | 3.0 | 6.5 | 7,340 | 223 | 23.9 |
| | | | 5.0 | 11.4 | 173,000 | 5,250 | 562 |
| 12 | B | 1 | 2.0 | 4.2 | 3,710 | 302 | 9.07 |
| | | | 3.0 | 6.5 | 5,550 | 451 | 48.2 |
| | | | 5.0 | 11.4 | 32,200 | 2,620 | 281 |
| 15 | A | 8 | 2.0 | 4.2 | 6,580 | 430 | 12.9 |
| | | | 3.0 | 6.5 | 9,000 | 588 | 62.9 |
| | | | 5.0 | 11.4 | 34,900 | 2,280 | 244 |
| 16 | A | 2 | 2.0 | 4.2 | 6,190 | 430 | 12.9 |
| | | | 3.0 | 6.5 | 8,470 | 588 | 62.9 |
| | | | 5.0 | 11.4 | 32,800 | 2,280 | 244 |
| 27 | C | 1 | 2.0 | 4.2 | 7,880 | 302 | 9.07 |
| | | | 3.0 | 6.5 | 11,800 | 451 | 48.2 |
| | | | 5.0 | 11.4 | 68,400 | 2,620 | 281 |
| 28 | A | 2 | 2.0 | 4.2 | 5,340 | 302 | 9.07 |
| | | | 3.0 | 6.5 | 7,980 | 451 | 48.2 |
| | | | 5.0 | 11.4 | 46,400 | 2,620 | 281 |

Table 14 (concluded)

| RTI Bldg. Number | Wall | Floor | Free-Field Overpressure (psi) Front Facing | Free-Field Overpressure (psi) Side Facing | Number of Fragments Produced, N | Spatial Density of Fragments (fragments/ft$^2$) At Window, $N_0$ | Spatial Density of Fragments (fragments/ft$^2$) 10 Feet from Window, $N_{10}$ |
|---|---|---|---|---|---|---|---|
| 35 | D | 2 | 2.0 | 4.2 | 7,340 | 302 | 9.07 |
| | | | 3.0 | 6.5 | 11,000 | 451 | 48.2 |
| | | | 5.0 | 11.4 | 63,700 | 2,620 | 281 |
| 38 | C | 1 | 2.0 | 4.2 | 12,800 | 197 | 5.91 |
| | | | 3.0 | 6.5 | 21,700 | 334 | 35.7 |
| | | | 5.0 | 11.4 | 256,000 | 3,940 | 422 |
| 39 | C | 6 | 2.0 | 4.2 | 10,900 | 302 | 9.07 |
| | | | 3.0 | 6.5 | 16,300 | 451 | 48.2 |
| | | | 5.0 | 11.4 | 94,800 | 2,620 | 281 |
| 43 | D | 2 | 2.0 | 4.2 | 5,280 | 302 | 9.07 |
| | | | 3.0 | 6.5 | 7,890 | 451 | 48.2 |
| | | | 5.0 | 11.4 | 45,800 | 2,620 | 281 |
| 44 | B | 2 | 2.0 | 4.2 | 7,340 | 302 | 9.07 |
| | | | 3.0 | 6.5 | 11,000 | 451 | 48.2 |
| | | | 5.0 | 11.4 | 63,700 | 2,620 | 281 |
| 48 | A | 1 | 2.0 | 4.2 | 9,450 | 302 | 9.07 |
| | | | 3.0 | 6.5 | 14,100 | 451 | 48.2 |
| | | | 5.0 | 11.4 | 82,000 | 2,620 | 281 |

The total number of fragments (N) emanating from each window, calculated by multiplying $N_0$ by the total glass area of a window, is also given in Table 14.

# Appendix A

## GLASS SELECTION PROCEDURE

## Appendix A

### GLASS SELECTION PROCEDURE

The usual situation in design would be a knowledge of the size, a X b, of the glass required and the location of the building. Building codes take over at this point and dictate the minimum thickness of glass required. Sheet glass is selected where surface quality is not paramount while plate glass is used where high surface quality is desired, such as for display windows.

Figure A-1 is used in the first design step to determine the resultant wind pressure for the particular locality. This information is used to enter Table A-1 to obtain the wind pressure in the height zone of the window above grade. The required thickness of either sheet or plate glass can then be found in Table A-2.

If the thickness of an existing window is not known but must be estimated to determine air blast response, the above procedure or the local building code can be used to obtain the minimum allowable thickness, which may be considered the most likely thickness used. If either side of an installed window pane is accessible, the thickness may be simply measured by light refraction.*

---

* An FHA Glass Thickness Gage, a two-inch by four-inch plastic card, was used to make glass thickness measurements for use in the applications chapter of this report. The card contains several lines corresponding to various glass thicknesses. Reflections of these lines from both glass surfaces readily indicate the glass thickness when the card is held at an angle of 45 degrees to the pane.

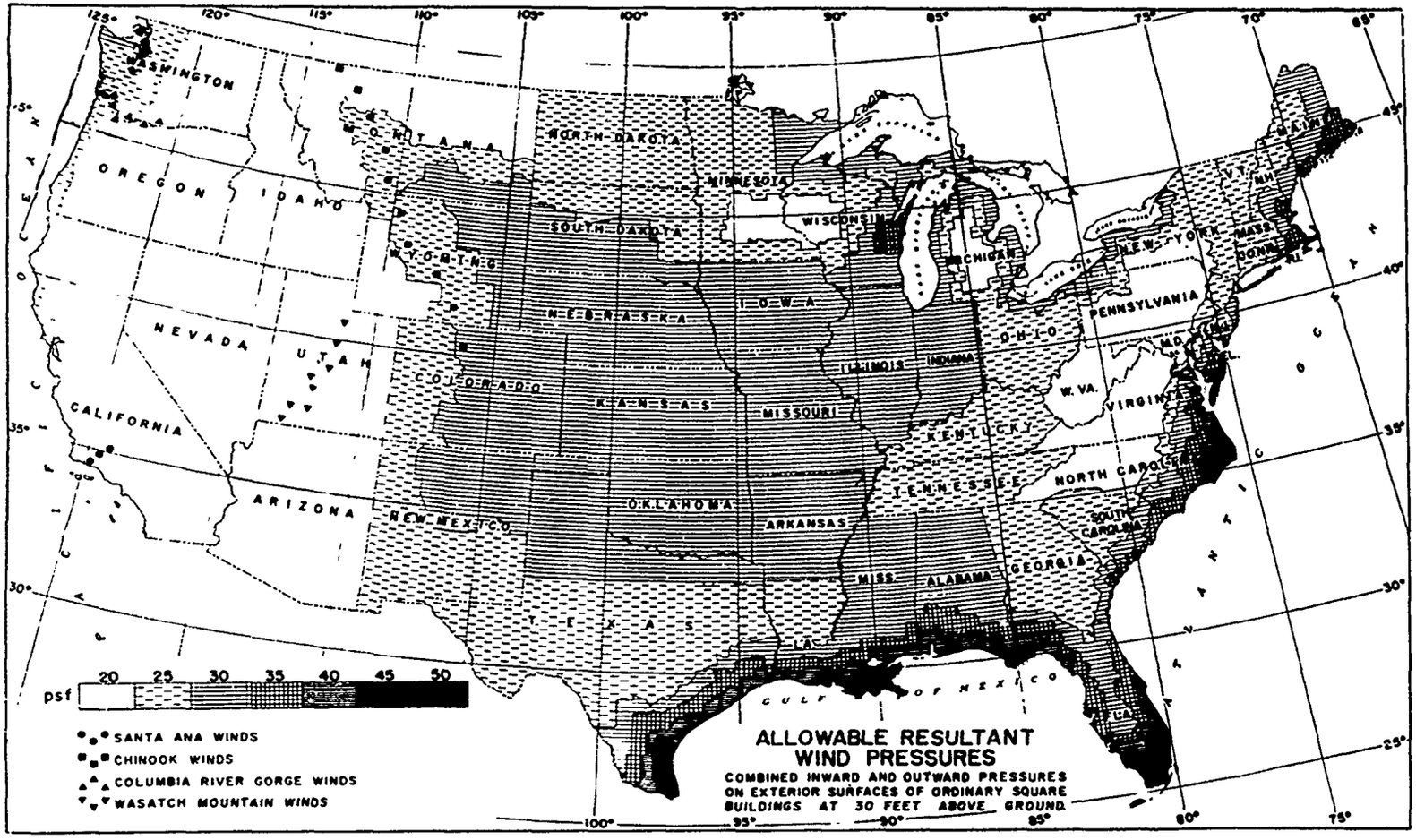


SOURCE: Reprinted through the courtesy of the International Conference of Building Officials (Ref. 28).

FIG. A-1 ALLOWABLE RESULTANT WIND PRESSURES

Table A-1

WIND PRESSURES AT VARIOUS ELEVATIONS ABOVE GRADE

| Pressure from Figure A-1 | 20 | 25 | 30 | 35 | 40 | 45 | 50 |
|---|---|---|---|---|---|---|---|
| Related pressure (psf) in various height zones: | | | | | | | |
| 0-29 feet above grade | 15 | 20 | 25 | 25 | 30 | 35 | 40 |
| 30-49 " " " | 20 | 25 | 30 | 35 | 40 | 45 | 50 |
| 50-99 " " " | 25 | 30 | 40 | 45 | 50 | 55 | 60 |
| 100-499 " " " | 30 | 40 | 45 | 55 | 60 | 70 | 75 |
| 500-1199 " " " | 35 | 45 | 55 | 60 | 70 | 80 | 90 |
| 1200 and over " " " | 40 | 50 | 60 | 70 | 80 | 90 | 100 |

Source: Reprinted through the courtesy of the International Conference of Building Officials (Reference 28).

Table A-2

MAXIMUM ALLOWABLE AREA OF GLASS*
(Square Feet)

| Wind Load ($lb/ft^2$) | Thickness (in.) | | | | | | | | | | |
|---|---|---|---|---|---|---|---|---|---|---|---|
| | SS | DS | 3/16 | 7/32 | 13/64 | 1/4 | 5/16 | 3/8 | 1/2 | 5/8 | 3/4 |
| 10 | 25 | 37 | 72 | 84 | 72 | 114 | 156 | 198 | 270 | 365 | 465 |
| 15 | 16 | 25 | 48 | 58 | 48 | 72 | 104 | 131 | 192 | 260 | 330 |
| 20 | 12 | 19 | 36 | 43 | 36 | 54 | 78 | 98 | 144 | 195 | 245 |
| 25 | 10 | 15 | 29 | 35 | 29 | 43 | 62 | 78 | 115 | 156 | 195 |
| 30 | 8 | 12 | 24 | 29 | 24 | 36 | 52 | 65 | 96 | 130 | 165 |
| 35 | 7 | 11 | 21 | 25 | 21 | 31 | 45 | 56 | 82 | 112 | 140 |
| 40 | 6 | 9 | 18 | 22 | 18 | 27 | 39 | 49 | 72 | 98 | 124 |
| 45 | 5 | 8 | 16 | 19 | 16 | 24 | 35 | 44 | 64 | 87 | 110 |
| 50 | 4 | 7 | 14 | 17 | 14 | 22 | 31 | 39 | 58 | 78 | 98 |
| 60 | -- | 6 | 12 | 15 | 12 | 18 | 25 | 32 | 48 | 65 | 81 |
| 70 | -- | -- | 10 | 12 | 10 | 15 | 22 | 28 | 40 | 55 | 70 |
| 80 | -- | -- | 9 | 11 | 9 | 13 | 19 | 24 | 35 | 47 | 61 |
| 90 | -- | -- | 8 | 9 | 8 | 12 | 17 | 22 | 32 | 42 | 55 |
| 100 | -- | -- | 7 | 8 | 7 | 11 | 16 | 20 | 29 | 39 | 50 |

* Maximum areas apply for rectangular lights of annealed glass firmly supported on all four sides in a vertical position. Glass mounted at a slope not to exceed one horizontal to five verticals may be considered vertical. Maximum areas based on minimum thicknesses set forth in Table No. 54-1-A, Volume III, U.B.C. Standard No. 54-1-67.

Source: Reprinted through the courtesy of the International Conference of Building Officials (Reference 28).

## Appendix B

## COMMON WINDOW TYPES AND SIZES

## Appendix B

### COMMON WINDOW TYPES AND SIZES

Single or double strength panes approximately 10" X 20" mounted in wood sash are typical of window installations used in houses today. Picture windows have panes as large as 110" X 80" and 7/32" or 1/4" thick. A common pane size for schools is 16" X 44" with a thickness of 3/16".[3]

Figure B-1 shows some of the common window types. The following list provides the standard sizes and types of windows used today.[40] An average pane size is indicated in some cases.

a. Aluminum casement windows

   Commercial: height 2'9" to 8'1"; width 1'8-7/8" to 6'8-7/8"

   Residential: height 2'2" to 5'3"; width 1'7-1/8" to 5'9-3/8"

b. Aluminum projected windows

   Commercial: height 1'5" to 8'1"; width 2'0-7/8" to 4'0-7/8"

   Residential: height 1'7-1/8" to 5'9-3/8"; width 2'2" to 4'2-5/8"

   Approximate average size of glass: 12" X 32".

c. Steel casement windows

   Residential: height 2'2" to 5'3"; width 1'7-1/8" to 7'7-3/8"

   Approximate average size of glass: 10" X 16".

d. Steel commercial projected windows

   Commercial: height 2'9" to 9'5"; width 1'8-7/8" to 6'8-7/8"

   Approximate average size of glass: 14" X 18".

e. Double-hung wood windows (all applications)

   Height 2'6" to 6'6"; width 1'4" to 4'4"; glass about 20" X 20"

f. Picture windows are made to sizes desired, as limited by building codes.

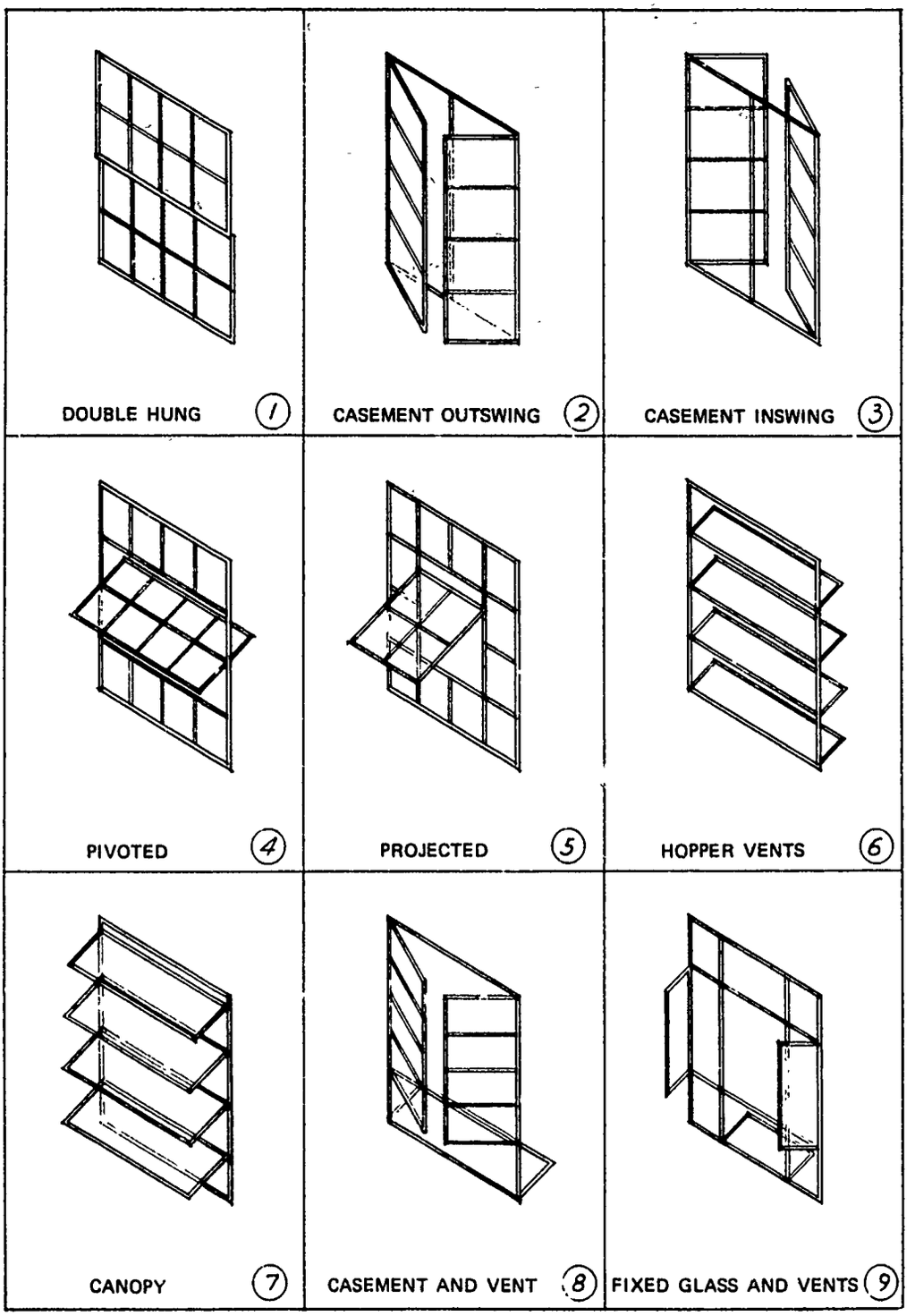


SOURCE: Ref. 41.

FIG. B-1 COMMON WINDOW TYPES

# Appendix C

## MODULUS OF RUPTURE DATA

## Appendix C

## MODULUS OF RUPTURE DATA

Tests to determine the modulus of rupture, $\sigma_r$, of plate glass have been made by the National Bureau of Standards.[12,42] The tests were performed on soda-lime-silica plate glass in varying conditions of anneal with as-cut edges. The test laths were all 10" X 1-1/2" X 1/4", the loading rate was 10,000 psi per minute, and the test temperature was 75°F. In an attempt to account for scratches, surface deterioration, and age, the surface of some of the laths was abraded by sand blasting. Results of the tests are shown in Table C-1. A sketch of the test loading arrangement is shown in Figure C-1.

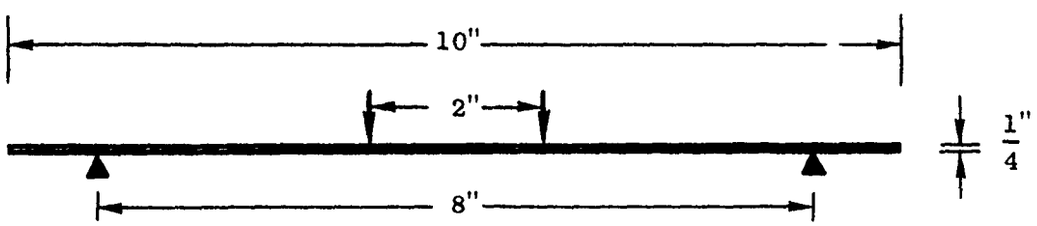


FIG. C-1 DIAGRAM OF TEST METHOD

---

Source: Reference 12.

A summary of the data presented in Table C-1 is given in Table C-2 for the purpose of having one value of the modulus of rupture, its standard deviation, and its coefficient of variation for each of the various conditions of anneal and abrasion.

Table C-1

MODULUS OF RUPTURE TESTS ON PLATE GLASS*

| Type† | Condition of Anneal‡ | Number Tested | Failure Type | Average $\sigma_r$ (psi) | High $\sigma_r$ (psi) | Low $\sigma_r$ (psi) | Standard Deviation (psi) | Coefficient of Variation (percent) |
|---|---|---|---|---|---|---|---|---|
| 1 | A | 30 | -- | 14,700 | 21,900 | 6,400 | 4,400 | 29.9% |
| 1 | A | 30 | -- | 15,900 | 21,700 | 9,300 | 2,900 | 18.2 |
| 1 | A | 30 | -- | 13,400 | 20,700 | 5,800 | 3,000 | 22.4 |
| 1 | A | 30 | -- | 15,000 | 22,700 | 5,000 | 4,100 | 27.3 |
| | A | 24 | Surface | 19,208 | -- | -- | 4,338 | 22.6 |
| | A | 26 | Edge | 14,801 | -- | -- | 5,127 | 34.6 |
| 1 | A | $\Sigma$ = 50 | All | 16,917 | -- | -- | 5,215 | 30.8 |
| | S | 36 | Surface | 23,426 | -- | -- | 3,995 | 17.1 |
| | S | 14 | Edge | 28,587 | -- | -- | 5,265 | 18.4 |
| 2 | S | $\Sigma$ = 50 | All | 24,871 | -- | -- | 4,923 | 19.8 |
| 3 | T | 30 | -- | 30,400 | 47,000 | 23,700 | 3,900 | 12.8 |
| 3 | T | 30 | -- | 33,300 | 41,500 | 25,500 | 4,500 | 13.5 |
| 3 | T | 30 | -- | 28,000 | 35,800 | 23,500 | 3,400 | 12.1 |
| 3 | T | 30 | -- | 36,400 | 48,400 | 27,000 | 4,300 | 11.8 |
| | T | 40 | Surface | 35,590 | -- | -- | 5,073 | 14.3 |
| | T | 10 | Edge | 39,363 | -- | -- | 8,037 | 20.4 |
| 3 | T | $\Sigma$ = 50 | All | 36,345 | -- | -- | 5,888 | 16.2 |
| 4 | Aa | 30 | -- | 10,100 | 11,200 | 8,500 | 600 | 5.9 |
| 4 | Aa | 30 | -- | 9,700 | 11,600 | 8,200 | 700 | 7.2 |
| 4 | Aa | 30 | -- | 10,100 | 11,400 | 6,200 | 800 | 7.9 |
| 4 | Aa | 30 | -- | 10,400 | 12,400 | 7,200 | 1,100 | 10.6 |
| 5 | Ta | 30 | -- | 23,400 | 28,500 | 20,500 | 1,100 | 4.7 |
| 5 | Ta | 30 | -- | 23,800 | 27,600 | 20,700 | 900 | 3.8 |
| 5 | Ta | 30 | -- | 24,600 | 26,500 | 21,600 | 900 | 3.6 |
| 5 | Ta | 30 | -- | 25,700 | 30,200 | 23,800 | 1,100 | 4.3 |

* Some of the data in this table were taken from a table in Ref. 12. The remainder of the data were estimated to the nearest 100 psi from a floating bar chart in Ref. 42.

† Same numbered lines were combined in the preparation of Table C-2.

‡ A = annealed, S = semitempered, T = tempered, Aa = annealed and abraded, and Ta = tempered and abraded.

Table C-2

SUMMARY OF TABLE C-1 DATA

| Condition of Anneal | Abraded | Modulus of Rupture (psi) | Standard Deviation (psi) | Coefficient of Variation (percent) |
|---|---|---|---|---|
| Annealed | No | 15,400 | 4,300 | 27.9% |
| Semitempered | No | 24,871 | 4,923 | 19.8 |
| Tempered | No | 33,300 | 5,700 | 17.1 |
| Annealed | Yes | 10,100 | 500 | 5.0 |
| Tempered | Yes | 24,400 | 800 | 3.3 |

Table C-3

MODULUS OF RUPTURE TESTS

| Number of Samples | Surface Condition | Strength (psi) | Standard Deviation (psi) | Coefficient of Variation (percent) |
|---|---|---|---|---|
| 247 | Ground and polished | 12,906 | 2,624 | 20.3% |
| 293 | Sandblasted | 6,789 | 464 | 6.8 |
| 287 | Ground and polished | 8,400 | 1,865 | 22.2 |

Source: Reference 3.

The results of other tests[3] taken under similar conditions to those previously described are presented in the first two rows of Table C-3. One difference noted was that the glass laths in this case were 1/2 in. wide rather than 1-1/2 in. wide as in the other tests. The third row of data came from concentric ring[17] tests carried to destruction.

The results of modulus of rupture tests[43] reported in 1923 are reproduced in Table C-4. The glass laths in this case were 18" X 2", the supports were 16 in. apart, and the load was applied at midspan at a rate of 10 pounds per minute.

It can be seen that the modulus of rupture values shown in Table C-1 are more than two times larger than the values for 1/4-in. plate shown in Table C-4. Even the strengths of the abraded laths of Table C-1 are larger than those for the unabraded laths reported in Table C-4. This considerable difference illustrates the difficulty in assigning modulus of rupture values to a brittle material.

Table C-4

MODULUS OF RUPTURE TESTS

| Type* | Number Tested | Average Modulus of Rupture (psi) | Deflection (in.) | Load (lb) |
|---|---|---|---|---|
| A grade SS | 65 | 10,020 | .423 | 6.4 |
| A grade SS | 74 | 10,770 | .317 | 5.0 |
| A grade SS | 10 | 8,275 | .338 | 4.9 |
| A grade DS | 70 | 9,692 | .290 | 10.8 |
| A grade DS | 76 | 9,442 | .316 | 12.37 |
| A grade DS | 8 | 7,880 | .297 | 9.5 |
| 26-oz sheet | 10 | 7,460 | .213 | 10.8 |
| 29-oz sheet | 10 | 6,111 | .190 | 10.8 |
| 34-oz sheet | 10 | 7,230 | .182 | 15.2 |
| 39-oz sheet | 10 | 6,980 | .151 | 22.2 |
| 39-oz sheet | 10 | 5,970 | .127 | 18.8 |
| 1/4-in. polished plate | 9 | 6,027 | .109 | 33.0 |
| 1/4-in. polished plate | 9 | 6,977 | .124 | 33.4 |

* Types given in ounces may be converted to thicknesses by using Table 1 of this report.

Source: Reference 43.

## Appendix D

## WINDOWS SUBJECTED TO VARIOUS DYNAMIC LOADINGS

## Appendix D

## WINDOWS SUBJECTED TO VARIOUS DYNAMIC LOADINGS

The purpose of this appendix is to demonstrate the strength of glass in windows under various types of loading conditions. The most often quoted strength figures are reproduced in Table D-1. The table gives typical breaking stresses for large lights (panes) with normal surface quality, as glazed, thus accounting for temper, fabrication, support conditions, and type of loading. It is felt that breaking stress refers to the maximum tensile stress on the glass surface at the time of failure; however, a procedure for calculating such a large deflection plate stress for comparison with the tabulated values was not found in the literature.

Table D-1

THE RELATIONSHIP OF LOADING TO BREAKING STRESS

| Type of Loading | Approximate Load Duration | Plate Glass (psi) | Window Glass (psi) |
|---|---|---|---|
| Sonic booms, blasts | 0.1 second | 6,000 | 6,600 |
| Wind gusts | 5-10 seconds | 5,500 | 6,050 |
| Fastest mile wind | 60 seconds | 4,000 | 4,400 |
| Long term | 2 hours--indefinite | 3,000 | 3,300 |

Source: Reference 22.

Factors affecting the ability of windows to resist failure are numerous. Some factors affecting glass were mentioned in Chapter I. Other factors affecting the strength of glass panes in windows[9,10] are size,

thickness, shape, style, edge restraints, preloading, and uniformity of support. Of interest in sonic boom situations is that restraint may be different at different time points in the loading; that is, edge restraint may be different inward (frame) than outward (putty and glazers' points).[13] Again no method of applying a factor(s) to strength to account for each variable was found.

## Nuclear Explosion Data

A nuclear device with a magnitude of nearly 30 kt was detonated atop a 500-foot tower at a distance of 10,500 feet from four test houses during Operation Teapot.[44] The resulting peak free-field overpressure at that distance was measured and calculated to be about 1.7 psi. All glass in all windows facing the blast was blown in, and most of the side and rear windows were destroyed. Phrases such as "remained in place but were distorted in shape," . . . "warped and twisted but remained in place," . . . and "in place with minor distortions" were used to describe the steel sashes in three of the four buildings.

During the Upshot-Knothole test series,[45] a two-story frame house was located 7,500 feet from a 16.4-kt atomic device detonated atop a 300-foot tower. Using Figure 3.67b of ENW,[25] the peak free-field overpressure at the house was calculated to be nearly 1.9 psi, which means a peak reflected pressure of about 4 psi. Wood, double-hung, multipane windows with single strength, grade B window glass were used. All front and side windows failed, with glass broken into small fragments and muntins broken from the sashes. The sashes in the front wall were pushed into the rooms but this may have been the result of unconventional mounting procedure. Slightly less than one-half of the glass in the rear wall was destroyed. It was concluded that "major damage to multilight double-hung wood sash may be expected at overpressures of 2 psi."

A test structure was located 10,328 feet from a 46.7-kt atomic device detonated atop a 300-foot tower in the Operation Greenhouse series.[46]

The pressures were estimated at $p_{so}$ = 2 psi and $p_r$ = 4.2 psi. Aluminum and steel sashes were only slightly damaged when glazed with double strength glass, which failed readily. However, this type of sash was more severely damaged when glazed with heavier glass, such as 1/4-in. plate, because of the high forces transmitted to the frames by the ability of the stronger glass to resist breakage. Commercial, lightweight, double-hung, wooden, multipane windows glazed with double strength glass were almost completely destroyed even though they were located at the sides of the test house where there was no reflection.

Nuclear test results have indicated that the resistance of windows to atomic blast appears to be "approximately proportional to their strength in supporting static loads."[46] This observation has been summarized into five rules:[47]

1. If $p_{so} < 1/4\, q_{sf}$, windows facing the blast "will almost surely survive the blast." A value of $p_{so}$ = 0.25 psi was suggested for failure of usual lightweight, double-hung, wooden windows with ordinary glazing, facing ground zero.

2. If $p_{so} > q_{sf}$, windows facing the blast "will almost surely fail."

3. "Within these two extremes the situation is variable."

4. If $p_{so} < 1/2\, q_{sf}$, side windows "may have an excellent chance of surviving."

5. If the building interior is open, pressure equalization could reduce damage on rear windows.

Frame rigidity is important. A pane may survive in a rigid frame, whereas the same pane in a flexible frame would be broken by the frame as it distorted.[46] "Generally the weakest parts of a window assembly are the cross pieces (muntins) that divide the sashes into smaller glass areas. Sashes designed with intersecting muntins are particularly

susceptible to blast."[41] Table D-2, although not conclusive, gives some idea of the reaction of various sashes to atomic blast. All pressures shown in the table are peak reflected pressures.

A formula for calculating the shatter pressures of flat glazing materials exposed to blast, apparently derived empirically from nuclear weapons effects data, is as follows:[41]

$$q_s = \frac{KRh^2}{A} \qquad \text{(D-1)}$$

where $q_s$ = psi required to shatter,

$K$ = a constant (approximately 10,500 for ordinary window glass)

$h$ = thickness in inches

$A$ = area in square inches

$R$ = a shape factor

| Aspect Ratio | R |
|---|---|
| 1.0 | 1.000 |
| .9 | 1.005 |
| .8 | 1.02 |
| .7 | 1.07 |
| .6 | 1.14 |
| .5 | 1.25 |
| .4 | 1.45 |
| .3 | 1.8 |
| .2 | 2.6 |
| .1 | 5.0 |

The formula assumes that the frame is substantial for the type of glass it supports and that the frame does not deform.

From the best available field test data, it has been estimated that both large and small glass windows facing ground zero will shatter with some frame failures at $p_{so}$ = 0.5 - 1.0 psi.[25] Using scaling laws on other estimates presented in the same reference, it was found that $p_{so}$ = 0.25 psi is given as the pressure at which glass breakage in front-facing windows is possible. Light damage to frames is estimated to occur at $p_{so}$ = 0.75 psi.

Table D-2

BLAST EFFECTS ON WINDOW CONSTRUCTION AND GLAZING

| Type of Window | Size | Frame and Sash Condition | | Glass Breakage | |
|---|---|---|---|---|---|
| Lightweight wood, double-hung with 12 panes 10-1/2" X 15" double strength glass | 3'0" X 5'6" | At 2 psi, muntins broken, frame intact | | At 2 psi, all broken | |
| Lightweight aluminum outswinging casements<br>4 panes 1/8" glass 12" X 16"<br>4 panes 1/4" glass 12" X 16" | 3'2" X 4'2" | At 4.2 psi, frame bent | At 2 psi, no damage | At 4.2 psi, all broken | At 2 psi, none of 1/4" broken; 1/8" not tested |
| Steel intermediate projected<br>2 panes 1/4" plate 15" X 40"<br>2 panes 1/4" safety in vent | 3'6" X 5'6" | At 4.2 psi, muntin in vent bent | At 2 psi, no damage | At 4.2 psi, panes broken only in vent | None at 2 psi |
| Heavy aluminum inswinging casement<br>6 panes 18" X 22" X 1/4" tempered | 4'8" X 5'1" | At 7.4 psi, wrecked | At 3.2 psi, no damage | At 7.4 psi, all broken | None at 3.2 psi |
| Hopper vents, inswinging, steel<br>4 panes 12" X 42": 3/16" glass, 1/4" plate, tempered & plastic | 4'0" X 5'2" | At 7.4 psi, wrecked | At 3.2 psi, no damage | At 7.4 psi, all broken | At 3.2 psi, 1/4" plate and 3/16" broken |
| Hopper vents inswinging aluminum<br>4 panes 1/4" X 12" X 42" tempered | 4'0" X 5'2" | At 7.4 psi, sash torn from frame | At 3.2 psi, no damage | At 7.4 psi, one pane broken | None at 3.2 psi |
| Heavy steel double-hung<br>3 panes 1/4" plate and<br>1 DS 20" X 30" | 4'2" X 5'8" | At 4.2 psi, muntins bent | At 2 psi, no damage | At 4.2 psi, all broken | At 2 psi, only DS pane broken |
| Heavy steel double-hung<br>4 panes 3/16" glass 12" X 28" | 2'8" X 4'5" | At 3.2 psi, no damage | At 3.2 psi, no damage | At 3.2 psi, all broken | At 1.5 psi, only 2 panes broken |
| Canopy aluminum<br>2 panes plate 1/4" X 19" X 33"<br>1 pane 1/8" X 19" X 33" | 3'1" X 5'4" | At 4.2 psi, no damage | At 2 psi, latch broken | At 4.2 psi, all broken | At 2 psi, 1/8" pane broken |

Source: Reference 41.

## Conventional Explosion Data

Considerable work has been done, especially during World War II, on the problem of blast loading of windows; however, none of this previous work is believed to be applicable to this investigation. To clarify this statement, the work of Schardin[14] who indicated the similarity between the responses of a simple oscillator and a window pane to an explosive force must be considered. If $t_o$ is the positive pressure phase duration and T is the natural period of vibration of the system, then:

> If the system has a large natural period, or if the strain is caused by a shock wave coming from a small explosive charge at a short distance $[t_o < T]$, then the destruction depends on the momentum of the shock wave. If the system has a low natural period, or if the strain is caused by a shock wave coming from large explosive charges at a great distance $[t_o > T]$, then the destruction depends on the maximum pressure of the shock wave. Between those two limits there is a transition range.[14]

The natural period of usual sizes of single and double strength panes varies from 10 to possibly 100 milliseconds. Positive phase durations for the conventional explosions reviewed during this investigation were all less than the natural period of the window being tested. On the other hand, the positive phase duration of a 1-Mt nuclear explosion exceeds several seconds. Therefore, on the basis of the above quotation, window failures caused by conventional explosions are a result of the momentum of the shock wave, while failures caused by nuclear detonations are dependent on $p_{so}$.

Since it has been shown above that window failures for a conventional explosion are not dependent on $p_{so}$, the results of only one, large magnitude conventional explosion with a considerable amount of window data are presented here. Other sources of conventional explosion data can be found in the bibliography.

An accidental detonation of conventional explosives occurred at Medina Facility near San Antonio, Texas, in November 1963.

> Storage records showed that 111,500 lbs. of chemical high explosives with a TNT yield equivalent of 145,000 lbs. were destroyed. The burst was partially contained in its storage bunker and it was not one uniform sphere, because many more missiles were ejected to the west. It is reasonable, however, to assume that its blast yield equalled its weight, free air burst. An ideal 145,000 lbs. TNT sphere, if surface burst, and restricted to hemispheric expansion, would have given a blast wave more like 290,000 lbs. TNT free air burst. . . . One million pounds of TNT, or one-half kiloton, is assumed to be the air blast generating equivalent of one-kiloton nuclear explosives.[48]

On the basis of the above quotation, the yield of the explosion was assumed to be 145,000 lb. TNT (equal to 0.0725 kt TNT). The air blast generating equivalent was therefore 0.145 kt nuclear. Prevailing weather conditions were carefully analyzed, and window damage claims were categorized by pane size and location.[48] One of the results of the extensive research performed is the following equation:

$$D = 3.71 \times 10^{-3} A^{1.22} \Delta p^{2.78} \qquad \text{(D-2)}$$

where $D$ = damage intensity in number of panes broken per 1,000 panes exposed

$A$ = area of pane in square feet

$\Delta p$ = incident overpressure in millibars.

Rewriting the above equation in terms of probability and psi, it becomes

$$\text{Probability of failure} = 0.48\, A^{1.22}\, p_{so}^{2.78} \qquad \text{(D-3)}$$

Equation D-2 was derived for windows with a wide range of areas and a pressure range of approximately 0.01 to 0.1 psi. The thickness of the window pane in the survey in Reference 48 is implied by the area. As an example, the 50 percent probability of failure of a 40" x 40" window, which would probably be a double strength window in San Antonio, is

$$0.50 = 0.48 \times 11.1^{1.22} p_{so}^{2.78}$$

$$p_{so} = 0.35 \text{ psi}$$

Shock Tube Test[49]

The shock tube used was designed to simulate the shock wave of a large bomb with one slight, inherent difference. The test specimens experienced reflected pressures for a longer time than a building since the specimens closed off the end of the tube. The tests were done on both 1/8-in. and 7/32-in. thick, 16-in. X 16-in. sheet glass panes, with a 1/4-in. engagement on all sides. It was found that the 1/8-in. specimens survived $p_{so}$ = 0.7 psi and failed at $p_{so}$ = 0.8 psi. The 7/32-in. specimens survived $p_{so}$ = 0.9 psi and failed at $p_{so}$ = 1.1 psi.

Sonic Boom Data

References concerned with the study of sonic booms generally agree that the window damage threshold is near $p_{so}$ = 2 psf or 0.014 psi. Because of the pressure, the duration of the pulse, and the "N" shape of sonic boom pressure signatures, window natural frequency becomes important since resonance can increase the stress significantly.[3] Windows responding to sonic booms have been known to deflect inward and then fail on an outward deflection that has no comparison to nuclear explosion response; however, a few sonic boom test results are reported here.

The following results were taken from one series of tests.[50] A sonic boom with $p_{so}$ = 0.26 psi caused deflections up to 1.5 in. in twelve 5 ft X 10 ft X 1/4 in. windows causing some molding damage in one of them, but none broke. One of five 32-1/2 in. X 48-1/2 in. X 0.115 in. windows broke at $p_{so}$ = 0.15 psi. Glass fell equally on both sides of the window. When a greenhouse having 120 panes 0.085 in. thick was exposed to a boom

with $p_{so}$ = 0.26 psi, 12 panes broke and 4 cracked, mostly on the side facing the pressure wave.

A case of an accidental boom without warning over Cedar City, Utah, has been documented.[50] Claims for damage were reported in a path where the estimated overpressure ranged from about 0.125 psi to 0.04 psi at a lateral distance of about 2,000 feet. No claims were reported beyond 2,000 feet laterally from the flight path.

Two airplanes were used to create sonic booms with overpressures much higher than usual for normal supersonic flight.[11] One of the planes produced a pressure signature with a longer duration than the other. The data concerning that plane, which caused greater damage, are given in Table D-3. The number of window units (not panes) is reported for multi-pane windows.

Table D-3

SONIC BOOM EXPOSURE

| 3' X 3' Double Strength Window | | | | Nine 11" X 11" Single Strength Panes in 3' X 3' Wooden Frame | | | |
|---|---|---|---|---|---|---|---|
| $p_{so}$ (psi) | Number Exposed | Number Broken | Percent Broken | $p_{so}$ (psi) | Number Exposed | Number Broken | Percent Broken |
| 0.16<br>0.24 | 28 | 9 | 32% | 0.16<br>0.18 | 13 | 3 | 23% |
| 0.29 | 3 | 2 | 67 | 0.29 | 3 | 0 | 0 |
| 0.33 | 10 | 4 | 40 | 0.43 | 10 | 4 | 40 |
| 0.39 | 6 | 6 | 100 | 0.50 | 3 | 2 | 67 |
| 0.50 | 2 | 2 | 100 | 0.60 | 6 | 3 | 50 |
| 0.53 | 1 | 1 | 100 | | | | |
| 0.65 | 6 | 6 | 100 | | | | |

Source: Reference 11.

# Appendix E

## TIME TO FAILURE

## Appendix E

### TIME TO FAILURE

The purpose of this appendix is to provide a measure of the elapsed time between loading and failure for windows.

The computer program described in Chapter II was used to provide the data plotted in Figures E-1 through E-4. The times associated with the lowest overpressure are for incipient failure. To plot other points for determining the curves for each window size shown, use was made of the program feature which permits overpressures above the incipient failure overpressure to be used as inputs.

No test data were found to confirm or deny the values provided in the figures. It is suggested that these values be used in the interim until test data become available.

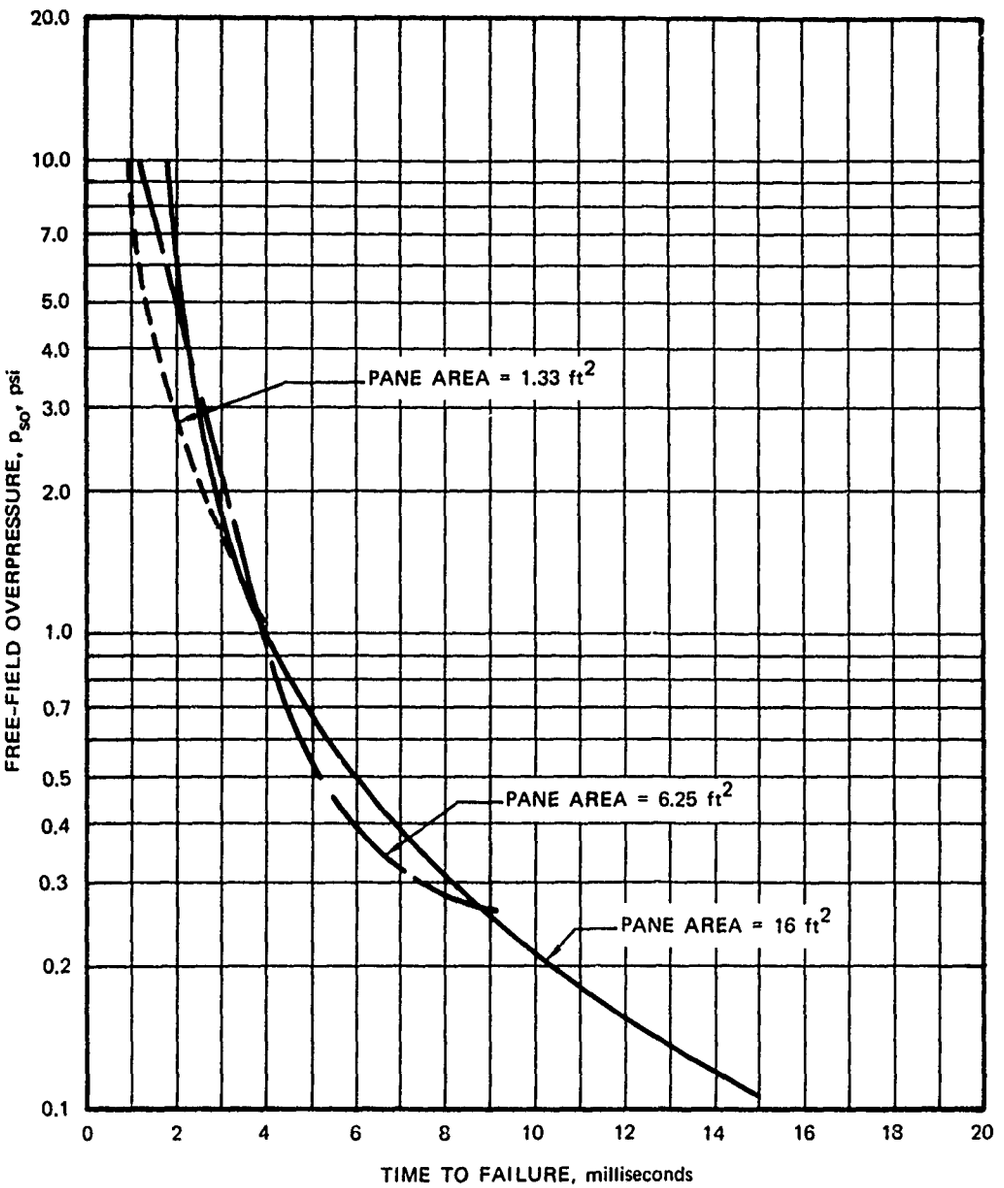


FIG. E-1 FREE-FIELD OVERPRESSURE VERSUS TIME TO FAILURE FOR PANES OF GLASS MOUNTED IN HOUSE WALLS
Single Strength Glass, Front-Face Loading

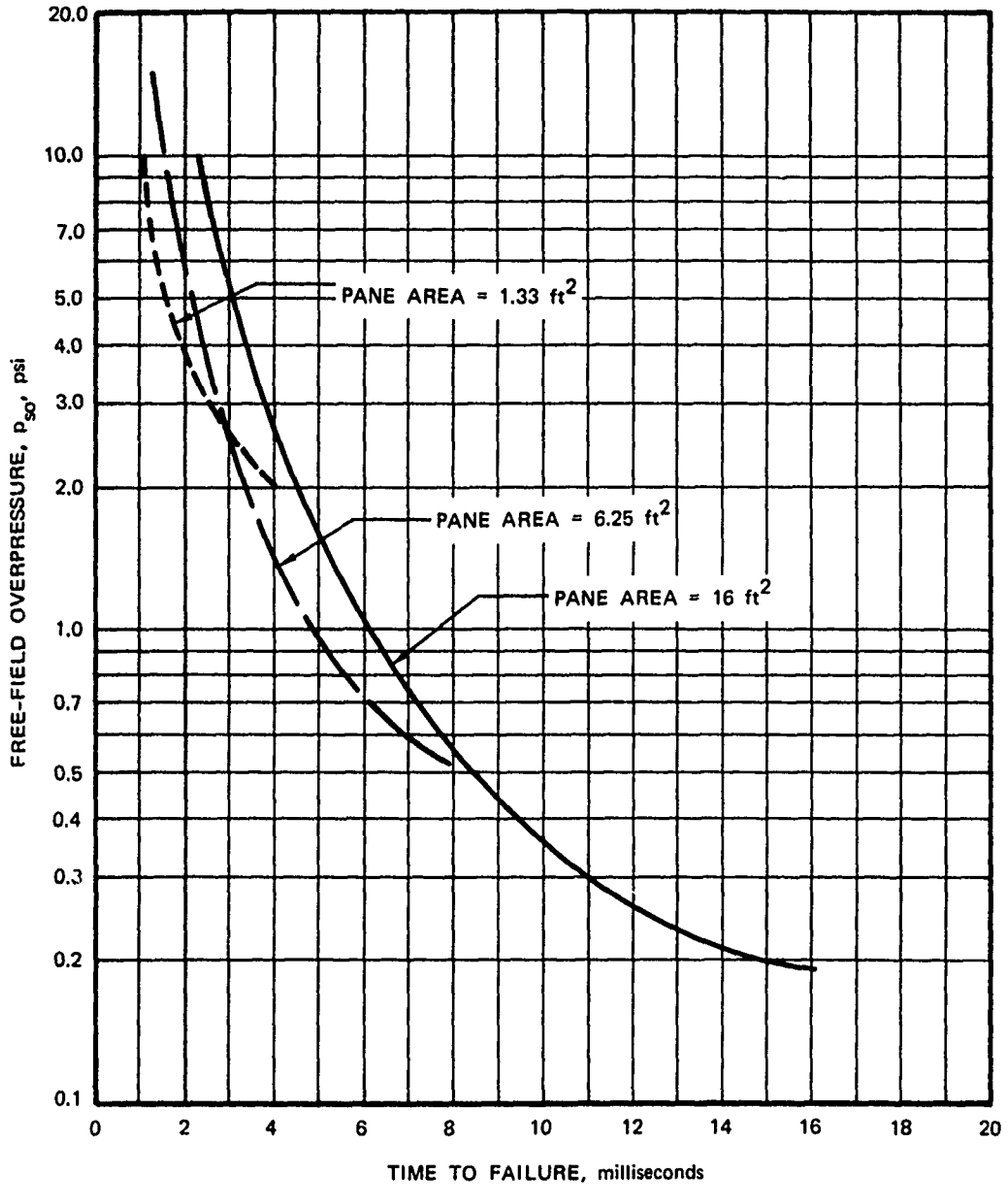


FIG. E-2 FREE-FIELD OVERPRESSURE VERSUS TIME TO FAILURE FOR PANES OF GLASS MOUNTED IN HOUSE WALLS
Single Strength Glass, Side-Face Loading

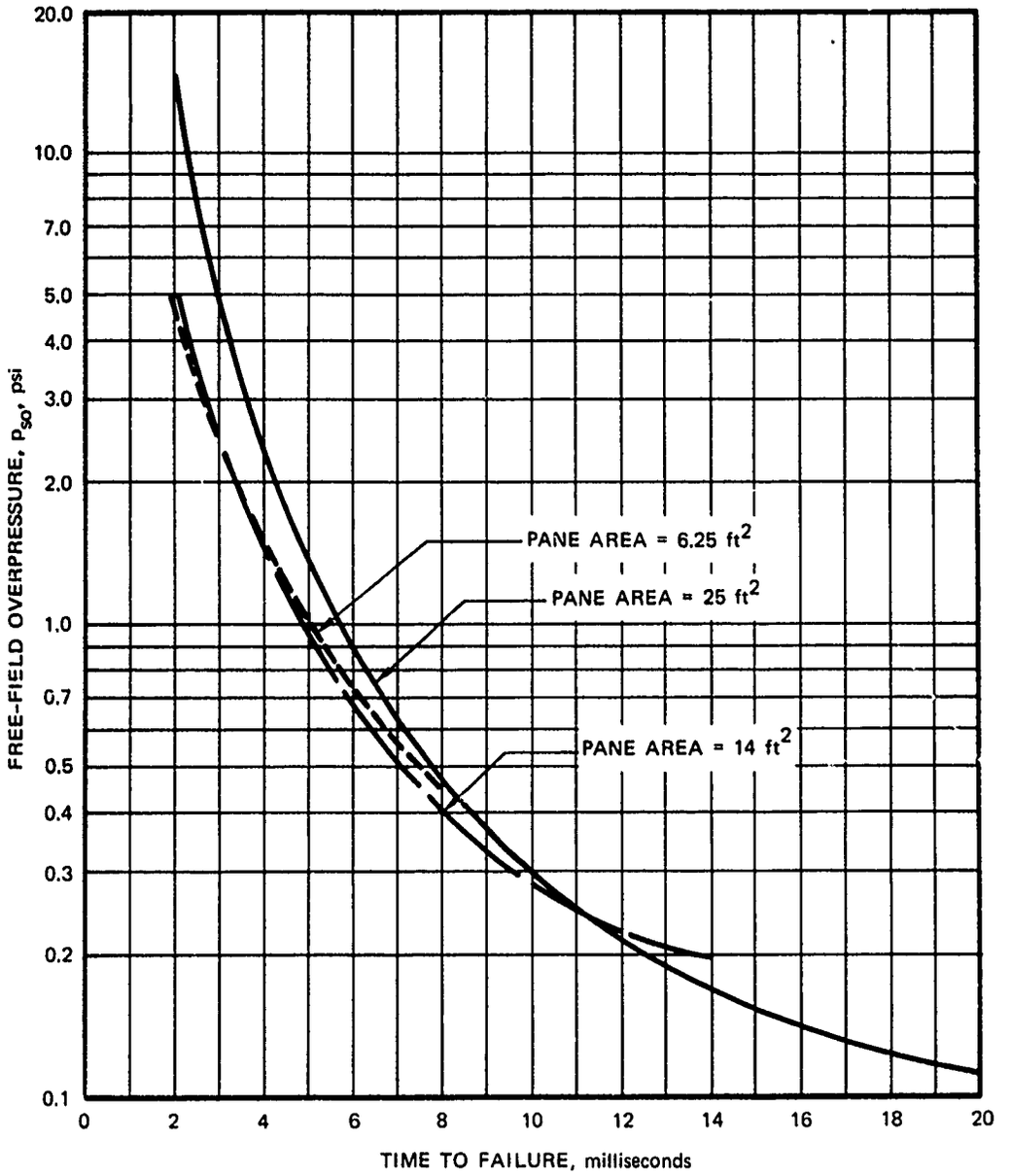


FIG. E-3 FREE-FIELD OVERPRESSURE VERSUS TIME TO FAILURE FOR PANES OF GLASS MOUNTED IN HOUSE WALLS
Double Strength Glass, Front-Face Loading

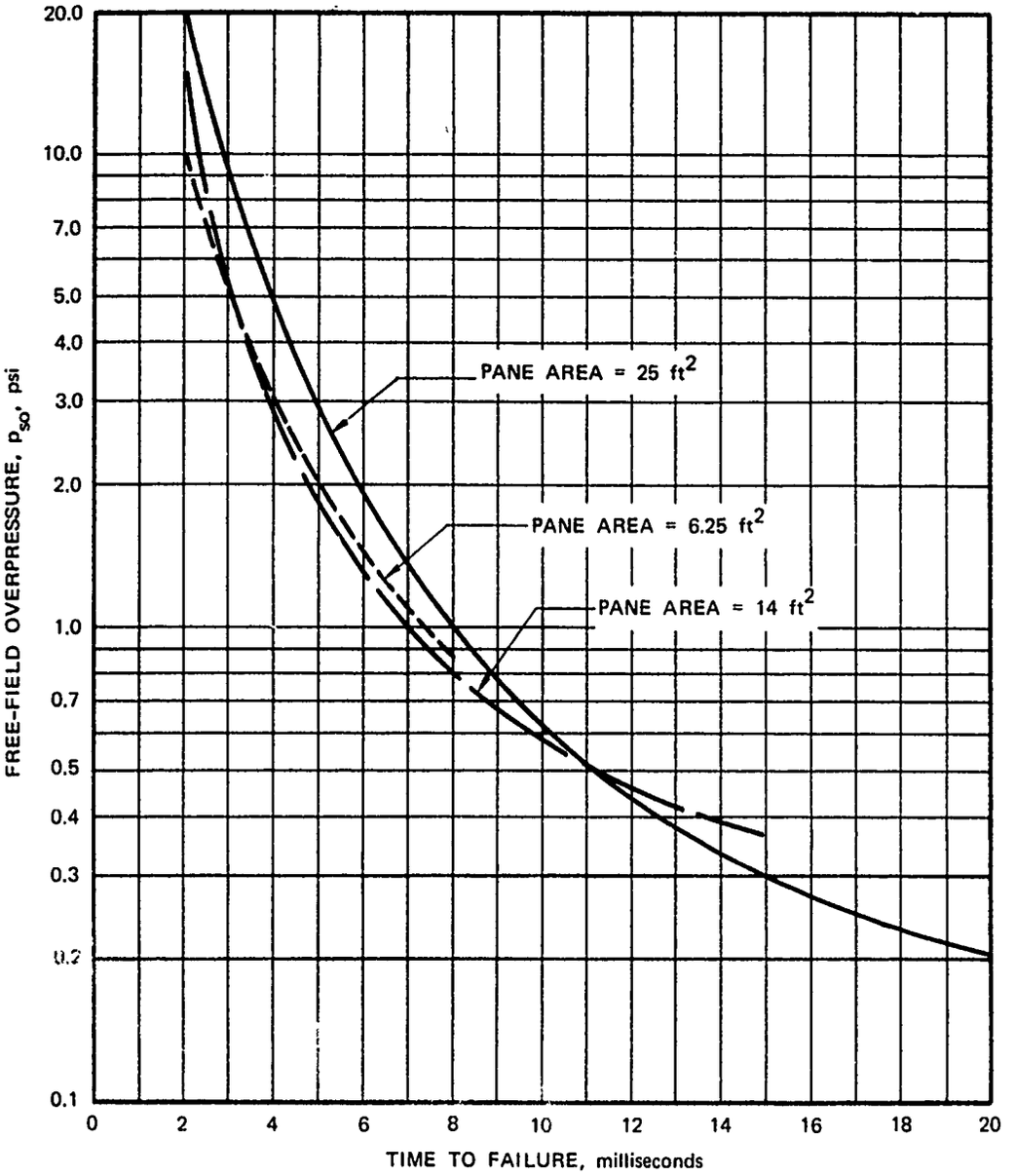


FIG. E-4 FREE-FIELD OVERPRESSURE VERSUS TIME TO FAILURE FOR PANES OF GLASS MOUNTED IN HOUSE WALLS
Double Strength Glass, Side-Face Loading

Addendum

# A MULTIPLE REGRESSION ANALYSIS APPROACH

By H. L. Murphy

## Addendum

### A MULTIPLE REGRESSION ANALYSIS APPROACH

By H. L. Murphy

As stated in the report, one must conclude from the literature that the fracture behavior of window glass principally depends on the flaws and scratches in the glass, and the unevenness and other variations in the mounting and frame. A brief statistical study, therefore, appeared to be indicated for at least part of the problem. Such an approach was undertaken following the technical work reported; results are described in the following paragraphs.

For incipient collapse prediction in terms of free-field air blast overpressure, no further study was made - the approach described in the report appeared to be supported by many tests and much research.

When higher overpressures than sufficient for incipient collapse were assumed, prediction of window glass behavior must be based on sparse nuclear test data and thus was considered appropriate for a simple statistical analysis. Table An-1 shows TEAPOT nuclear test data (Table 7 plus average and geometric mean velocity data at the trap).

Independent variables involved were:

| | |
|---|---|
| Free-field air blast peak overpressure | A |
| Total glass area of window | C |
| Window pane area | D |
| Thickness of glass | E |
| Total volume of glass | F |
| Glass travel distance to point of interest | K |
| Unit weight of glass | $\gamma$ |

It was desired to predict values for four dependent variables in a statistical (multiple regression analysis) approach:

| | |
|---|---|
| Average fragment weight | B |
| Total number of glass fragments | G |
| Geometric mean fragment weight | H |
| Geometric mean velocity (at K) | J |

Since F can be calculated as a function of C and E, or $F = f(C,E)$, and G can be calculated from B, F and $\gamma$, or $G = f(B,F,\gamma)$, both F and G merited no further study.

It was reasoned that the following relationships for predicting the dependent variables should be tried:

$B = f(A,C,D,E)$ or $f(A,C,E)$ or $f(A,D,E)$ or $f(A,E)$ or $f(A)$

$H$ = same functional equations as for B

$J = f(A,H,K)$ or $J = [f(A,H,K)]^{1/2}$

The latter was actually handled as $J^2 = f(A,H,K)$. It may be noted that J as a function of H was considered sounder, technically, than J as a function of B.

Because Equation 6 indicates that the glass behavior is closer to a linear function of glass thickness, than to some (whole-numbered) power or root, only the linear function of this variable was tried. Time did not permit trial of nonlinear functions for any of the other variables except as indicated for J and for both B and H as functions of several roots of A. The latter were all poorer fits than obtained for B and H as functions of A.

Tables An-2 through An-6 show the results of trying the functions shown above for B, using a library program of a commercial time-sharing computer service and the Table An-1 data on seven windows. All things considered, the best function for use seemed to be the last one shown

above, i.e., B = f(A). Similar results were obtained in trying the five functions shown above for H; Table An-7 shows the data on the function considered best for use, i.e., H = f(A).

The two functions shown above for J were tried, with the results for the first one being somewhat the better of the two. However, considering that the user must, in practice, calculate H before using one of these functions for J, results of a trial of J = f(A,H,K), with H values computed from H = f(A), were compared with results of a trial of J = f(A,K) which needs no H calculation. The latter results were considered best for use and are shown in Table An-8.

For the nonstatistician: the smaller the absolute value of beta, the lower the influence of that independent variable in the linear equation for the dependent variable; the "F-ratio test statistic" must be considered in connection with an F Table from standard statistical texts, and together with the index of determination (higher values equal better least squares fit), indicates the overall statistical merit of the derived linear equation.

From all of the foregoing, the most useful linear equations derived appear to be the following:

$$B = 2.96068 - 0.537311A$$

$$H = 1.97486 - 0.368371A$$

$$J = 132.36 + 17.8936A - 5.12857K$$

That the computer program routinely prints out six significant figures should not be taken as an implication of prediction accuracy, of course.

Much more confidence would be engendered by this approach if it could be based on more than seven test windows; however, that was all that seemed to be available.

Table An-1

WINDOW GLASS FRAGMENT WEIGHT DATA*

| Free-Field Overpressure, $P_{so}$ (psi) | Trap Designation | Average Thickness of Panes h (in.) | Number of Fragments Caught in Traps† | Geometric Mean Weight, $M_{50}$ (gm) | Average Weight, $\bar{M}$ (gm) | Distance from Window to Trap, x (ft) | Size of Individual Panes (in.) | Number of Panes per Window | Frame Material | Average Velocity at Trap (fps) | Geometric Mean Velocity at Trap (fps) |
|---|---|---|---|---|---|---|---|---|---|---|---|
| 5.0 | 2A | .092 | 254 | .140 | .226 | 8.83 | 12 x 12 | 16 | Wood‡ | 176 | 171 |
| 5.0 | 2C | .096 | 423 | .140 | .282 | 13.50 | 12 x 16 | 20 | Steel | 151 | 146 |
| 5.0 | $2D_1$ | .094 | 247 | .113 | .307 | 9.00 | 12 x 16 | 12 | Steel | 180 | 176 |
| 5.0 | $2D_2$ | .089 | 231 | .095 | .140 | 9.00 | | | | 184 | 180 |
| | | | 478 | .104 | .226 | | | | | 182 | 178 |
| 5.0 | $2E_1$ | .124 | 242 | .153 | .415 | 10.50 | 12 x 23.5 | 9 | Steel§ | 170 | 166 |
| 5.0 | $2E_2$ | .122 | 732 | .142 | .241 | 10.50 | | | | 186 | 178 |
| | | | 974 | .145 | .284 | | | | | 182 | 175 |
| 3.8 | $3C_1$ | .120 | 61 | .810 | 1.275 | 7.00 | 12 x 12 | 16 | Wood‡ | 148 | 146 |
| 3.8 | $3C_2$ | .118 | 259 | .540 | .993 | 7.00 | | | | 179 | 175 |
| | | | 320 | .580 | 1.047 | | | | | 173 | 169 |
| 1.9 | $4B_1$ | .124 | 1 | 2.125 | 2.125 | 10.67 | 15 x 18 | 20 | Steel‡ | 111 | 111 |
| 1.9 | $4B_2$ | .123 | 11 | 1.322 | 1.677 | 10.67 | | | | 98 | 94.8 |
| 1.9 | $4B_3$ | .124 | 5 | 1.596 | 1.704 | 10.67 | | | | 99 | 98.7 |
| 1.9 | $4B_4$ | .124 | 5 | 4.407 | 5.260 | 10.67 | | | | 109 | 107.4 |
| | | | 22 | 1.854 | 2.518 | | | | | 101.3 | 99.2 |
| 1.9 | 4D | .088 | 15 | .694 | 1.312 | 13.50 | 12 x 16 | 20 | Steel‡ | 111 | 107.8 |

* All data were taken from 13 traps located behind 7 windows mounted in house walls that faced ground zero. In cases of more than one trap per window, data from traps have been combined to provide results for each window as well as each trap.

† The number of fragments given is limited to the number for which the velocity could be calculated.

‡ Window covered with venetian blinds.

§ Window covered with curtains.

Source: Reference 29.

Table An-2

B = f(A,C,D,E)

| VARIABLE | REGR COEFF | BETA | MEAN VALUE | STD DEV |
|---|---|---|---|---|
| 0 (DEP VAR) | 2.58206 $-2 | (=CONSTANT) | .842143 | .86176 |
| 1 | -.374546 | -.635738 | 3.94286 | 1.46271 |
| 2 | 2.52484 $-4 | .348795 | 3218.57 | 1190.48 |
| 3 | -2.71972 $-3 | -.173108 | 202.286 | 54.8504 |
| 4 | 19.3855 | .366469 | .10475 | .016291 |

| SOURCE OF VARIATION | DEGREES OF FREEDOM | SUM OF SQUARES | MEAN SQUARE |
|---|---|---|---|
| TOTAL | 6 | 4.45578 | .742629 |
| REGRESSION | 4 | 4.28226 | 1.07056 |
| ERROR | 2 | .173521 | 8.67605 $-2 |

| | |
|---|---|
| INDEX OF DETERMINATION | .961057 |
| F-RATIO TEST STATISTIC | 12.3393 |

| Y-ACTUAL | Y-CALCULATED | DIFFERENCE | PERCENT |
|---|---|---|---|
| .226 | .126636 | -9.93644 $-2 | -78.4649 |
| .282 | .461446 | .179446 | 38.8877 |
| .226 | -1.36035 $-2 | -.239604 | 1761.34 |
| .284 | .411345 | .127345 | 30.9583 |
| 1.047 | 1.0995 | 5.24987 $-2 | 4.77478 |
| 2.518 | 2.34222 | -.175778 | -7.50473 |
| 1.312 | 1.46746 | .155455 | 10.5935 |

Table An-3

B = f(A,C,E)

| VARIABLE | REGR COEFF | BETA | MEAN VALUE | STD DEV |
|---|---|---|---|---|
| 0 (DEP VAR) | .330447 | (=CONSTANT) | .842143 | .86176 |
| 1 | -.406869 | -.690601 | 3.94286 | 1.46271 |
| 2 | 1.73418 $-4 | .23957 | 3218.57 | 1190.48 |
| 3 | 14.8712 | .281131 | .10475 | .016291 |

| SOURCE OF VARIATION | DEGREES OF FREEDOM | SUM OF SQUARES | MEAN SQUARE |
|---|---|---|---|
| TOTAL | 6 | 4.45578 | .742629 |
| REGRESSION | 3 | 4.219 | 1.40633 |
| ERROR | 3 | .236773 | 7.89242 $-2 |

| | |
|---|---|
| INDEX OF DETERMINATION | .946862 |
| F-RATIO TEST STATISTIC | 17.8188 |

| Y-ACTUAL | Y-CALCULATED | DIFFERENCE | PERCENT |
|---|---|---|---|
| .226 | 6.38125 $-2 | -.162188 | -254.163 |
| .282 | .389668 | .107668 | 27.6307 |
| .226 | 5.63769 $-2 | -.169623 | -300.874 |
| .284 | .565401 | .281401 | 49.7701 |
| 1.047 | .953579 | -9.34215 $-2 | -9.79694 |
| 2.518 | 2.33417 | -.183829 | -7.87554 |
| 1.312 | 1.53199 | .219992 | 14.3599 |

Table An-4

B = f(A,D,E)

| VARIABLE | REGR COEFF | BETA | MEAN VALUE | STD DEV |
|---|---|---|---|---|
| 0 (DEP VAR) | 1.17925 | (=CONSTANT) | .842143 | .86176 |
| 1 | -.508773 | -.863568 | 3.94286 | 1.46271 |
| 2 | -2.79582 $-4 | -1.77952 $-2 | 202.286 | 54.8504 |
| 3 | 16.4722 | .311396 | .10475 | .016291 |

| SOURCE OF VARIATION | DEGREES OF FREEDOM | SUM OF SQUARES | MEAN SQUARE |
|---|---|---|---|
| TOTAL | 6 | 4.45578 | .742629 |
| REGRESSION | 3 | 4.10103 | 1.36701 |
| ERROR | 3 | .354742 | .118247 |

| | |
|---|---|
| INDEX OF DETERMINATION | .920386 |
| F-RATIO TEST STATISTIC | 11.5606 |

| Y-ACTUAL | Y-CALCULATED | DIFFERENCE | PERCENT |
|---|---|---|---|
| .226 | .110572 | -.115428 | -104.392 |
| .282 | .163041 | -.118959 | -72.9629 |
| .226 | 8.89157 $-2 | -.137084 | -154.173 |
| .284 | .582629 | .298629 | 51.2554 |
| 1.047 | 1.16585 | .11885 | 10.1942 |
| 2.518 | 2.17553 | -.342466 | -15.7417 |
| 1.312 | 1.60846 | .296459 | 18.4313 |

Table An-5

B = f(A,E)

| VARIABLE | REGR COEFF | BETA | MEAN VALUE | STD DEV |
|---|---|---|---|---|
| 0 (DEP VAR) | 1.17116 | (=CONSTANT) | .842143 | .86176 |
| 1 | -.507385 | -.861212 | 3.94286 | 1.46271 |
| 2 | 15.9573 | .301661 | .10475 | .016291 |

| SOURCE OF VARIATION | DEGREES OF FREEDOM | SUM OF SQUARES | MEAN SQUARE |
|---|---|---|---|
| TOTAL | 6 | 4.45578 | .742629 |
| REGRESSION | 2 | 4.1001 | 2.05005 |
| ERROR | 4 | .355672 | .088918 |

| | |
|---|---|
| INDEX OF DETERMINATION | .920177 |
| F-RATIO TEST STATISTIC | 23.0555 |

| Y-ACTUAL | Y-CALCULATED | DIFFERENCE | PERCENT |
|---|---|---|---|
| .226 | .102309 | -.123691 | -120.899 |
| .282 | .166138 | -.115862 | -69.7379 |
| .226 | 9.43308 $10^{-2}$ | -.131669 | -139.583 |
| .284 | .596985 | .312985 | 52.4276 |
| 1.047 | 1.14202 | 9.50175 $10^{-2}$ | 8.32015 |
| 2.518 | 2.18185 | -.336154 | -15.4069 |
| 1.312 | 1.61137 | .299373 | 18.5788 |

Table An-6

B = f(A)

| VARIABLE | REGR COEFF | BETA | MEAN VALUE | STD DEV |
|---|---|---|---|---|
| 0 (DEP VAR) | 2.96068 | (=CONSTANT) | .842143 | .86176 |
| 1 | -.537311 | -.912008 | 3.94286 | 1.46271 |

| SOURCE OF VARIATION | DEGREES OF FREEDOM | SUM OF SQUARES | MEAN SQUARE |
|---|---|---|---|
| TOTAL | 6 | 4.45578 | .742629 |
| REGRESSION | 1 | 3.70613 | 3.70613 |
| ERROR | 5 | .749649 | .14993 |

| | |
|---|---|
| INDEX OF DETERMINATION | .831758 |
| F-RATIO TEST STATISTIC | 24.7191 |

| Y-ACTUAL | Y-CALCULATED | DIFFERENCE | PERCENT |
|---|---|---|---|
| .226 | .274128 | .048128 | 17.5568 |
| .282 | .274128 | -7.87201 $-3 | -2.87165 |
| .226 | .274128 | .048128 | 17.5568 |
| .284 | .274128 | -9.87201 $-3 | -3.60124 |
| 1.047 | .918902 | -.128098 | -13.9404 |
| 2.518 | 1.93979 | -.578207 | -29.8077 |
| 1.312 | 1.93979 | .627793 | 32.3639 |

Table An-7

H = f(A)

| VARIABLE | REGR COEFF | BETA | MEAN VALUE | STD DEV |
|---|---|---|---|---|
| 0 (DEP VAR) | 1.97486 | (=CONSTANT) | .522429 | .634543 |
| 1 | -.368371 | -.849146 | 3.94286 | 1.46271 |

| SOURCE OF VARIATION | DEGREES OF FREEDOM | SUM OF SQUARES | MEAN SQUARE |
|---|---|---|---|
| TOTAL | 6 | 2.41587 | .402645 |
| REGRESSION | 1 | 1.74196 | 1.74196 |
| ERROR | 5 | .673909 | .134782 |

| | |
|---|---|
| INDEX OF DETERMINATION | .721049 |
| F-RATIO TEST STATISTIC | 12.9243 |

| Y-ACTUAL | Y-CALCULATED | DIFFERENCE | PERCENT |
|---|---|---|---|
| .14 | .133008 | -6.99197 $-3 | -5.25681 |
| .14 | .133008 | -6.99197 $-3 | -5.25681 |
| .104 | .133008 | .029008 | 21.8092 |
| .145 | .133008 | -.011992 | -9.01598 |
| .58 | .575053 | -4.94704 $-3 | -.860275 |
| 1.854 | 1.27496 | -.579043 | -45.4166 |
| .694 | 1.27496 | .580957 | 45.5668 |

Table An-8

$J = f(A,K)$

| VARIABLE | REGR COEFF | BETA | MEAN VALUE | STD DEV |
|---|---|---|---|---|
| 0 (DEP VAR) | 132.36 | (=CONSTANT) | 149.429 | 33.1315 |
| 1 | 17.8936 | .789976 | 3.94286 | 1.46271 |
| 2 | -5.12857 | -.375367 | 10.4286 | 2.42494 |

| SOURCE OF VARIATION | DEGREES OF FREEDOM | SUM OF SQUARES | MEAN SQUARE |
|---|---|---|---|
| TOTAL | 6 | 6586.2 | 1097.7 |
| REGRESSION | 2 | 6167.96 | 3083.98 |
| ERROR | 4 | 418.235 | 104.559 |

| | |
|---|---|
| INDEX OF DETERMINATION | .936498 |
| F-RATIO TEST STATISTIC | 29.4952 |

| Y-ACTUAL | Y-CALCULATED | DIFFERENCE | PERCENT |
|---|---|---|---|
| 171 | 176.543 | 5.543 | 3.13975 |
| 146 | 152.593 | 6.59259 | 4.32039 |
| 178 | 175.671 | -2.32885 | -1.32569 |
| 175 | 167.978 | -7.02171 | -4.18013 |
| 169 | 164.456 | -4.54399 | -2.76304 |
| 99.2 | 111.636 | 12.4364 | 11.1401 |
| 107.8 | 97.1226 | -10.6774 | -10.9938 |

## REFERENCES


1. Garden, G. K., "Characteristics of Window Glass," Canadian Building Digest, Division of Building Research, National Research Council, Canada, December 1964.

2. Shand, E. B., Glass Engineering Handbook, 2nd Edition, McGraw-Hill Book Company, Inc., New York, 1958.

3. McKinley, R. W., "Response of Glass in Windows to Sonic Booms," Materials Research and Standards, November 1964.

4. Architectural Data Handbook, Fifth Edition, Pittsburgh Plate Glass Company, Pittsburgh, Pa., 1965.

5. Sakhnovsky, A. A., "New ASTM Structural Testing Procedures for Sash and Glass," Building Research, the Journal of the Building Research Institute, Vol. 4, No. 3, May-June 1967.

6. Preston, F. W., "The Mechanical Properties of Glass," Journal of Applied Physics, Vol. 13, No. 10, October 1942.

7. Swarts, E. L., "Fundamental Strength Considerations," Building Research, The Journal of the Building Research Institute, Vol. 4, No. 3, May-June 1967.

8. Haward, R. N., The Strength of Plastics and Glass, Cleaver-Hume Press, Ltd., New York, 1949.

9. Parrott, T. L., "Experimental Studies of Glass Breakage due to Sonic Booms," Sound, Vol. 1, No. 3, May-June 1962.

10. Gurney, C., "Sources of Weakness in Glass," Royal Society Proceedings, A, Vol. 282, 1964.

11. Maglieri, D. J., V. Huckel, and T. L. Parrott, Ground Measurements of Shock-Wave Pressure for Fighter Airplanes Flying at Very Low Altitudes and Comments on Associated Response Phenomena, NASA TN D-3443, Langley Research Center, July 1966.

12. Kerper, M. J., T. G. Scuderi, and E. H. Eimer, Strength of Glass as Related to Edge Finish, National Bureau of Standards Report No. 9069, December 1965. (AD 480 215L)

13. Freynik, H. S., Jr., "Response of Windows to Random Noise," Sound, May-June 1963.

14. Schardin, H., "The Physical Principles of the Effects of a Detonation," German Aviation Medicine, World War II, Chapter XIV - A, Vol. 2, U.S. Government Printing Office, Washington, D.C., 1950.

15. Orr, L., "Engineering Properties of Glass," Windows and Glass in the Exterior of Buildings, Building Research Institute, NAS-NRC, Publication 478, March 1957.

16. Bowles, R. and B. Sugarman, "The Strength and Deflection Characteristics of Large Rectangular Glass Panels Under Uniform Pressure," Glass Technology, Vol. 3, No. 5, October 1962.

17. Seely, F. B. and J. O. Smith, Advanced Mechanics of Materials, Second Edition, John Wiley and Sons, Inc., New York, 1952.

18. Timoshenko, S. and S. Woinowsky - Krieger, Theory of Plates and Shells, McGraw-Hill Book Company, Inc., New York, 1959.

19. Greene, C. ..., "Fundamental Strength Considerations," Building Research, The Journal of the Building Research Institute, Vol. 4, No. 3, May-June 1967.

20. Mould, R. E., "The Strength of Inorganic Glasses," Fundamental Phenomena in the Materials Sciences, Vol. 4, Fracture of Metals, Polymers, and Glasses, Plenum Press, New York, 1967.

21. Seaman, L., Response of Windows to Sonic Booms, prepared by Stanford Research Institute for the Dept. of the Air Force, SRI Project ETU-5897, June 1967.

22. "Glass Product Recommendations - Structural," Technical Service Report No. 101, Pittsburgh Plate Glass Company, Pittsburgh, Pa., March 1964.

23. Glass Performance Under Wind Load, Part II - Supplementary Data, Technical Memorandum, Product Development Dept., Pittsburgh Plate Glass Company, Pittsburgh, Pa., February 1962.

24. Fitzgerald, J. E., Blast Loading and Response of Prototype Structures and Quarter Scale Model, Operation Greenhouse WT-86 Interim Report, prepared by Armour Research Foundation of Ill. Inst. of Tech. for the U.S. Air Force, August 1951. (AD 460 274)

25. Glasstone, S., The Effects of Nuclear Weapons, Department of Defense and Atomic Energy Commission, 1962 edition, reprinted February 1964.

26. Kaplan, K. and C. Wiehle, Air Blast Loading in the High Shock Strength Region (U), Part II - Prediction Methods and Examples (U), DASA 1460-1, URS Corporation (for Defense Atomic Support Agency), Burlingame, California, February 1965.

27. Newmark, N. M., "A Method of Computation for Structural Dynamics," J. Engineering Mechanics Div., Proceedings Vol. 85, American Society of Civil Engineers, New York, July 1959; ASCE Transactions, Paper No. 3384, Vol. 127, 1962, Part I.

28. "Glass and Glazing," Uniform Building Code, Chapter 54, International Conference of Building Officials, Pasadena, California, 1967 Edition.

29. Bowen, I. G., A. F. Strehler, and M. B. Wetherbe, Distribution and Density of Missiles from Nuclear Explosions, Operation Teapot WT-1168, prepared by Lovelace Foundation for the AEC, March 1956.

30. Bowen, I. G., D. R. Richmond, M. B. Wetherbe, and C. S. White, Biological Effects of Blast from Bombs. Glass Fragments as Penetrating Missiles and Some of the Biological Implications of Class Fragmented by Atomic Explosions, AECU-3350, prepared by Lovelace Foundation for the AEC, June 1956.

31. Bowen, I. G., et al., A Model Designed to Predict the Motion of Objects Translated by Classical Blast Waves, Report CEX-58.9, prepared by Lovelace Foundation for the AEC, June 1961.

32. Fletcher, E. R., et al., Determination of Aerodynamic Drag Parameters of Small Irregular Objects by Means of Drop Tests, Report CEX-59.14, prepared by Lovelace Foundation for the AEC, October 1961.

33. Bowen, I. G., et al., Secondary Missiles Generated by Nuclear-produced Blast Waves, Operation Plumbbob WT-1468, prepared by Lovelace Foundation for the AEC, October 1963. (AD 436 391)

34. Goldizen, V. C., D. R. Richmond, and T. L. Chiffelle, Missile Studies with a Biological Target, Operation Plumbbob WT-1470 Report, prepared by Lovelace Foundation for the AEC, January 1961.

35. Bowen, I. G., private communication.

36. White, C. S., I. G. Bowen, and D. R. Richmond, Biological Tolerance to Air Blast and Related Biomedical Criteria, Report CEX-65.4, prepared by Lovelace Foundation for the AEC, October 1965.

37. Liber, T. and R. L. Barnett, An Experimental Investigation of Frangible Plate Fragmentation, IITRI Project M6095 for OCD, October 1966.

38. Barnett, R. L., J. F. Costello, and D. I. Feinstein, Debris Formation and Translation, IITRI Project M6103 for OCD, November 1966. (AD 657 603)

39. Hill, E. L., A. A. Qadeer, and A. B. Nicholls, Structural Characteristics of NFSS Buildings, Volume V - San Jose, California, Research Triangle Institute Final Report R-OU-237 prepared for OCD, June 1967.

40. Ramsey, C. G. and H. R. Sleeper, Architectural Graphic Standards, Fifth Edition, John Wiley and Sons, Inc., New York, 1956.

41. Clark, W. C., Window and Glass Hazards Under Wartime Conditions and Recommended Protective Measures, U.S. Atomic Energy Commission, AECU-3037, 1954.

42. Kerper, M. J. and T. G. Scuderi, "Mechanical Properties of Glass at Elevated Temperatures," American Ceramic Society Bulletin, December 1963.

43. Williams, A. E., "The Mechanical Strength of Glazing Glass," Journal of the American Ceramic Society, Vol. 6, No. 9, 1923.

44. Randall, P. A., Damage to Conventional and Special Types of Residences Exposed to Nuclear Effects, Operation Teapot WT-1194 Report, Office of Civil and Defense Mobilization, March 1961. (AD 611 160)

45. Byrnes, J. B., Effects of an Atomic Explosion on Two Typical Two-Story-and-Basement Wood-Frame Houses, Operation Upshot-Knothole WT-792 Report, Federal Civil Defense Administration, September 1953.

46. Clark, W. C., The Effect of Atomic Weapons on Glazing and Window Construction, Operation Greenhouse WT-7 Report, Public Buildings Service, August 1951. (AD 482 990L)

47. Chilton, CDR A. B., USN, "Resistance of Glass Windows to Atomic Blast," Chapter 12 of Studies in Atomic Defense Engineering, Navdocks P-290, Revised June 1962.

48. Reed, J. W., Evaluation of Window Pane Damage Intensity in San Antonio Resulting from Medina Facility Explosion on 13 November 1963, Sandia Laboratory and Southwest Research Institute supported by USAEC.

49. Taylor, W. J. and R. O. Clark, Shock Tube Test of Glazing Materials, BRL Memorandum Report No. 626, November 1952.

50. Wiggins, J. H. Jr., "Effect of Sonic Boom on Structural Behavior," Materials Research and Standards, June 1967.

# BIBLIOGRAPHY*

## Background information


Archer, J. S., E. A. Lawlor, and C. F. Long, Study of Atomic Blast Damage to Buildings at Hiroshima and Nagasaki, Department of Civil and Sanitary Engineering, MIT, AFSWP-808, July 1954 (regraded unclassified December 1966).

Brode, H. L., A Review of Nuclear Explosion Phenomena Pertinent to Protective Construction, prepared by Rand Corporation for the U.S. Air Force, May 1964.

Fletcher, E. R. et al., Nuclear Bomb Effects Computer, Report CEX 62.2, February 1963.

"Flexure Testing of Glass," ASTM Standards, Part 13, ASTM Designation C158-43, April 1965.

Keefer, J. H., Air Blast Predictions for Operation Distant Plain, Ballistic Research Laboratories, Tech. Note No. 1612, June 1966.

Levy, S., Bending of Rectangular Plates with Large Deflections, National Bureau of Standards, Report No. 737, 1942.

Weibull, W., A Statistical Theory of the Strength of Materials, Generalstabens Litografiska Anstalts Forlag, Stockholm, 1939.

Wiehle, C. K., and W. L. Durbin, Combined Effects of Nuclear Weapons on NFSS Type Structures, URS Corporation, September 1966.


## General glass and window information


Building Research, the Journal of the Building Research Institute, Vol. 4, No. 3, May-June 1967. (A collection of articles concerning glass in windows.)


---

* These books, reports, and articles were reviewed during the course of this investigation but not used specifically in preparing the report.

Haward, R. N., "The Behaviour of Glass under Impact and Static Loading," Society of Glass Technology-Journal, Vol. 28, 1944.

Haward, R. N., "The Behaviour of Laminated and Toughened Glass under Impact by a Falling Bolt," Journal of the Society of Glass Technology, Vol. 29, 1945.

Reinhart, F. W., R. A. Kronstadt, and G. M. Kline, Antiscatter Treatments of Glass, National Bureau of Standards Miscellaneous Publication M175, June 1944.

Shand, E. B., "Experimental Study of Fracture of Glass: I, The Fracture Process, and II, Experimental Data," Journal of the American Ceramic Society, Vol. 37, No. 2, February 1954, and Vol. 37, No. 12, December 1954.

"Testing Window Glass for Concussion Damage," Engineering News-Record, Vol. 128, 521, April 2, 1942.

Conventional Explosion information related to glass

Adams, F. W., "Behavior of Glazing Material Subjected to Explosion," ASTM Bulletin No. 122, May 1943.

Eilenberg, T. R., and W. K. Jones, "Discussion of Paper on Behavior of Glazing Material Subjected to Explosion," ASTM Bulletin No. 124, October 1943.

Grossman, J. R., Methods of Reducing the Flying Glass Hazard From Blast Shattered Windows, Atlantic Research Corporation, TR-PL-9222, for the Dept. of State, December 1966.

Ilsley, R., Glass and Plaster Damage from Small Explosions, Armed Services Explosives Safety Board, Technical Paper No. 7, March 1950. (AD 637 835)

Moore, H., "Physics and Windows in War-time," Journal of Scientific Instruments, Vol. 17, 237-241, October 1940.

Report of Blast Tests on Glass, prepared by the Fortification Section, Construction Division, Office of Chief of Engineers, War Dept., March 1943.

Thompson, N. J., and E. W. Cousins, "Explosion Tests on Glass Windows; Effect on Glass Breakage of Varying the Rate of Pressure Application," Journal of the American Ceramic Society, Vol. 32, 1949.

"Windows and Bomb Blast," Nature, Vol. 146, 435-6, September 28, 1940.

Wise, J. A., Rupture of Glass by Blast, Monthly Report EWT-5e (OSRD-5405e), Div. 2, NDRC, August 1945.

Sonic boom information

Bailey, D., A Sonic Boom Study for the Structural Engineer, Air Force Weapons Laboratory, Tech. Report No. AFWL-TR-66-154, March 1967.

Structural Response to Sonic Booms, Vols. 1 and 2, prepared by Andrews Associates, Inc. and Hudgins, Thompson, Ball and Associates, Inc. for the Federal Aviation Agency, February 1965.

Proceedings of the Sonic Boom Symposium, Acoustical Society of America, November 1965.

Young, J. R., "Energy Spectral Density of the Sonic Boom," The Journal of the Acoustical Society of America, Vol. 40, No. 2, 1966.

Biological information

McDonnell, G. M., W. H. Crosby, C. F. Tessmer, et al., Effects of Nuclear Detonation on a Large Biological Specimen (Swine), Operation Plumbbob Report WT-1428, Project 4.1, prepared by Walter Reed Army Institute of Research, For Official Use Only, August 1961. (AD 460 308)

Missile Effects of Flying Glass, OCD, MPM #263-276, PSD-Project No. NF-55, October 1963.

Richmond, D. R., and C. S. White, Biological Effects of Blast and Shock, Technical Progress Report on Contract No. DA-49-146-XZ-055, DASA-1777, April 1966.

White, C. S., Biological Blast Effects, presented before the Special Subcommittee on Radiation of the Joint Committee on Atomic Energy During Public Hearings on the Biological and Environmental Effects of Nuclear War, Washington, D.C., Report TID-5564, June 24, 1959.

White, C. S., I. G. Bowen, and D. R. Richmond, "A Comparative Analysis of Some of the Immediate Environmental Effects at Hiroshima and Nagasaki," Health Physics, Vol. 10, pp. 89-150, March 1964.

White, C. S., I. G. Bowen, D. R. Richmond, and R. L. Corsbie, Comparative Nuclear Effects of Biomedical Interest, Report CEX-58.8, January 1961.

## NOTATION

| | |
|---|---|
| a | Short side dimension of a rectangular window pane |
| A | Pane area; nondimensional missile parameter in translation model |
| $A_f$ | Area of fragment presented to the wind |
| b | Long side dimension of a rectangular window pane |
| $c_o$ | Speed of sound in undisturbed air |
| $C_d$ | Drag coefficient |
| D(n) | Nondimensional fragment displacement in translation model |
| E | Modulus of elasticity |
| g | Acceleration of gravity |
| h | Average thickness of a glass pane |
| m | Mass of an entire window (Equation 1); glass fragment weight |
| $\bar{M}$ | Average weight of a number of fragments |
| $M_{so}$ | Geometric mean weight of a number of fragments |
| n | Decimal point locator in translation model equations |
| N | Estimated total number of glass fragments produced by the failure of a given window |
| $N_x$ | Spatial density of fragments at x feet from a window, fragments/unit area |
| $N_o$ | Spatial density of fragments zero feet from a window, fragments/unit area (x may be replaced by a number to denote a specific distance from a window) |
| $N_{10}$ | Spatial density of fragments 10 feet from a window, fragments/unit area |

| | |
|---|---|
| $p(t)$ | Time dependent pressure against any surface |
| $p_c$ | Pressure exerted at time $t_c$ |
| $p_d$ | Dynamic pressure varying with time |
| $p_{do}$ | Peak dynamic pressure |
| $p_r$ | Reflected pressure |
| $p_s$ | Free-field overpressure varying with time |
| $p_{so}$ | Peak free-field overpressure |
| P | Nondimensional peak free-field overpressure used in translation model; probability of penetration or serious injury |
| $P_o$ | Ambient atmospheric pressure of undisturbed air |
| q | Applied pressure to glass panes |
| $q_{sf}$ | Static failure pressure for glass panes |
| $q_{df}$ | Dynamic failure pressure for glass panes |
| s | Length of a side of a square glass pane |
| S | Clearing distance |
| t | Time |
| $t_c$ | Clearing time, front-face |
| $t_o$ | Duration of positive overpressure phase |
| $t_u$ | Duration of dynamic pressure phase |
| T | Nondimensional time used in translation model |
| U | Shock front velocity |
| v | Fragment velocity |
| $v_m$ | Maximum fragment velocity |
| $\dot{v}$ | Fragment acceleration |

| | |
|---|---|
| $V(n)$ | Nondimensional fragment velocity used in translation model |
| $\dot{V}(n)$ | Nondimensional fragment acceleration used in translation model |
| $w_o$ | Mean central deflection of a glass pane |
| $W$ | Weapon yield, kilotons |
| $x$ | Pane displacement at center during loading (Equation 1); distance of travel for a glass fragment |
| $\alpha$ | Fragment acceleration coefficient, area/weight |
| $\gamma$ | Unit weight |
| $\nu$ | Poisson's ratio |
| $\sigma$ | Stress |
| $\sigma_r$ | Modulus of rupture |

UNCLASSIFIED

Security Classification

## DOCUMENT CONTROL DATA - R & D

*(Security classification of title, body of abstract and indexing annotation must be entered when the overall report is classified)*

| 1. ORIGINATING ACTIVITY (Corporate author) | 2a. REPORT SECURITY CLASSIFICATION |
|---|---|
| STANFORD RESEARCH INSTITUTE<br>Menlo Park, California 94025 | Unclassified |
| | 2b. GROUP<br>Not applicable |

3. REPORT TITLE

EXISTING STRUCTURES EVALUATION - PART II: WINDOW GLASS AND APPLICATIONS

4. DESCRIPTIVE NOTES (Type of report and inclusive dates)

Final Report

5. AUTHOR(S) (First name, middle initial, last name)

James H. Iverson

| 6. REPORT DATE | 7a. TOTAL NO. OF PAGES | 7b. NO. OF REFS |
|---|---|---|
| December 1968 | 164 | 50 |

| 8a. CONTRACT OR GRANT NO. | 9a. ORIGINATOR'S REPORT NUMBER(S) |
|---|---|
| OCD-DAHC20-67-C-0136<br>b. PROJECT NO.<br>Work Unit No. 1126C | None |
| c.<br>d. | 9b. OTHER REPORT NO(S) (Any other numbers that may be assigned this report) |

10. DISTRIBUTION STATEMENT

This document has been approved for public release and sale; its distribution is unlimited.

| 11. SUPPLEMENTARY NOTES | 12. SPONSORING MILITARY ACTIVITY |
|---|---|
| | Office of Civil Defense<br>Office of the Secretary of the Army<br>Washington, D.C. 20310 |

13. ABSTRACT

This report covers one portion of a research project to evaluate existing National Fallout Shelter Survey (NFSS) structures for resistance to combined nuclear weapons effects. The objective of this investigation was to determine the response of windows to air blast overpressures generated by nuclear explosions, including glass fragment characteristics (weights, velocities, numbers produced, and spatial densities) that could be used to predict statistically the effects of window glass failure on humans.

The analysis leading to the presentation of graphs, which can be used to predict the free-field overpressure at incipient failure for sheet and plate glass, was based on the theoretical load-deflection equation for large deflections of plates, modified by test results found in the literature. Glass panes were changed to equivalent single-degree-of-freedom systems in the analysis. The analysis was also used to estimate the time to failure for windows at various overpressures. Methods for predicting glass fragment characteristics were obtained empirically from Operation Teapot nuclear test data. The procedures for estimating incipient failure overpressures and fragment weights, spatial densities, numbers, and velocities were applied to windows in 14 buildings (located in San Jose and Palo Alto, California) that were part of the NFSS.

DD FORM 1 NOV 68 1473 REPLACES DD FORM 1473, 1 JAN 64, WHICH IS OBSOLETE FOR ARMY USE.

UNCLASSIFIED

Security Classification

| 14: KEY WORDS | LINK A | | LINK B | | LINK C | |
|---|---|---|---|---|---|---|
| | ROLE | WT | ROLE | WT | ROLE | WT |
| Nuclear weapon effects<br>Response of windows to air blast<br>Glass fragment characteristics<br>Window glass failure<br>Incipient failure for sheet and plate glass<br>Time to failure for window | | | | | | |